

12-2014

# Cellulose Nanofibers Use in Coated Paper

Finley Richmond

Follow this and additional works at: <http://digitalcommons.library.umaine.edu/etd>

 Part of the [Chemical Engineering Commons](#)

---

## Recommended Citation

Richmond, Finley, "Cellulose Nanofibers Use in Coated Paper" (2014). *Electronic Theses and Dissertations*. 2242.  
<http://digitalcommons.library.umaine.edu/etd/2242>

This Open-Access Dissertation is brought to you for free and open access by DigitalCommons@UMaine. It has been accepted for inclusion in Electronic Theses and Dissertations by an authorized administrator of DigitalCommons@UMaine.

# CELLULOSE NANOFIBERS USE IN COATED PAPER

By

Finley Richmond

B.S. Widener University, 2006

M.S. Widener University, 2008

A DISSERTATION

Submitted in Partial Fulfillment of the

Requirements for the Degree of

Doctor of Philosophy

(in Chemical Engineering)

The Graduate School

The University of Maine

December 2014

Advisory Committee:

Douglas W. Bousfield, Professor of Chemical & Biological Engineering, Advisor

Albert Co, Associate Professor of Chemical & Biological Engineering

Douglas Gardner, Professor of Forest Operations, Bioproducts & Bioenergy

Joseph M. Genco, Professor of Pulp and Paper Science and Engineering

William Desisto, Associate Professor of Chemical & Biological Engineering

# CELLULOSE NANOFIBERS USE IN COATED PAPER

By Finley Richmond

Dissertation Advisor: Dr. Douglas W. Bousfield

An Abstract of the Dissertation Presented  
in Partial Fulfillment of the Requirements for the  
Degree of Doctor of Philosophy  
(in Chemical Engineering)  
December 2014

Cellulose Nanofibers (CNF) are materials that can be obtained by the mechanical breakdown of natural fibers. CNF have the potential to be produced at low cost in a paper mill and may provide novel properties to paper, paper coatings, paints, or other products. However, suspensions have a complex rheology even at low solid contents. To be able to coat, pump, or mix CNF at moderate solids, it is critical to understand the rheology of these suspensions and how they flow in process equipment; current papers only report the rheology up to 6% solids. Few publications are available that describe the coating of CNF onto paper or the use of CNF as an additive into a paper coating.

The rheology of CNF suspensions and coatings that contain CNF were characterized with parallel-disk geometry in a controlled stress rheometer. The steady shear viscosity, the complex viscosity, the storage modulus, and the yield stress were determined for the range of solids or concentrations (2.5-10.5%). CNF were coated onto paper with a laboratory rod coater, a size press and a high speed cylindrical laboratory coater (CLC). For each case, the coat weights were measured and the properties of the papers were characterized.

CNF water base suspension was found to be a shear thinning with a power law index of around 0.1. Oscillatory tests showed a linear viscoelastic region at low strains and significant storage and loss moduli even at low solids. The Cox Merz rule does not hold for CNF suspensions or coating formulations that contain CNF with complex viscosities that are about 100 times larger than the steady shear viscosities. Paper coating formulations that contain CNF were found to have viscosities and storage and loss moduli that are over ten times larger than coatings that contain starch at similar solids.

CNF suspensions were coated on papers with low amount transferred on paper either at high solids or high nip loadings. The amount transferred appears to be controlled by an interaction of filtration and fluid flow mechanisms. Coatings with CNF of 5 pph (part per hundred) were not able to be applied with CLC coater due to solid like behavior of the coating: the issue seems to be the ability of the coating to flow in the pond by gravity to the blade-paper nip and not the flow in the blade region itself.

Some improvement of the paper properties were found by coating CNF onto paper, but some improvements were much less than expected. This may be due to CNF soaking into the paper. Air permeability decreased and stiffness increased.

Paper coatings with CNF had higher stiffness and coating strength than coatings that contained starch. CNF acts similar to starch in terms of being a co-binder. A decrease in pick resistance is seen at 5 pph CNF or starch content; this decrease likely comes from the coating layer becoming more brittle.

**COPYRIGHT NOTICE**

© Finley Richmond

All Rights Reserved

## ACKNOWLEDGEMENTS

I would like to thank many people throughout the course of my sejourney here at University of Maine; without them this work would be possible. I wish to thank Dr. Douglas W. Bousfield for providing guidance, opportunity to work on this project and valuable suggestions that he gave through the whole process. I also thank Dr. Albert Co for suggestions on the rheological experiments and the use of his laboratory equipment. Thanks to Dr. Douglas Gardner for discussions on the analysis of the diffusion data. I also like to thank Dr. Joseph M. Genco for his vibrant suggestions and the direction to go, and Dr. William Desisto for advice and discussions on work progress.

I wish to thank The Paper Surface Science Program at The University of Maine for support and excellent discussions. I would like to thank the Process development Center team at University of Maine for supplying the materials and Special thanks to the faculty, staff and graduate students of the Chemical and Biological Engineering Department over the past years.

## TABLE OF CONTENTS

ACKNOWLEDGEMENTS .....	iv
LIST OF TABLES .....	viii
LIST OF FIGURES .....	ix
1. INTRODUCTION .....	1
1.1 Cellulose Nanofibers .....	1
1.2 Thesis Objectives.....	2
1.3 Literature Reviews.....	4
1.4 Cellulose Nanofibers (CNF) and their Production .....	5
1.5 Thesis Format .....	7
1.6 Summary.....	8
2. RHEOLOGY OF CELLULOSE NANOFIBERS (CNF) SUSPENSIONS.....	9
2.1 Abstract.....	9
2.2 Introduction .....	10
2.3 Experimental Methods.....	14
2.4 Results and Discussion .....	15
2.5 Conclusion.....	29
3. PREDICTION OF COAT WEIGHT OF CNF OBTAINED WITH DIFFERENT COATING METHODS .....	31
3.1 Abstract.....	31
3.2 Introduction .....	32
3.3 Experimental Methods.....	34

3.4	Results and Discussion .....	38
3.5	Model prediction of CNF coated on paper with size press.....	45
3.6	Filtration theory .....	51
3.7	Conclusion .....	55
4	PROPERTIES OF COATED PAPERS COATED WITH CELLULOSE NANOFIBERS (CNF).....	56
4.1	Abstract.....	56
4.2	Introduction .....	56
4.3	Experimental Methods.....	58
4.4	Results and Discussion .....	60
4.5	Conclusion .....	72
5	THE RHEOLOGY OF COATING FORMULATION THAT COATAIN CELLULOSE NANOFIBERS.....	73
5.1	Abstract.....	73
5.2	Introduction .....	73
5.3	Experimental Methods.....	75
5.4	Theory.....	78
5.5	Results and Discussion .....	81
5.6	Conclusion .....	95
6	THE USE OF CELLULOSE NANOFIBERS IN PAPER COATING FORMULATION.....	96
6.1	Abstract.....	96
6.2	Introduction .....	97
6.3	Cellulose Nanofibers as a coating additive.....	100

**LIST OF TABLES**

Table 2-1 Solids of CNF suspension on shear viscosity for different materials.....	12
Table 2-2 Effect of solid contents on shear viscosity for NCC. ....	13
Table 3-1 Carreau model parameters that fit the steady shear data .....	47
Table 5-1 Coating formulations for constant latex amount .....	76
Table 6-1 Coating formulations for constant latex amount .....	102
Table 6-2 Coating formulations that reduce latex and increase CNF and starch.....	102

## LIST OF FIGURES

Figure 2-1 Steady shear viscosity and shear stress as a function of shear rate.....	16
Figure 2-2 Steady shear viscosity as a function of shear rate for different solids of CNF .....	17
Figure 2-3 Comparison of geometry measurements for the steady shear viscosity .....	18
Figure 2-4 Power law index $n$ as a function of solids for old sample (OS) and new sample (NS).....	19
Figure 2-5 Power law parameter $m$ as a function of solids for old sample (OS) and new sample (NS) .....	20
Figure 2-6 Comparison of results with Haavisto et al. (2011) data for power law index.....	21
Figure 2-7 Comparison of our results with Haavisto et al data on power law parameter $m$ of CNF (2011).....	21
Figure 2-8 Elastic stress as a function of strain for various solids of CNF .....	22
Figure 2-9 Stress as a function of time used to determine the yield stress of CNF for various solids.....	23
Figure 2-10 Storage modulus as a function of strain for various solid levels of CNF.....	24
Figure 2-11 Loss modulus of CNF as a function of strain for various solid levels .....	25
Figure 2-12 Complex viscosity as a function of shear rate for different solids of CNF.....	26
Figure 2-13 Complex viscosity and steady viscosity for different solids.....	27

Figure 2-14 Comparison of our results with Pääkkö et al data on viscosity of CNF (2007) .....	29
Figure 3-1 Laboratory scale size press device. ....	36
Figure 3-2 Coat weight results for two sheets of paper sent through the nip .....	38
Figure 3-3 Coat weight obtained for 3.5% solid of CNF using the flooded size press method at three nip loads.....	40
Figure 3-4 Coat weight for different solids and nip loads of CNF .....	40
Figure 3-5 Coat weight obtained for different solid levels of CNF at the speed of 0.5 m/s using the metered size press method. ....	42
Figure 3-6 Coat weight obtained for 3.5 and 8.5% solids of CNF using the rod draw down method and coated only on side.....	43
Figure 3-7 Coat weight obtained for three different papers coated with CNF for various nip loads.....	44
Figure 3-8 Coat weight obtained for 3.5% solids of CNF using the flooded size press method.....	44
Figure 3-9 Coat weight obtained for different solid levels of CNF and different speeds using the cylindrical laboratory coater (CLC).....	45
Figure 3-10 Schematic of the forward rolling nip geometry .....	47
Figure 3-11 An example output of the model for a) velocity magnitude field .....	48
Figure 3-12 Predicted coat weight as a function of nip load for two solid contents and roll surface velocities .....	50
Figure 3-13 Predicted coat weight as a function of roll surface velocity .....	51
Figure 3-14 Predicted coat weight compared to the experimental coat weight.....	54

Figure 4-1 Water retention value of CNF as a function of time for different solid contents.....	61
Figure 4-2 Gloss as a function of coat weight for CNF .....	62
Figure 4-3 Brightness as a function of coat weight for CNF .....	63
Figure 4-4 Roughness as a function of coat weight for CNF coated with the CLC coater .....	64
Figure 4-5 Roughness as a function of coat weight coated with a rod draw down coater.....	65
Figure 4-6 Stiffness as a function of coat weight for CNF.....	66
Figure 4-7 Air permeability as a function of coat weight for CNF for CLC coated samples.....	67
Figure 4-8 Darcy permeability as a function of coat weight for CNF coated with rod draw down coated. ....	68
Figure 4-9 Contact angle as a function of coat weight for CNF .....	69
Figure 4-10 Bristow wheel as a function of coat weight for CNF .....	70
Figure 4-11 Porosity of rod coated samples at various solids and coat weights.....	71
Figure 4-12 Volume as a function particle size for different solids of CNF .....	72
Figure 5-1 Steady shear viscosity as a function of shear rate for different concentrations of CNF holding the latex content constant at 10 pph .....	82
Figure 5-2 Steady shear viscosity as a function of shear rate for different concentration of starch with constant 10 pph of latex .....	83
Figure 5-3 Steady shear viscosity as a function of shear rate for different concentrations of CNF, starch.....	83

Figure 5-4 Power law index $n$ as a function of pph for coatings with CNF, starch and as a function of weight percent in CNF-water system (pure CNF).....	84
Figure 5-5 Power law parameter $m$ as a function of pph for coatings with CNF, starch and pure CNF .....	85
Figure 5-6 Viscosity of starch as a function of shear rate for different solids for ethylated starch Ethylex 2025 .....	86
Figure 5-7 Viscosities of coatings that contain starch as a function of shear rate for different 5 and 10pph .....	87
Figure 5-8 Viscosities of proposed scaling for coatings that contain CNF as a function of shear rate for different pph .....	88
Figure 5-9 Viscosities of proposed scaling for coatings that contain CNF as a function of shear rate for different pph of a constant factor .....	89
Figure 5-10 Complex viscosity and steady shear viscosity as a function of shear rate-frequency for different concentrations of CNF into a coating .....	90
Figure 5-11 Complex viscosity and steady shear viscosity as a function of shear rate-frequency for different concentration of starch in a coating .....	90
Figure 5-12 Storage and loss moduli as a function of frequency for coatings that contain 5 pph starch or CNF and 10 pph latex.....	91
Figure 5-13 Storage and loss moduli as a function of frequency for coatings that contain 10 pph starch or CNF and 10 pph latex.....	92
Figure 5-14 Complex viscosity ( $C_v$ ) and steady shear viscosity ( $v$ ) as a function of shear rate-frequency for different concentrations of CNF into a coating .....	93

Figure 5-15 Complex viscosity ( $C_v$ ) and steady shear viscosity ( $v$ ) as a function of shear rate-frequency for different concentration of starch into a coating.....	94
Figure 5-16 Stress as a function of time used to determine the yield stress of CNF-starch into a coating .....	95
Figure 6-1 An AFM image of the refiner produced CNF .....	101
Figure 6-2 Comparison of steady shear viscosity as a function of shear rate for different pph of coatings with CNF and starch .....	105
Figure 6-3 Steady shear viscosity as a function of shear rate for different pph of coatings with CNF, starch and latex .....	106
Figure 6-4 Storage and loss moduli as a function of frequency for coatings that contain 0 CNF and 5 pph starch or CNF and 10 pph latex .....	107
Figure 6-5 Storage and loss moduli as a function of frequency for coatings that contain 10 pph starch or CNF and 10 pph latex.....	107
Figure 6-6 Water retention value for coatings with CNF and starch as a function of time for series 2 formulations.....	109
Figure 6-7 Coat weight as a function speed for different coating formulation by using the CLC coater.....	110
Figure 6-8 Gloss as a function of coat weight for coatings with CNF and starch applied with CLC coater.....	111
Figure 6-9 Roughness as a function of coat weight for coatings with CNF and starch.....	112
Figure 6-10 Brightness as a function of coat weight for coatings with CNF and starch.....	113

Figure 6-11 Air permeability as a function of coat weight for coatings with CNF and starch.....	114
Figure 6-12 Stiffness as a function of coat weight for coatings with CNF and starch.....	115
Figure 6-13 Pick velocity as a function of coat weight for coatings with CNF and starch.....	116

## CHAPTER 1

### INTRODUCTION

#### 1.1 Cellulose Nanofibers

Nanotechnology has enabled the development of new products that can have a dramatic influence on the economy and standard of living. Nanotechnology is the manipulation of materials at the nanometer length scale. Nanotechnology can influence many applications such as medical diagnostics, separations, composite materials, insulation, energy storage, and consumer products (Bhat & Lee, 2003).

Consumers, industries, governments and scientists are all interested in products made from renewable resources that have low environmental impact and minimal safety risks. Cellulose nanofibers (CNF) are a biodegradable, natural, and renewable resource that is made from wood. The CNF suspension can also be extracted from sources other than wood, such as bananas, bamboo, cotton, sugar cane, straw, sugar beets, and potatoes (Klemm et al., 2006 & 2009). It is expected that this material can be produced at a low cost in paper mills (Spence et al., 2011). In the paper industry, nano-scale cellulose fibers have gained attention due to a number of potential applications. A number of recent journal review articles describe various aspects of the production and use of these materials and much attention is paid to using this material in plastic composites and other applications (Moon et al., 2011; Eichorn et al., 2010; Klemm et al., 2006; Hubbe et al., 2008; Sairo et al., 2010).

Many of these reviews are focused on using these fibers as reinforcement agents in plastics. However, a natural uses for these fibers is in the production of paper and packaging materials. Recent work has shown that CNF coated on paper can increase the capture of ink pigments at the top surface which leads to an increase in print density for ink jet and flexographic printing (Hamada & Bousfield 2010; Hamada et al., 2010; Luu et al.,2011). The use of CNF in the wet-end has also been reported (Torvinen et al., 2011; Morseburg et al., 2009) resulting strength benefits. CNF coated on a paper surface with a pigment pre-coat has also been shown to increase the stiffness of the sheet (Ridgeway & Gane, 2011).

This thesis explores the potential use of CNF as a coating layer and as a component of a paper coating formulation. The rheology of CNF suspensions and coating that contain CNF is reported. An understanding the coat weight that is obtained with various coating parameters is obtained. The final properties of paper coated with CNF suspensions and with coatings that contain CNF is given.

## **1.2 Thesis Objectives**

The overall objective of this dissertation is to enable the use of mechanically made cellulose nanofibers either as an additive to paper coating formulation or as a coating layer itself. One of the key technical challenges is related to the rheological behavior of CNF suspensions and coating formulation that contain CNF. Even at low concentrations of CNF, the viscosity increase is significant. The rheology of these coatings will influence the coating operations in unknown ways. Also, the resulting paper properties after coating with CNF or with coatings that contain CNF are not widely known. The defining key points of this project are:

- 1) To characterize the effect of solids on CNF suspension rheology, especially high solids.
- 2) To understand the mechanisms that determine the coat weight obtained in size press geometry when coating CNF suspension onto papers.
- 3) To determine the potential of using CNF as a coating layer and the properties of paper coated with CNF.
- 4) To characterize the rheology of paper coating that contains CNF and the resulting coated paper properties.

The first objective is to understand how various rheological properties change as the solids change. Other researchers have reported results for low solids (less than 5% solids), but few have reported for solids over 5%. The second objective is to develop a better understanding of the coat weight obtained when CNF is coated onto paper with size press geometry. There has been no other published work on this topic; however, work around starch application at a size press is related. The rheology of the CNF suspension is expected to influence the coat weight obtained. The third objective relates to determining the properties of the paper coated with CNF. The last objective is concerned with the rheology of paper coatings that contain CNF and the properties of these layers: if these coating layers are as strong as standard coating layers, CNF may be able to reduce the latex needed in a coating formulation. Two groups have published work on this topic, but a systematic study is lacking in the literature.

### 1.3 Literature Reviews

The significance of cellulose was first recognized by a French chemist, Anselme Payen. After a long time studying the subject, he found cellulose in the cell walls of higher plants, algae, bacteria, fungi and more. Due to its availability and the fact that it can be extracted from wood fibers with the chemical formula  $(C_6H_{10}O_5)_n$ , it is the most abundant and natural renewable polymer on earth. It is found to have high stiffness, and its high strength biocompatibility could be used in many different products to make cellulose used for numerous applications such as drug barriers, pharmaceutical formulations and more. Cellulose is a polymer that consists of repeated linear  $\beta(1-4)$  linked anhydro-D-glucose units that are called cellobioses. Each glucose unit is composed of three hydroxyl groups connected to the ring.

The parallel straight cellulose chains that are present in bundles are called microfibrils. The formation is due to plant cell processes and the microfibrils that are wood based fibers that are made of bundles of cellulose chains. There are intermolecular hydrogen bonds with each individual chain between the ring oxygen and c-3 hydroxyl group, and between the c-2 and c-6 hydroxyl groups. The cellulose chains are often tightly packed together forming the microfibrillar units (Klemm et al., 2005).

Wood fibers are primarily composed of lignin, cellulose, and hemicelluloses (Klemm et al., 2005). The lignin and hemicellulose act as adhesives which bind wood fibers together. Hemicellulose is present within wood fibers in order to provide the necessary support to maintain the wood fibers' natural structure. The dimensions of wood fibers vary among plant type. However, the standard model for wood fiber consists of a middle lamella, primary wall, an outer, middle, and an inner layer of the secondary wall,

as well as the warty layer (Gardner, 1974). The dispersion of lignin, cellulose, and hemicellulose is not constant within the cell walls of the hardwoods and softwoods (Wielen, 2004). The mechanical interlocking, electrostatic, and diffusion which are theorized to occur within wood fibers may potentially explain why adhesion is promoted among the fibers (Higuchi, 1990).

#### **1.4 Cellulose Nanofibers (CNF) and their Production**

Three methods to produce CNF are bacterial cultures, chemical methods, and mechanical methods. Some methods reported involve chemical or enzyme pre-treatment followed by mechanical treatment, but these will be considered mechanical methods here.

Bacterial cellulose is an attractive natural nanomaterial produced by various strains of acetobacterial species which are able to produce cellulose in large scale in culture medium containing carbon and nitrogen sources in either stagnant or disturbed surroundings (Hon & Shiraishi, 2000). Bacterial cellulose can form a group of ribbon-shaped cellulose fibers that is less than 100 nm in length and less than 5 nm in diameter (Gardner et al., 2008). This material has unique structural applications and properties that are different from the wood cellulose such as high purity, a high degree of polymerization, high crystallinity, high water content, and high mechanical stability (Barud et al., 2007)

The chemical method requires sulfuric acid hydrolysis to break down amorphous cellulose regions to leave crystalline cellulose with uniform dimensions. This form of converting wood pulp into nanoscale fibers is commonly referred to as cellulose nanocrystals (CNC) or simply called nano-crystalline cellulose (NCC). Because of its nanoscale, it can also be used as a reinforcing component in the high performance

nanocomposites. This simple chemical modification on the NCC surface can improve its dispersability in different solvents and expand its utilization in nano-related applications, such as drug production, protein immobilisation, and inorganic reaction template. These review paper provides an overview on this emerging nanomaterial, focusing on the surface modification, properties, and applications of NCC (Klemm et al., 2009);

The first successful mechanical production of nanometer scale cellulose was in the 1980's when a research group passed a wood pulp suspension several times through a homogenizer, resulting in a gel-like suspension of highly fibrillated cellulose that was named microfibrillated cellulose (MFC) (Turbak et al., 1983). This process involved forcing the material through a small capillary to break apart fibers. This requires high pressure allowing the wood fibers to break down from a dimension of 30  $\mu\text{m}$  into dimensions of 20-50 nm in diameter. Other mechanical methods have been reported such as microfluidization, micro-grinding, refiners, and cryocrushing. Today, the nanoscale material generated through mechanical process is often called nanofibrillated cellulose (NFC) or cellulose nanofibrils (CNF). (Revol et al., 1992; Turbak et al., 1983). The standard and nomenclature of the suspension are currently under development. The advantages of mechanical methods are high yield, no chemical costs and no chemical disposal costs. The disadvantage of the mechanical methods is non-uniform fibers that are not well dispersed.

Other studies have been focused on many aspects of CNF production. For example chemical pretreatment for reducing energy consumption, such as enzymatic hydrolysis (Henriksson et al., 2007), and TEMPO-mediated oxidation (Saito et al., 2007).

This suspension was obtained around 3.5% solid and the solid was increase up to 10.5% by using the simple filtration process. Some trails were filled with 3.5 and 10.5% solids of CNF that placed under the frozen process. The wet sample undergoes unto the low temperature process to form a foam material as the final product. Once the foam is received in a conversion of it to a powder form by using the blending process and the laboratory mill was used to obtain a coarse material of grill of 0.5 mm in diameter. A ball mill was activated to make this material the finest of it level by allowing to ball mill for a period of four days before we can obtain a very tiny fine length in diameter. This process is very useful to make the coarse material to a smaller particle size of the final product that was considered to measure the particle size distribution.

## **1.5 Thesis Format**

This thesis is written as separate publications or potential publications. Therefore, some of the background and literature review is repeated in the chapters. Chapter 2 contains details of the rheology of CNF and will be part of a paper that is planned to be submitted to the journal Applied Rheology. Chapter 3 reports the coat weight of CNF on papers as a function of speed, solids and nip loading: this chapter was published as a proceeding to the technical association of pulp and paper (TAPPI) Papercon conference. Chapter 4 discusses the properties of CNF coated papers; this work is part of a publication at the TAPPI Nanotechnology conference in June 2014. Chapter 5 presents the rheology of coatings containing CNF and starch and was presented at the fall meeting of the Society of Rheology meeting in October, 2013. Chapter 6 summaries the results of adding CNF to a paper coating formulation: these results were published as a conference

proceeding at the TAPPI Papercon conference in 2014. Chapter 7 contains the suggestions for future work.

## **1.6 Summary**

CNF is an innovative material that has become of high interest in recent years. While most of the research has focused on methods to produce and characterize CNF, only limited publications deal with the applications of CNF into products. The key technical challenges are linked to the change in rheology of these coatings and the relationship between the rheology and the coating process. The work proposed for this dissertation will improve our understanding of this process and document the final properties of paper that have been coated with these materials.

## CHAPTER 2

### RHEOLOGY OF CELLULOSE NANOFIBERS (CNF) SUSPENSIONS

#### 2.1 Abstract

Cellulose Nanofibers (CNF) are materials that can be obtained by the mechanical breakdown of natural fibers. These materials have the potential to be produced at low cost in paper mills and provide novel properties to paper, paper coatings, paints, or other products. However, suspensions of these materials may have a complex rheology even at low solids. To be able to coat, pump, or mix CNF at moderate solids, it is critical to understand the rheology of these suspensions and how they flow in process equipment. No other reports in literature discuss CNF rheology at moderate solids.

The rheological properties of CNF were characterized with parallel-disk geometry in a controlled stress rheometer. The solids of the material were changed by a filtration and evaporation process in the range of 3.5 to 10.5% by weight. CNF was found to be a highly shear thinning material with a power law index of around 0.1. Oscillatory tests provided consistent results and showed a linear viscoelastic region at low strains. The complex viscosity, the storage modulus, and the yield stress were determined for the range of solids.

## 2.2 Introduction

Interest is increasing with regard to products made from renewable resources that have low environmental impact and minimal safety risks. Cellulose nanofibers (CNF) are biodegradable, natural, and renewable resources that are made from wood. It is expected that CNF can be produced at a low cost in paper mills (Spence et al., 2011). In the paper industry, CNF has gained attention due to a number of potential applications. A number of recent journal review articles describe various aspects of the production and use of these materials (Moon et al., 2011; Eichorn et al. 2010; Klemm et al., 2006; Hubbe et al., 2008; Sairo et al., 2010). Because of recent advances, the nomenclature is not fully settled: CNF is also referenced in the literature as microfibrillated cellulose (MFC) and nanofibrillated cellulose (NFC).

To use CNF in products, the rheology of CNF suspensions is important. At even low solids, suspensions of CNF exhibit complex behavior. To be able to design and operate pumps, mixing systems, and coaters, the rheology of CNF suspensions is important. High solids suspensions are also important to characterize because handling CNF at high solids leads to less water removal in the production of the final product.

The steady shear viscosities for different solid contents as a function of shear rate were investigated by (Pääkkö et al., 2007; Haavisto et al., 2010; Karppinen et al. 2012; Hentze, 2010). All suspensions showed a large decrease in viscosity with an increase in shear rate. The dynamic rheological properties were studied as well and it has been found that the storage and loss moduli were independent of the angular frequency for the 0.125 – 5.9% solids of CNF. The storage modulus values are quite high even at low concentration (100,000 Pa at 3% solid). The results showed that CNF is highly shear

thinning and this behavior could be useful in many coating applications (Siqueira et al., 2009).

In another study, the high elastic modulus was found to be due to the long fibrils, which form a naturally knotted network structure (Missoum et al., 2010). Even at the low solids of 3%, the storage moduli were almost ten times higher than the loss moduli. These results confirm that even at the lowest concentration, the CNF suspensions form a network.

Table 2.1 below is the summary of different groups and their contribution to the literature. In all published reports, the suspensions showed a large decrease in viscosity with an increasing shear rate or shear thinning behavior. An exact explanation for this phenomenon is not clear, but it could be due to the fact that the packing aggregation limits the formation and the shear seems to break down the fiber network (Missoum et al., 2010; Hentze, 2010).

Haavisto et al. 2010 conducted a study of CNF that involved the steady shear viscosity, the oscillatory shear tests. The concentrations they used were as low as 0.3-1.5% solids. The past measurement of this material was mostly investigated at low concentrations.

The additional studies on MFC have confirmed their study (Hentze, 2010). They conducted a detailed study of MFC water dispersion at various concentrations (1–4%) and different temperatures (25, 60°C). As in the other studies, this group emphasized the steady shear rate-viscosity hysteresis loop, and measured the MFC network-forming capacity in slow dynamics studies. In addition, they investigated measurements obtained at high shear rates (above 100,000 s<sup>-1</sup>), which revealed a dilatant behavior of MFC

suspensions. According to their results, a 1% MFC water dispersion cannot be used for high shear coating applications (Missoum et al., 2010).

More recently some work has been performed and published on the rheological behavior of MFC (Karppinen et al., 2012). To further understand and characterize the steady shear viscosity and oscillatory shear were considered to analyze the flow properties of this suspension. In this work, the starting material was a bleached kraft birch pulp that was prepared by mechanical disintegration. This material was obtained from UPM- Kymmene Corporation and the pulp was changed to its sodium form and treated with deionized water that followed the procedure introduced by Swerin et al. The dynamic viscosity of the suspension showed shear thinning behavior even at low solid contents of the suspension (Karppinen et al., 2012). The shear rate was measured at the interval of  $(0.01-100 \text{ s}^{-1})$  and the results that were obtained are summarized in Table 2.1.

Table 2-1 Solids of CNF suspension on shear viscosity for different materials

Authors	Sources	Range of solids (%)	Range of viscosities (Pas)
Pääkkö et al	Bleached sulphite pulp	0.25-5.9	1.5-20000
Haavisto	Purified wood pulp	0.3-1.5	0.095-100
Karppinen	Birch pulp	0.1-2	1.5-3500
Hentze	wood pulp	1-4	35-4000
Marco	Bleached sulphate pulp	1-4	0.09-600

While those references above have some limited data, to be economical for some coating applications, the rheology at higher solids is needed. In addition, these studies

had a limited number of rheological tests. In this dissertation, higher solids levels are of interest as well as a wider range of rheological tests.

The rheology of nanocrystalline cellulose (NCC) has also been reported in the literature. Hatzikiriakos et al., (2012) give the most recent investigation on the viscosity of NCC suspension as function of shear rate and the solids concentrations and viscosity ranges are summarized in Table 2.2 with shear rate of 0.1 to 100 s<sup>-1</sup>. The concentrations were varied from 1 to 7% solids. The suspension exhibited the shear thinning behavior for all solid contents. However, after the sonication of NCC suspensions at 1000 J/g of NCC for the same solid levels, a decrease in viscosity by orders 2-3 of magnitude for all the solids was observed (Hatzikiriakos et al., 2012). The viscosity of NCC is lower than CNF at the same solids level by a factor of 100.

Table 2-2 Effect of solid contents on shear viscosity for NCC.

Solids (%)	Range of viscosity (Pas)
1	0.2-0.0045
2	0.48-0.015
3	2.1-0.04
4	23-0.087
5	170-0.16
7	2250-0.35

In this work, the rheology of NFC suspensions is characterized by a range of test methods at solids levels of up to 10.5% by weight. Steady shear viscosity, storage and loss moduli, and yield stress are reported. Results are compared to others in the literature.

### 2.3 Experimental Methods

The CNF used in this experiment was produced by the University of Maine Process Development Center. The sample was prepared mechanically by using a pilot scale refiner to break down the wood fibers. The wood fibers were a bleached softwood Kraft pulp. The suspensions were obtained at around 3.5% solid. The solid was increased up to 10.5% by using the filtration process. Filtration was done with standard laboratory equipment using a vacuum and standard filter paper (1003-150, Whatman).

The rheology of the CNF suspensions was measured by using a controlled stress rheometer (Bohlin CVO). Steady shear and oscillatory shear tests were used to characterize the flow properties. The parallel disk geometry was used to measure the steady shear and the oscillatory shear tests. The plate had a 40 mm radius for steady shear measurements, the stress was controlled in a ramped pattern and the rotation rate is recorded. For oscillatory tests, the upper plate was used to cause the motion sinusoidally in the  $\theta$ -direction with the frequency and the angular amplitude  $\theta_0$ , and the time dependent torque on the fixed, and lower the plate measurement. The torque measurements are used to calculate the storage and loss moduli. Enough materials were added to the bottom plate and the excess material was trimmed away after the gap was set. The steady shear was performed at 25°C and different gap sets of 800, 1000 and 1500  $\mu\text{m}$  to determine the consistency of the method used in this experiment. The shear rate was measured using a 30 second delay time with a 10 second integration time. Early tests with the cone and plate geometry showed poor results because the sample would eject from the gap even at moderate shear rates.

For the oscillatory tests, a shear stress ramp was performed to find the linear viscoelastic region that was less than 0.1 units of strain. This was followed by a frequency sweep, with a range of 0.01 to 30 Hz at a strain value of 0.06.

In addition, to measure the yield stress of CNF at low solids. A vane geometry that contains a baffle housing was designed in order to eliminate the slip at wall when measure the yield with the regular geometry.

## **2.4 Results and Discussion**

In order to check the consistency of the viscometric tests for CNF, an initial test was done using three different gaps; the results are shown in Figure 2.1. In figure 2.3 displays the steady shear viscosity and shear stress as a function of shear rate for 3.5% solids of CNF suspension for three different gap heights using the parallel disk geometry. The steady shear viscosity was found to be the same for different gaps, and the shear stress was observed to be an increasing function of shear rate. Each point is an average of three tests. If there was a slip at the surface or some other artifact, the viscosity values at different gaps would be different.

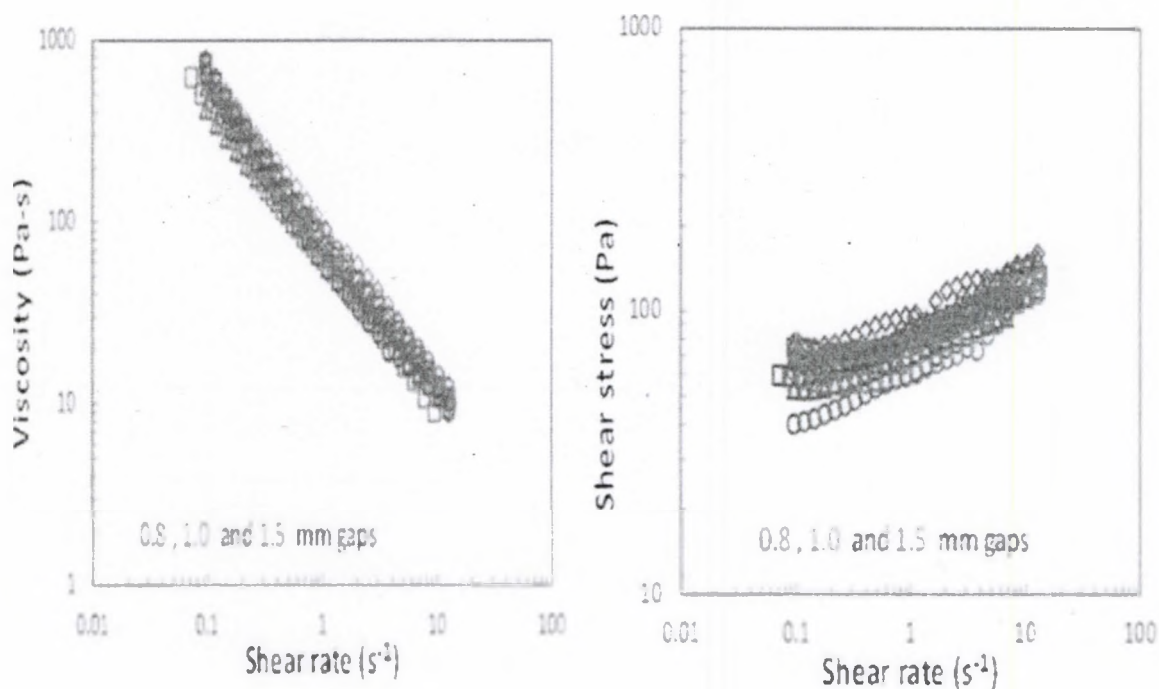


Figure 2-1 Steady shear viscosity and shear stress as a function of shear rate

An attempt was made to measure the rheology of this CNF suspension by using the cone and plate geometry. However, with these results we observed a non physical behavior of a decreasing shear stress with increasing shear rates: this was caused by the ejection of the material from the gap at shear rates around  $1\text{ s}^{-1}$ .

The steady shear viscosities of CNF suspensions at different solids as a function of shear rate with the parallel-disk geometries are given in Figure 2.2. The suspensions for all solids show shear thinning behavior. As expected, the viscosities increase as solids increase. The viscosity results show consistency for all solid levels and follow a shear thinning curve and a consistent pattern. The slopes of the lines are nearly parallel indicating that the power-law exponents are similar for different solids. Note that for the 3.5% solids, the viscosity at a shear rate of  $1\text{ s}^{-1}$  shear rate is 100 Pa-s.

The results in Fig. 2.2 were repeated, two years after they were obtained with fibers produced in a similar manner. Each set is an average of three runs in the parallel-disk geometry with 1mm gap. The results are quite similar. The data for 5.5% solids is around 20% higher. The data for the 2.5% case are 15% higher. The power law indexes for 3.5 and 10.5% are 0.15 and 0.09 for the old data and 0.12 and 0.06 for the recent data.

The maximum shear rate that could be obtained for the results was around 100 1/s. The reason for this is that material is ejected from the gap for shear rates larger than 100 1/s, resulting in values that are in error. This ejection is not from centrifugal forces, but seems to be caused by the formation of hard flocks or clumps of fibers that roll out from the gap. This mechanism is not well understood and is similar to what happens for the cone and plate geometry.

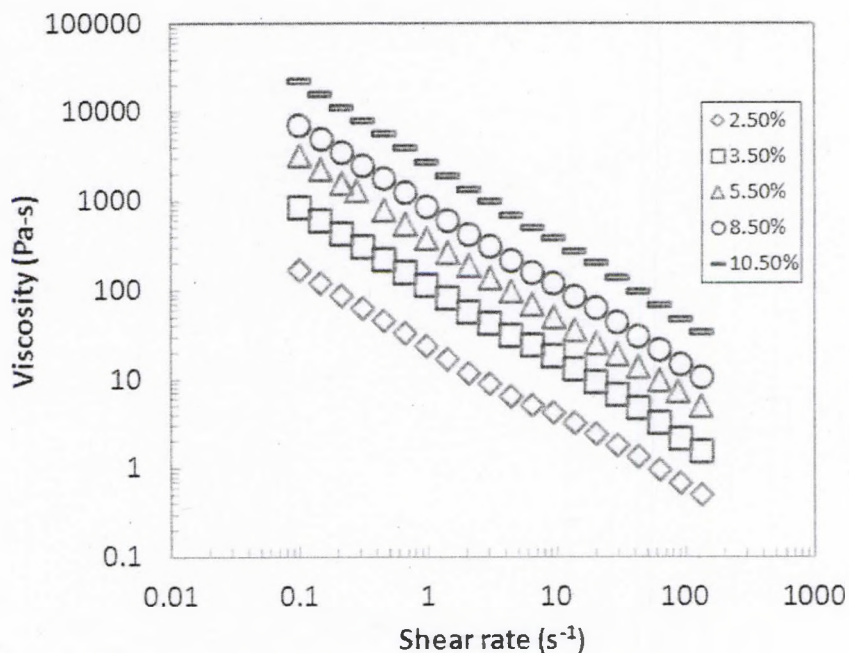


Figure 2-2 Steady shear viscosity as a function of shear rate for different solids of CNF

The results with concentric cylinder geometry are compared to the parallel plate geometry in Figure 2.3. The letter (PP) denotes the parallel plate geometry measurement and (CC) denotes the concentric cylinder geometry measurement. Each set is an average of three separate repeated trials. The shear rates for the concentric cylinder geometry are repeatable, even to values up to 1000 s<sup>-1</sup>. The results show excellent agreement between the two geometries. However, at solid higher 5% the torque measurement for the concentric cylinder is beyond the limits of the device.

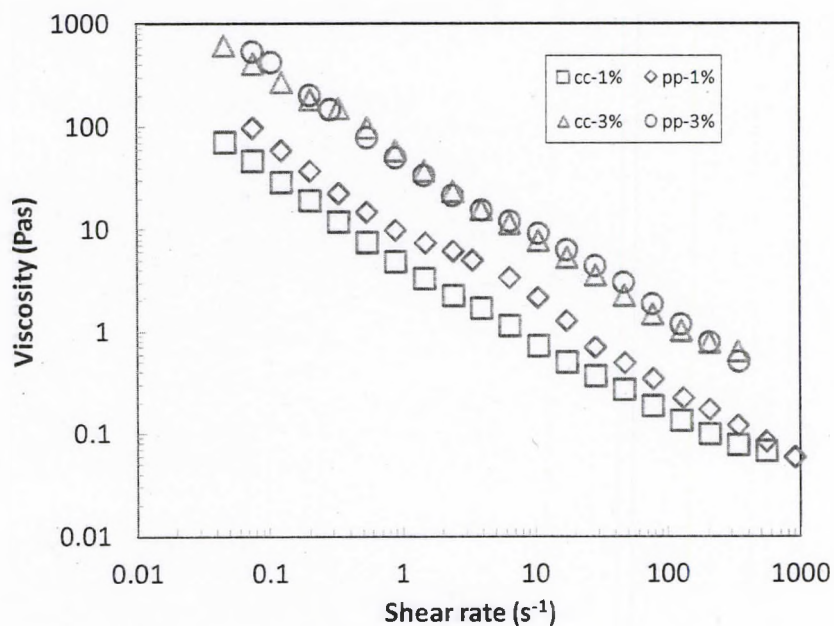


Figure 2-3 Comparison of geometry measurements for the steady shear viscosity

The power law model is an empirical expression to describe the shear thinning of fluids expression is

$$\eta = m \gamma^{n-1} \quad (2.1)$$

Where  $\eta$  is the viscosity,  $\gamma$  is the shear rate;  $m$  and  $n$  are the parameter index and the power law exponent, respectively. When  $n = 0$  this indicates a Newtonian fluid. When  $n$  is between 0 and 1.0, this is a shear thinning behavior. For  $n > 1$ , the fluid is shear thickening. The results for  $n$  and  $m$  at different solids are displayed in the Figures 2.4 and 2.5, comparing the early sample of the material to a recent sample. The power law index ( $n$ ) decreases to around 0.1 as the solids increases. The data point for the old sample at 2.5% solids may just be caused by some early issue with sample loading. Both cases showed shear thinning behavior which may indicate the strong gelation properties of CNF pure water base suspension. We also observe the same behavior for the parameters ( $m$ ) for the CNF in water base suspension

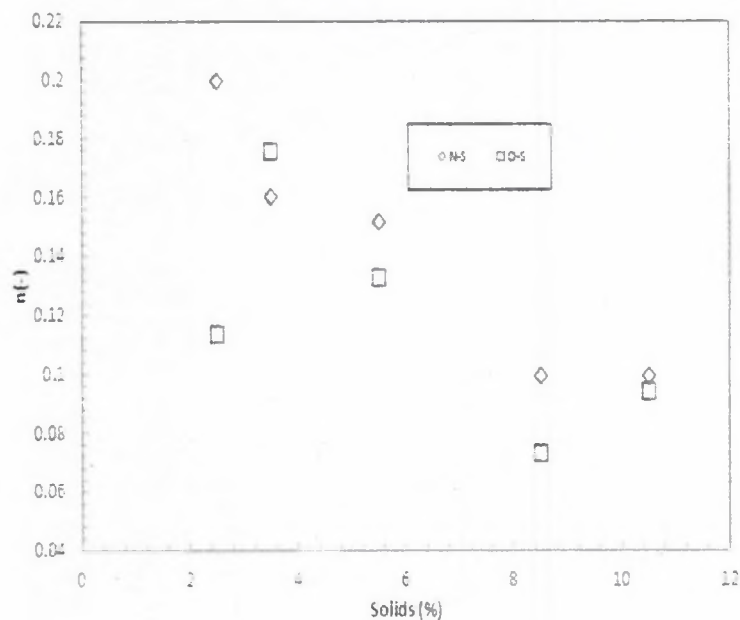


Figure 2-4 Power law index  $n$  as a function of solids for old sample (OS) and new sample (NS)

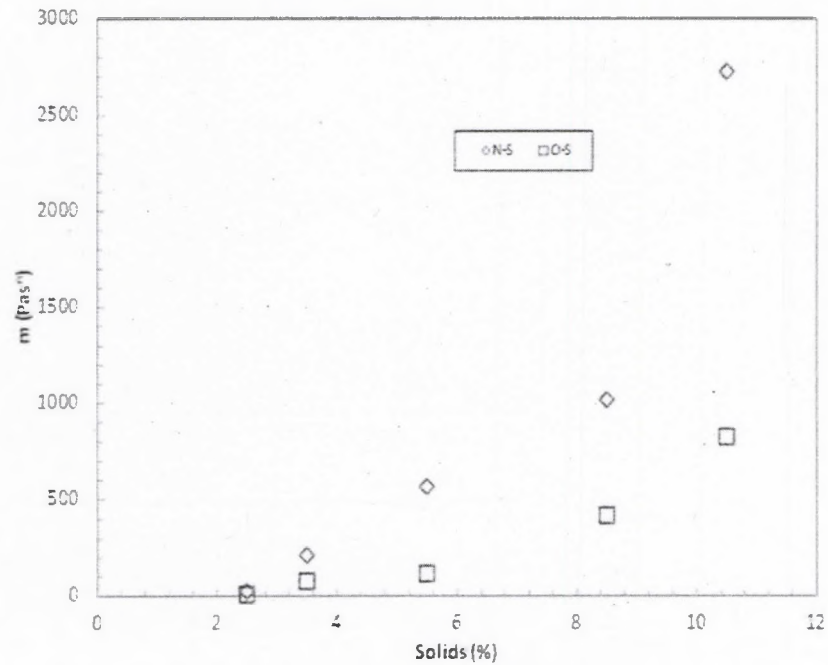


Figure 2-5 Power law parameter  $m$  as a function of solids for old sample (OS) and new sample (NS)

Figure 2.6 and 2.7 below displayed the results of the slope  $n$  and power law parameter  $m$  for different solids of CNF suspensions. The material produced at the University of Maine with the refiner method continues the trend of the Haavisto et al., data. in a reasonable way, even though the fibers were produced in different manners.

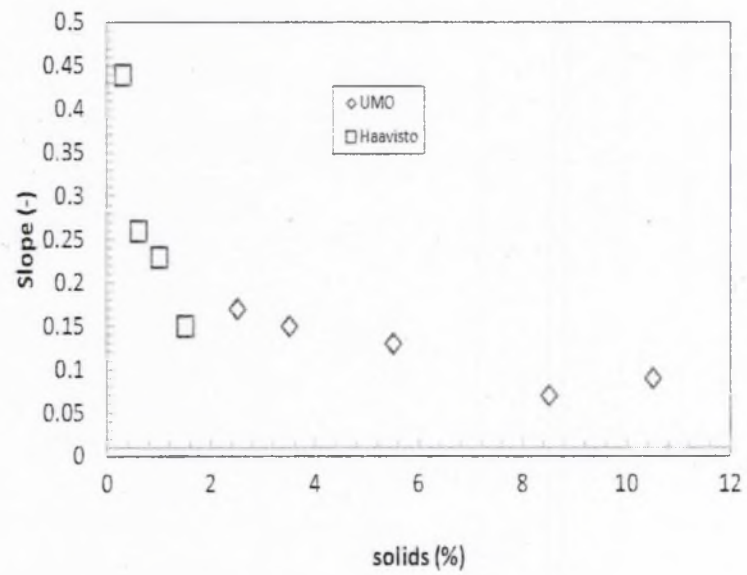


Figure 2-6 Comparison of results with Haavisto et al. (2011) data for power law index

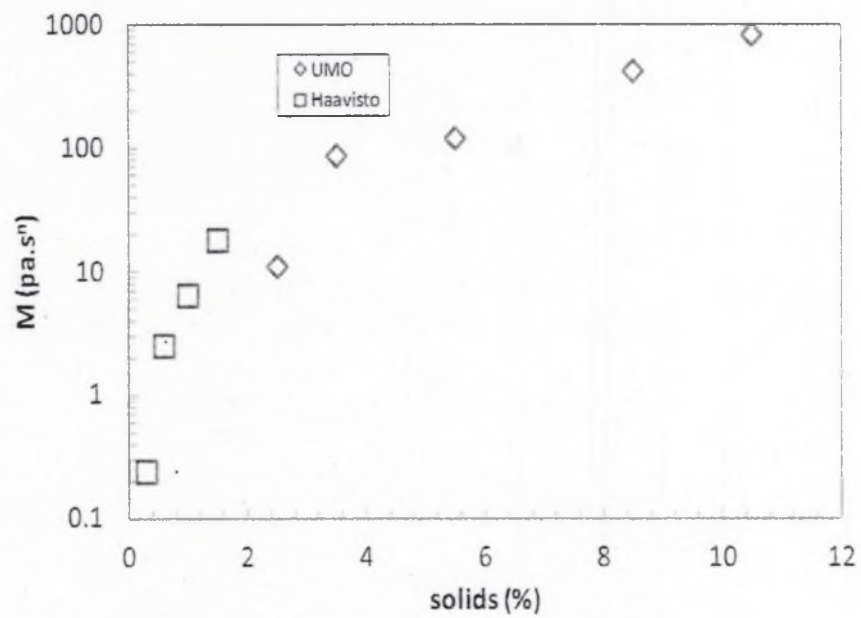


Figure 2-7 Comparison of our results with Haavisto et al data on power law parameter  $m$  of CNF (2011)

The yield stress is considered as stress needed to begin flow of a fluid and would be important in the design of a coating system. One way to obtain an effective yield stress for any substance is to plot the elastic stress, which is the storage modulus times the strain, as a function of strain (Walls et al., 2003). Figure 2.5 shows the results for different solid levels. The peak value of each curve is taken as the effective yield stress. As expected for all solids, the yield stress increases along with the solids of the suspension. Using this method, the yield stress of the 3.5 and 10.5% solids cases are 85 and 2500 Pa, respectively.

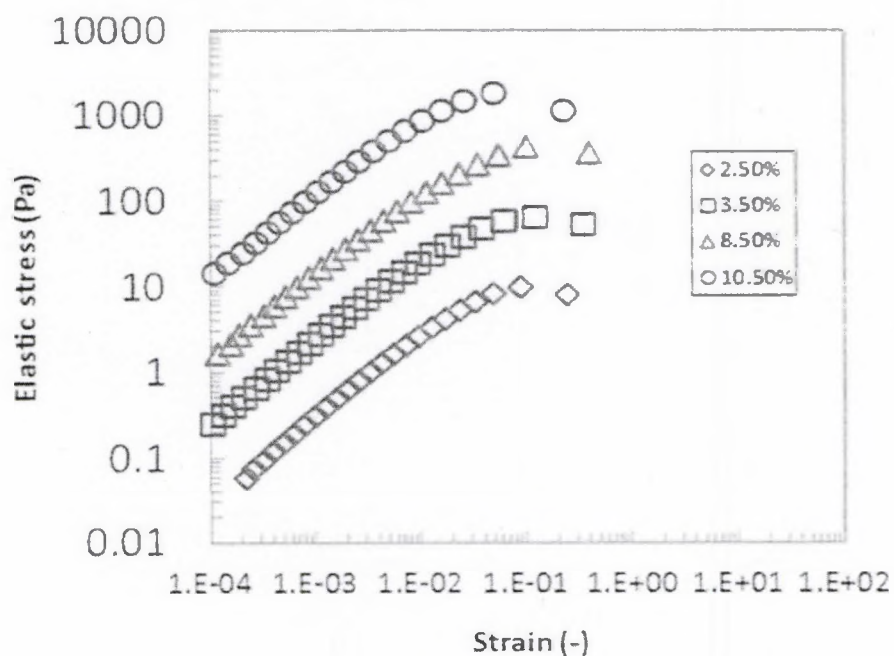


Figure 2-8 Elastic stress as a function of strain for various solids of CNF

Figure 2.6 is an example of the results obtained with the vane geometry. As the vane is set in motion at a constant speed it is experienced a torque by the shaft which is the sum up of the shear stress along the side of the sheared cylinder. Torque is converted

to stress by calibration with Newtonian fluids. As expected for all solid levels, the yield stress increases along with the solid contents of the cellulose nanofibers suspensions. Using this method, the yield stress of the 1 to 3.5% solids cases are 4 to 120 Pa, respectively. The value of 120 Pa is higher than the value obtained with the elastic stress method above 85 Pa for the 3.5% solids, but it is in the same range of magnitude. The difference may come from slip of material at the plate surface, but the values are at least in the same order of magnitude. The rheometer was not able to use the vane geometry for values over 3.5% solids because of the stress limitation. Therefore, the oscillatory method is the only method possible for solids over 3.5%.

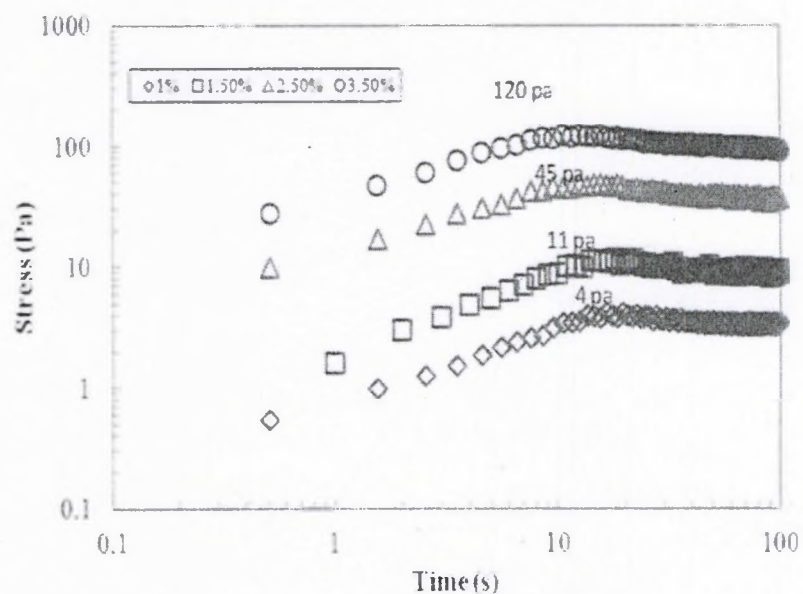


Figure 2-9 Stress as a function of time used to determine the yield stress of CNF for various solids

Storage and loss moduli obtained from amplitude sweep for different solids of CNF are shown in Figures 2.10 and 2.11. For the amplitude sweep test, the frequency was set at a constant 1 Hz while the strain was varied from 0.1% to 100%. During the test and at low strain the substance exhibited a linear viscoelastic response for all solids of CNF. After the linear viscoelastic region, the storage modulus decreases with increases of strain for all the solid contents. The storage modulus is around one order of magnitude larger than loss modulus for CNF water based suspension.

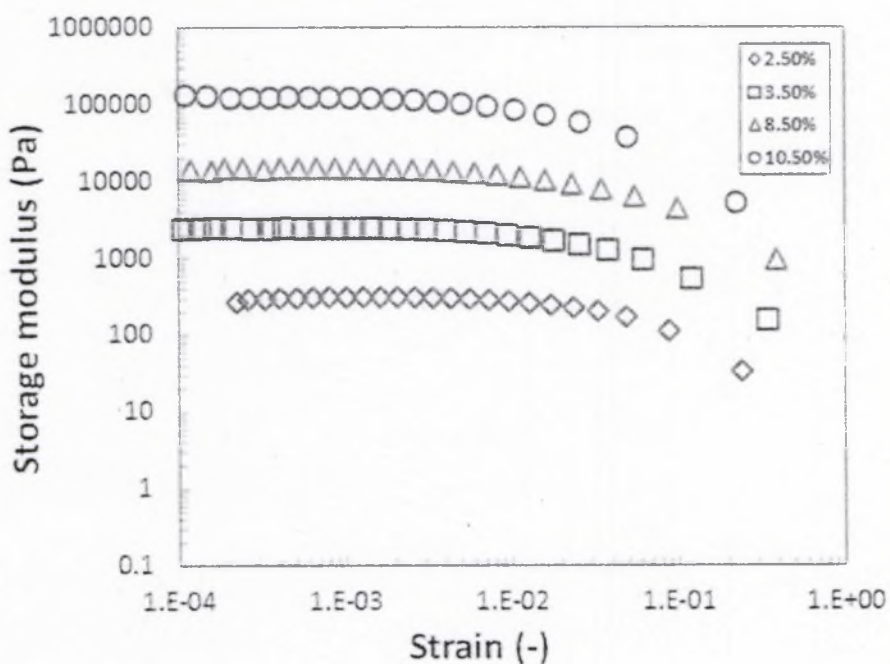


Figure 2-10 Storage modulus as a function of strain for various solid levels of CNF

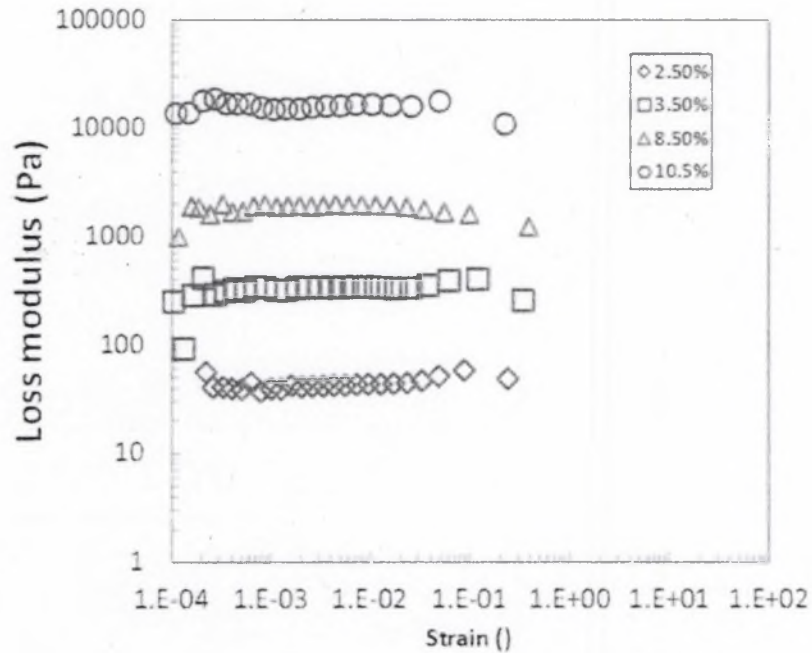


Figure 2-11 Loss modulus of CNF as a function of strain for various solid levels

The complex viscosity is the mathematical representation of a viscosity as the sum of a real part and an imaginary part. The real part is usually called dynamic viscosity, and the imaginary part is related to the real of the complex modulus or it is the ratio of complex modulus by the frequency. This expression can be described in the following equation.

$$\eta^* = \frac{G^*}{f} \quad (2.2)$$

Where  $\eta^*$  is the complex viscosity (Pas),  $G^*$  is the complex modulus (Pa) which is the ration of stress divided by strain and strain is the deformation or movement that occurs in a material. Expressed as the amount of movement that occurs in a given sample dimension this makes it dimensionless and  $f$  is the hertz or radian/s (Barnes et al, 1989).

The complex viscosity is obtained from frequency sweep tests and helps to analyze the rheological properties of the suspension. Complex viscosity should characterize the resistance to deformation for small deformations. Figure 2.12 shows the complex viscosity as a function of angular frequency for different solids. Each set is an average of three runs in the parallel-disk geometry with 1mm gap.

The complex viscosity decreases as the angular frequency increases, similar to the behavior of the steady shear viscosity. This indicates that CNF suspensions have a yield stress in shear corresponding to the plateau value of the storage modulus ( $G'$ ) for all solids. The change in slope of the values at higher frequencies may be an indicator of material ejection from the gap or some other artifact.

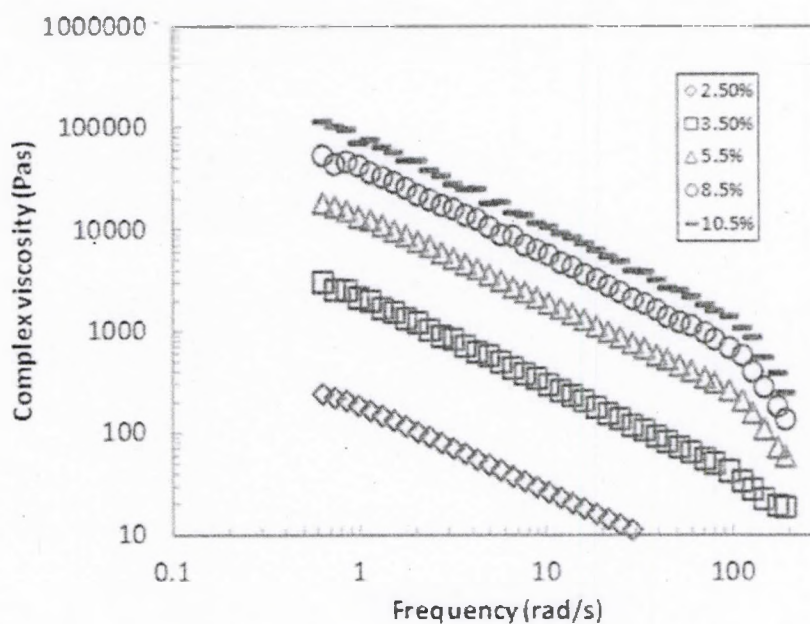


Figure 2-12 Complex viscosity as a function of shear rate for different solids of CNF.

The empirical expression Cox-Merz rule states that complex viscosity versus the angular frequency obtained from small-amplitude oscillatory shear flow should be similar

to the steady shear viscosity against the shear rate (Gleissle et al., 2003). Although there is no fundamental explanation for such a relationship, it is widely accepted and used for isotropic polymeric solutions and polymer melts. Figure 2.13 indicates that the Cox-Merz rule does not hold for this system for 3.5 and 10.5% solids. The complex viscosity is 50-100 times larger in magnitude than the steady shear viscosity data. The slopes of the lines are similar for the different solid levels. Other investigations (Doraiswamy et al., 1991) have shown that the complex viscosity is a factor of two larger than the steady shear viscosity for a colloidal suspension. Here, the complex viscosity at certain angular frequencies is over 100 times larger than the steady shear viscosity at the equivalent shear rate-frequency. In figure 2.13, the complex viscosity (CV) and the steady shear viscosity (V). Each line is an average of three repeats.

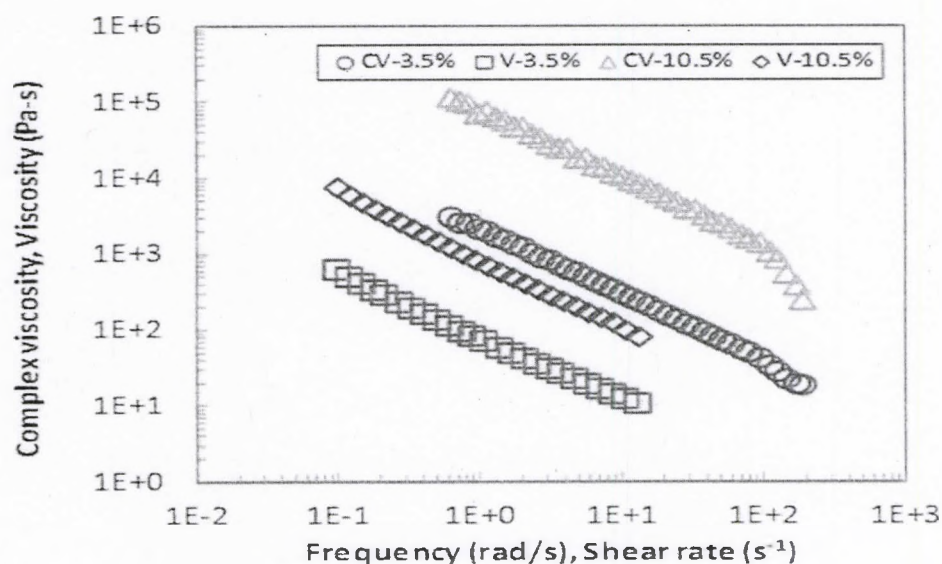


Figure 2-13 Complex viscosity and steady viscosity for different solids

All the past results obtained on steady shear viscosities and the oscillatory shear tests were studied at moderate or low concentration of CNF and they were made by using

different treatments. However, our current work here focused on the higher concentration of CNF. The different results obtained on the steady shear viscosity as a function of shear rates as indicated Table 1.1. Figure 2.14 compares the steady shear viscosity of CNF from two different studies. The “P” corresponds for Pääkkö et al., 2007 data obtained for the steady shear viscosity for different solids and UMO correspond to our present results. At 3% and 3.5% solids, the results are quite close. However, at 5.9% solids, Pääkkö results are more than an order of magnitude higher in viscosity than our results at 5.5% solids. The same conclusion was obtained for the oscillatory shear. The difference in the behavior may come from the different methods to generate the CNF, here in our case the material was generated by refiner, but in the other case with a fine grinder.

Material produced at the University of Maine with the refiner was sent to a research group at VTT in Finland. This group has published results on flocculation of CNF and rheology as determined with a pipe rheometer (Haavisto et al., 2011, and Saarikoki 2012). Results they obtained at lower solids were within 20% of the parallel plate results. A manuscript is in preparation that will combine the results presented here with those from the pipe rheometer to give a comprehensive report on the rheology of CNF suspensions at solids up to 10%.

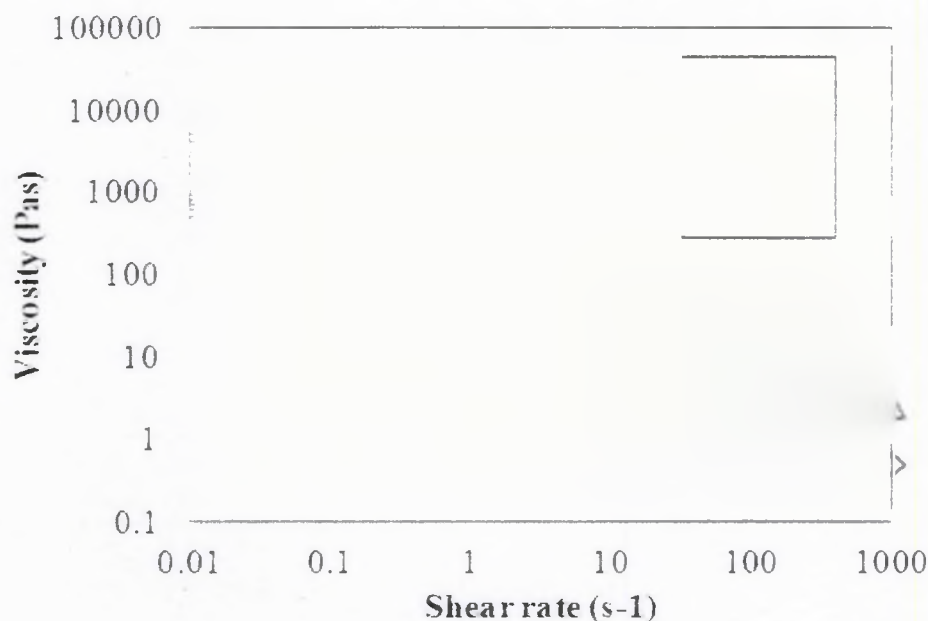


Figure 2-14 Comparison of our results with Pääkkö et al data on viscosity of CNF (2007)

## 2.5 Conclusion

The cone and plate geometry was found to not be useful for characterizing CNF because of sample ejection from the instrument. The reason for this ejection is not clear, but may be related to the generation of flocs in the material during shear. The concentric cylinder geometry results match with the parallel plates, but those results are limited on our device to CNF suspension solid contents less than 5%. The steady state shear rheological results showed that CNF suspension to have a strong shear thinning behavior, and compares with what others have reported at low solids. Oscillatory tests showed that CNF had a significant viscoelastic characteristic response and a large yield stress. The dynamic rheology response showed that the complex viscosity of CNF suspension at certain angular frequencies is much larger in magnitude than the steady shear viscosity at

equivalent shear rates. The past results obtained on steady shear viscosities and the oscillatory shear tests were studied at very low concentration of CNF and they were made by using different treatments. Even at moderate solids their results were shown to be closed and roughly exhibited the same behavior for the steady state shear response.

## CHAPTER 3

### PREDICTION OF COAT WEIGHT OF CNF OBTAINED WITH DIFFERENT COATING METHODS

#### 3.1 Abstract

Cellulose Nanofibers (CNF) and microfibrillated cellulose (MFC) can be obtained by the mechanical breakdown of natural fibers. These materials have the potential to be produced at low cost in paper mills and may give many novel properties to paper, paper coatings, paints, or other products. However, suspensions of these materials have a complex rheology even at low solids. To be able to coat, pump, or mix CNF at moderate solids, it is critical to understand the mechanism of the suspensions when coated on papers and how they flow in process equipment due to rheological influence of these suspensions. Only a limited number of reports have been published in the literature on CNF coated on paper about these suspension.

A laboratory size press device was used to apply CNF to the paper surface at various solids using two different application methods (flooded and metered size press methods). The coat weight of CNF was reported as a function of speed, nip loading and solids. A model was developed to predict the coat weight obtained in the device that accounts for the non-Newtonian aspects of the suspension as well as dewatering effects. The variation in coat weight as a function of speed and nip loading was minimal. While solids of 10.5% gave higher coat weights than solids of 3.5%, the increase is much less than what would be expected for the same volumetric application of the suspension. A pre-metered method of applying CNF using steel and rubber rolls resulted in a non-uniform application from side to side. While glycerin and other Newtonian fluids gave

rise to an even film split, CNF suspensions in the device did not experience a 50-50 film split, but material preferentially followed the steel roll. This behavior may be linked to the rheology of the CNF suspensions. The model under predicted the results but gave the correct order of magnitude. The coat weight was determined by a combination of flow and dewatering in the nip region of the size press.

### **3.2 Introduction**

Nanotechnology has the potential to be utilized by a number of industries due to the development of new methods to characterize and manipulate fine scale material. In the paper industry, nano-scale cellulose fibers have attracted attention due to a number of potential applications; a number of recent journal review articles describe various aspects of the production and use of these materials (Moon et al, 2011; Eichorn et al, 2010; Klemm et al, 2006; Hubbe et al, 2008; Siro et al, 2010). Two key methods are used to produce cellulose nanofibers from wood fibers. Chemical methods use a strong acid to break down amorphous cellulose regions to leave crystalline cellulose with uniform dimensions. This form of fibers is often called nano-crystalline cellulose (NCC). Mechanical methods use a high pressure homogenizers, micro-fluidic cells, refiners or micro-grinders to break up wood fibers to dimensions of 20-50 nm in diameter. The energy requirements and costs are documented in a recent presentation (Spence et al 2010). Originally, the material produced with mechanical methods was called microfibrillated cellulose (MFC) (Turbak et al, 1983), but because of the resulting length scales of recent methods, the material is now usually referred to as cellulose nanofibers (CNF) (Spence et al 2010). Another method using wood fibers is called TEMPO-mediated oxidation; this chemical pretreatment of wood fibers causes the fibers to break

down with simple stirring and produces excellent quality samples composed of stable fibers (Saito et al, 2006) Certain strains of bacteria also produce fine scale cellulose nanofibers (Moon et al, 2011; Siro et al, 2010; Yano et al, 2010).

There has been much attention paid to using this material in plastic composites and other applications (Moon et al, 2011; Eichorn et al, 2010; Klemm et al, 2006; Hubbe et al, 2008; Siro et al, 2010). Recently, a key advance was reported on how to treat the fibers to make them water redispersible (Eyholzer et al, 2010). However, there may be more natural uses of these fibers in the production of paper and packaging materials. Recent work has shown that CNF coated on paper can increase the capture of ink pigments at the top surface which leads to an increase in print density for ink jet and flexographic printing (Hamada et 2010; Luu et al, 2011; Richmond et al, 2011). The use of CNF in the wet-end has also been reported (Torvinen et al, 2011; Morseburg et al, 2009); some strength benefits were reported. CNF coated on a paper surface with a pigment pre-coat has also been shown to increase the stiffness of the sheet (Ridgeway et al, 2011).

A key issue that prevents the immediate use of CNF as a coating or a coating additive is the rheology of CNF suspensions. Even at a solid level of less than 2%, the behavior is non-Newtonian with significant viscosities (Haavisto et al, 2011). If this suspension is added into a coating or coated directly on paper, a large amount of water needs to be removed. Therefore, understanding the rheology of these suspensions and methods on how to apply at moderate solids is critical before economical use of this material is possible. There have been a limited number of reports on the viscosity of CNF suspensions even at low solids (Richmond et al, 2011; Haavisto et al, 2011).

In this work, these suspensions were applied to paper in a laboratory type size press device, laboratory rod coater, cylindrical laboratory coater (CLC). The coat weights obtained for various solids, speeds, and nip pressures were reported. A model was developed to describe the flow field in size press geometry as well as the dewatering of the suspension upon contact with the base paper. The coat weight results were compared with model predictions.

### 3.3 Experimental Methods

Coating of CNF suspension on paper was performed using different approaches (rolling nip device, laboratory rod coater, and cylindrical laboratory coater). The first approach, which is a bench scale rolling nip device is described in detail by Devisetti & Bousfield, 2010 and displayed in figure 3.1. The rolls were computer controlled to rotate at a given speed. Air pressure was used to adjust the nip load by generating a force on the rubber covered roll support that was on a free moving support. Based on the area of the pistons within the air actuator, the nip load was calculated from the pressure applied. A wire wound bar draw downs of the material on the paper often left wire marks, and this approach was abandoned. The paper used in the experiment was bleached wood free paper (Hansol Paper Inc.) with a basis weight around  $86 \text{ g/m}^2$ .

The nip device was operated using two methods. The first method used was to simulate a flooded size press. The paper was inserted in the nip and the air pressure was activated to close the nip and hold the paper in place. To each side of the paper, 20 mL of CNF suspension was added in the nip region, insuring good contact of the suspension with the paper and the roll surfaces as shown in Figure 3.1. The rolls were rotated one

time at a set speed. The paper commonly stuck to the steel roll surface and was peeled away from the surface after coating.

The second method simulated a metered size press. Here, the same amount of material was added to the nip while the nip was kept closed using air pressure. The rolls were rotated at a low speed to distribute the suspension on the roll surfaces. Excess material was squeezed from the edges on both sides of the nip. After about five revolutions, the rolls were stopped, and the speed of application was set. Then the rolls were started and the paper was sent through the nip. Again, the paper often stuck to the steel surface and was peeled from the surface. It should be noted that this method of operation is different from an industrial metered size press. In an industrial unit, the amount of material on each roll is controlled separately, often with a rod metering device working on the roll. In this unit, the material is metered by the rolls pressing against each other. Therefore, some of the results reported in the future may not have implications for industrial situations. Computer controlled rolls rotate a known number of rotations with a set speed. CNF suspensions are put at the nip inlet when the rolls are stationary

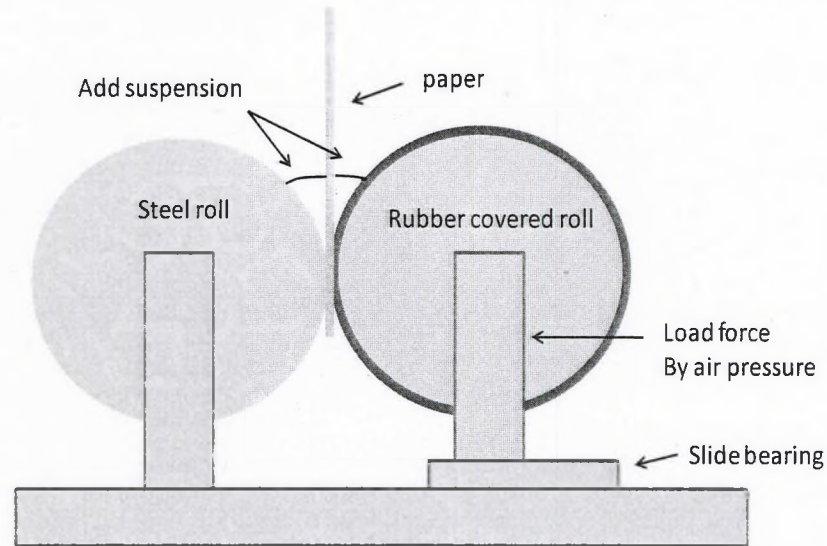


Figure 3-1 Laboratory scale size press device.

The coated paper samples were dried under a heat lamp. Excess material that stuck to the paper was peeled off. The paper was cut to eliminate starting, ending, and side effects. The paper was allowed to equilibrate at 25°C and 50% humidity for 12 hours before measuring coat weight. Each condition was repeated five times. An average and standard deviation were reported.

The process simulation was used as a tool to characterize the coat weight prediction obtained from the amount of CNF transferred when coated onto paper. We considered the flows in the nip of two rotating rolls that were moving in a forward direction. For the purpose of this work, the key concern was the amount of material that passed through this nip for various nip loading conditions, speeds, and rheology. A lot of previous work in this area had dealt with Newtonian fluids (Benjamin et al, 1995). Therefore, CNF suspension was shown to be highly shear thinning in figure 2 (please see chapter 2 and figure 2.2). Therefore, to predict the coat weight, a simulation was performed to describe the flow field in rolling nip geometry for a Carreau model fluid, where the viscosity  $\mu$  was given as

$$\mu = \mu_{\infty} + (\mu_0 - \mu_{\infty}) \frac{1 + (\lambda\dot{\gamma})^2}{2}^{\frac{n-1}{2}} \quad (3.1)$$

Where  $\mu_{\infty}$  and  $\mu_0$  are the high and low shear rate viscosities,  $\lambda$  is a constant, and  $n$  is a power law factor. The inlet and outlet regions were simplified by considering free surfaces and surface tension effects and neglecting any roll deformation, viscoelastic effects, and other phenomena such as cavitation.

A series of experiments were conducted to understand the film split behavior of the suspension and other model fluids. Two tests were conducted. First, CNF suspensions were inserted into the loaded nip and the rolls were turned as before to reach a steady film thickness on the roll surfaces. The rolls were then cleaned with pre-weighed paper towels to characterize the amount of material on the roll surfaces. Second, two sheets of paper were sent through the nip at the same time. The coat weight on each paper surface was measured. Some tests with glycerin were also conducted to understand the behavior of a Newtonian fluid.

The second approach of coating CNF suspension on paper is laboratory rod coater. The laboratory rod coater was used to coat the coatings with CNF. The procedures for this series of coatings are as followed. 1) Set up the gap size according to the dimensions of the rod. 2) Distribute enough material to fill up the gap size. 3) Cut the excess material and peel off from the edges of the coated region and 4) Calender, condition. and weigh the paper before and after to determine the coat weight and the physical properties.

The third approach of coating CNF on paper is the cylindrical laboratory coater (CLC) was used also to coat CNF on paper at a moderate solids. The speed was changed but the blade setting was held constant. This gave a range of coat weights.

### 3.4 Results and Discussion

To further characterize the behavior of the material on the rolls, two sheets of paper were sent through the nip at the same time. It was operated at constant solid 3.5% and nip load 2300 N/m. The coat weight was obtained for each sheet as given in Figure 3.2. When the device is operated as a flooded size press, the coat weight on each paper is similar at high speed but shows a small preference for the steel roll at low speeds.

These two-sided results would not be important for a commercial metered size press unit because the coat weight on each roll surface is controlled separately by a pressure loaded rod in an industrial unit. In this bench scale unit, the amount on the roll surfaces is controlled by a single pressure that presses the rolls together. Excess material finds its way to the sides of the unit. This issue does not allow an equal coating pickup on each side of the paper in the laboratory device.

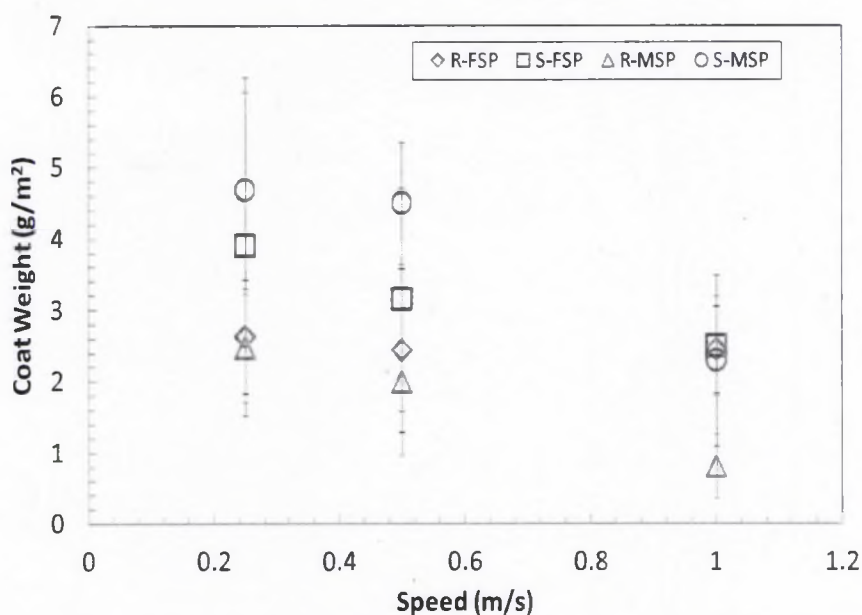


Figure 3-2 Coat weight results for two sheets of paper sent through the nip

Figure 3.3 shows the results for the flooded size press application method. Coat weight is the total coat weight for both sides. The tests were conducted at constant solid (3.5%) for different nip loads of the material. Again, within experimental error the speed of operation had little influence. Within the scatter of the data, it is hard to say if nip load influences the results. In general, an increase in nip load should allow less material to travel through the nip giving a lower coat weight.

Figure 3.4 compares the CNF coat weight as a function of speed for 3.5 and 10.5 % solid cases using the flooded size press method. Coat weight is the sum of coat weights on both sides. Error bars are the standard deviation of five trials. The higher solids content of the suspension does give higher coat weight, except for the low speed case. However, the 10.5% solids case does not coat uniformly for nip loads below 4460 N/m; these results are not recorded, but this result sets a lower limit of the nip pressure that is needed to cause the high solid CNF to flow in a uniform manner.

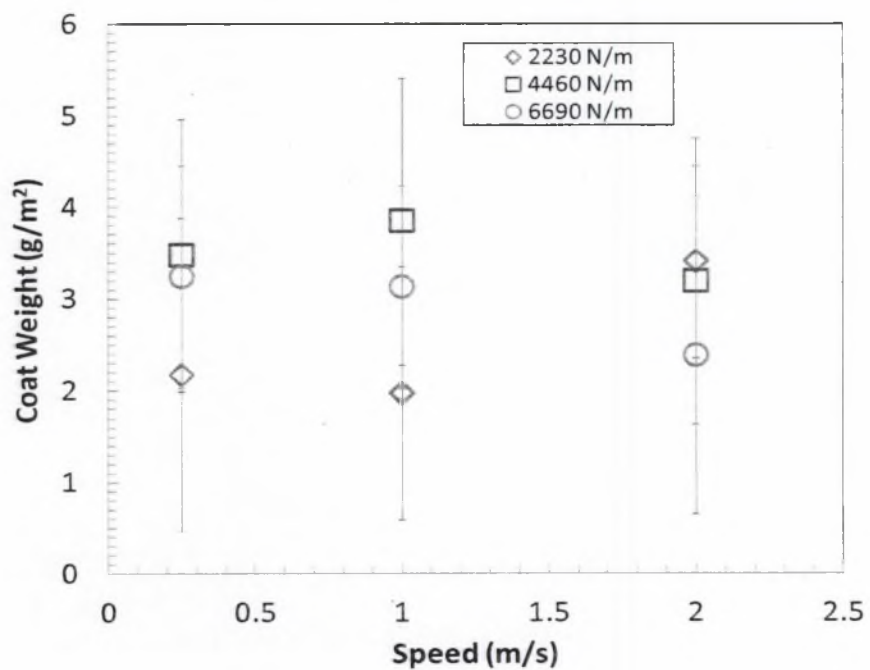


Figure 3-3 Coat weight obtained for 3.5% solid of CNF using the flooded size press method at three nip loads.

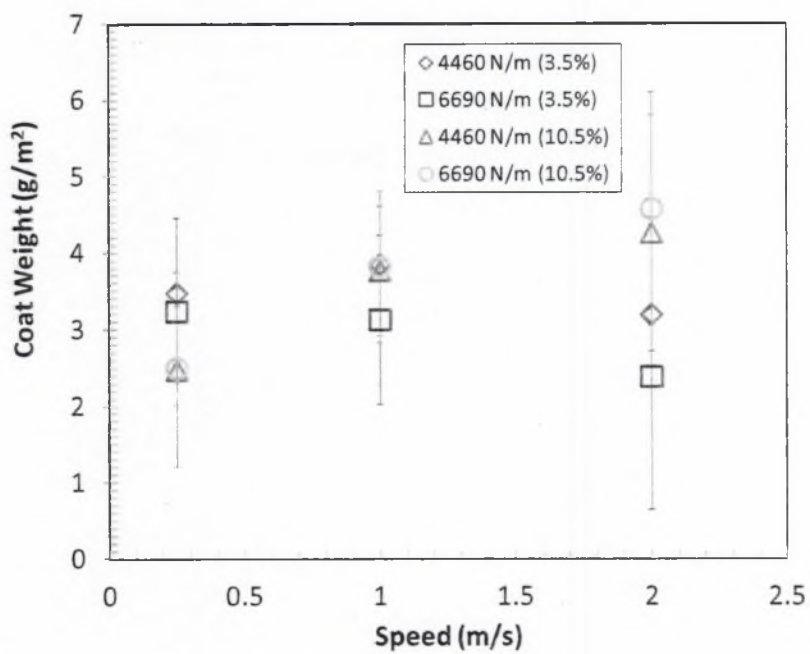


Figure 3-4 Coat weight for different solids and nip loads of CNF

Figure 3.5 shows the coat weight results as a function of nip load for the speed of 0.5 m/s using the metered size press method. Coat weight is the sum of the coat weight of both sides. The tests were conducted with different solid contents of the material. As the nip load increases, the coat weight increases. This increase is the opposite of what would be expected from a pure fluid flow; higher nip pressures should allow less material to pass through the nip.

The increase in coat weight with solids must relate to the pickup mechanism in the nip itself and is related to dewatering. A filtercake of nanofibers may form on the paper surface as the paper passes through the nip. This would limit the dewatering of the CNF suspension in the nip and the pick up in the nip. Therefore, as the solids increase, the dewatering of the CNF suspension in the nip decreases, and the split of the film moves closer to the paper. The net result was a modest increase in coat weight with solids. Other issues may be related to how the paper is pulled off the roll or the way the suspension is distributed, but more tests are needed to understand this transfer better.

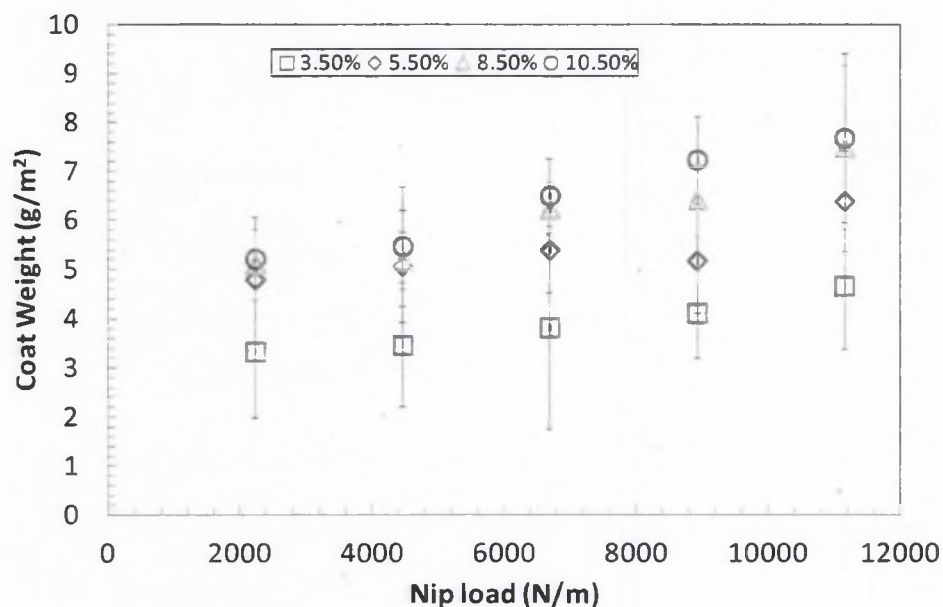


Figure 3-5 Coat weight obtained for different solid levels of CNF at the speed of 0.5 m/s using the metered size press method.

Figure 3.6 reports the behavior of CNF coat weight as a function of number rods for 3.5 and 8.5% solid cases for two different types of paper (copy paper and black construction). The results show that the coat weight increase with the number rods and the 3.5% and 8.5 % solids have similar coat for the regular copy paper. However, the results that the coat weight for black construction paper (BCP) gave a higher coat weight than the regular copy paper (RCP) under the same conduction. This could be because the black construction paper is much is easily to absorb water than regular copy paper. Absorption creates a thick layer of CNF that is not removed by the rod motion.

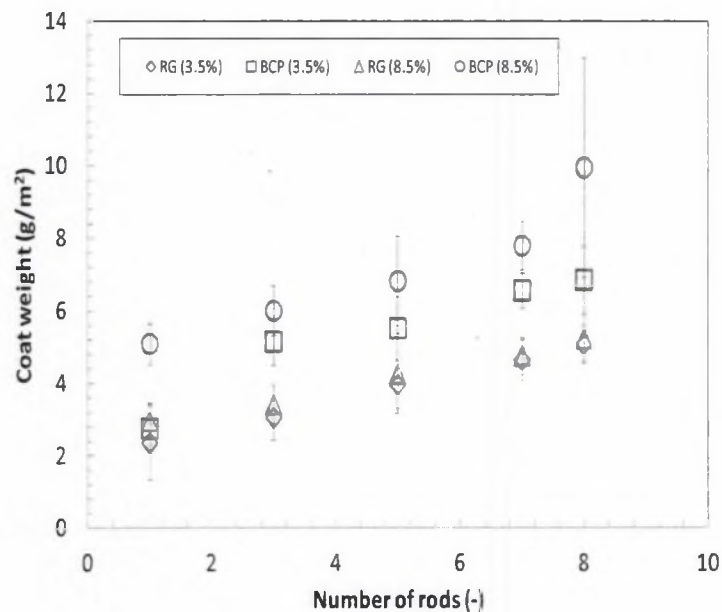


Figure 3-6 Coat weight obtained for 3.5 and 8.5% solids of CNF using the rod draw down method and coated only on side

Figure 3.7 displayed the results that were obtained by coating CNF into three different papers with the laboratory size press method. The symmetry paper represented by the symbol (S), the thermal mechanical pulp (T) and the wood free paper (W). The results showed that the coat weight for wood free paper is much higher than the coat for symmetry and thermal mechanical pulp paper. Figure 3.8 illustrates the coat weight as a function of speeds, and coated on both sides with constant nip lad (2300 N/m). Higher speeds result in a trend of lower coat weights, but the scatters in the data make it difficult to determine firm conclusions.

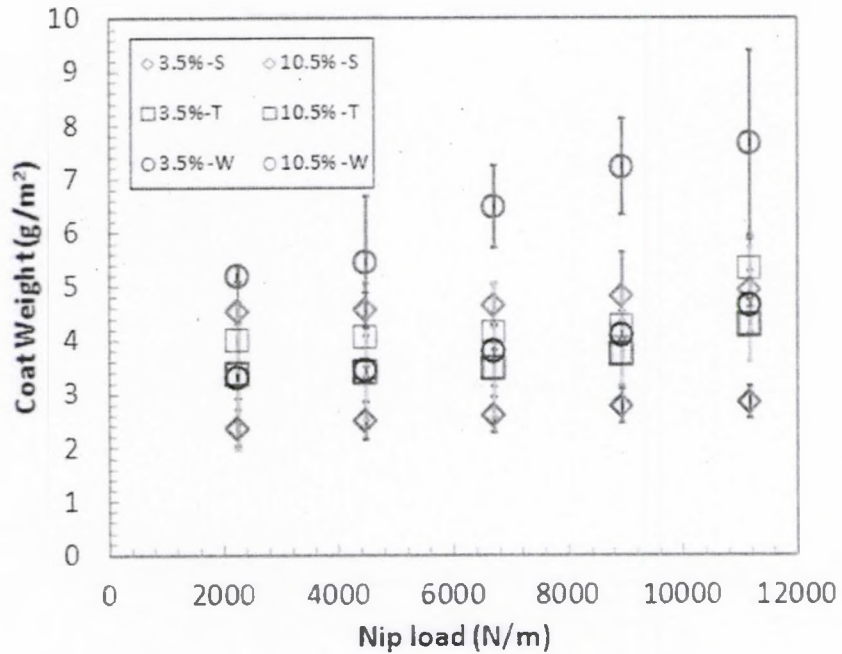


Figure 3-7 Coat weight obtained for three different papers coated with CNF for various nip loads.

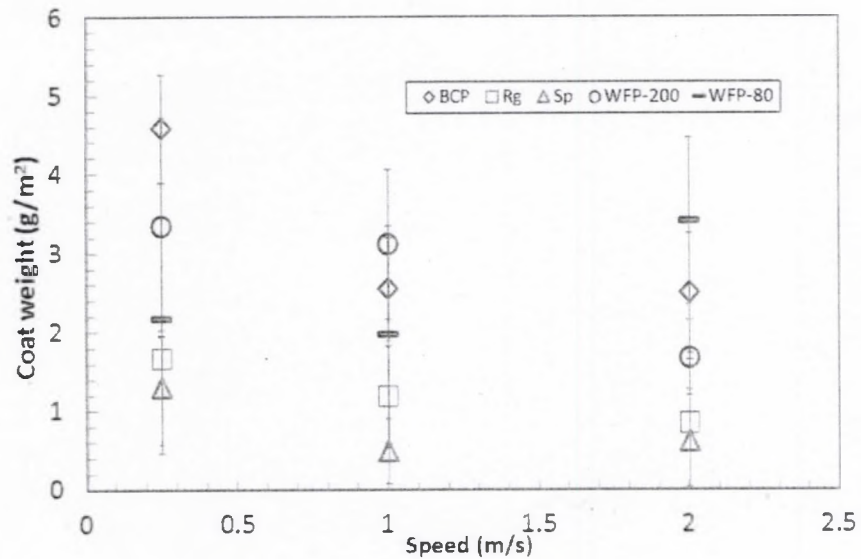


Figure 3-8 Coat weight obtained for 3.5% solids of CNF using the flooded size press method.

Figure 3.9 illustrates the coat weight as a function of speeds for samples coated using the high speed blade coater (CLC). Coat weight is for one side coated. It is important to note that solids over 3.5% were not possible to apply with this method because the material would not flow to the blade-paper nip by gravity in the time allowed in the test. The coatings were free of defects and had no obvious issues.

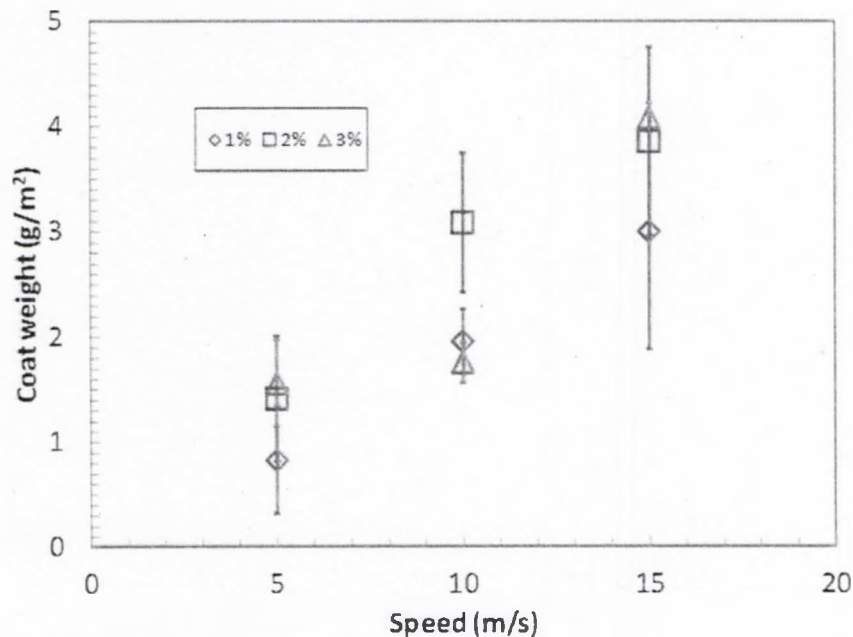


Figure 3-9 Coat weight obtained for different solid levels of CNF and different speeds using the cylindrical laboratory coater (CLC).

### 3.5 Model Prediction of CNF Coated on Paper with Size Press

Figure 3.10 indicates the geometry of concentration on the study of this process. Rolls are rotating at the same velocity. First of all, consider two rolls rotating at some speed  $U$ . The entry of any location is set to be zero gauge pressure and is assumed to be 10 mm upstream from the nip center. The exit location is set to 10 mm downstream of

the nip and is also set to zero gauge pressure. Some cases were also run assuming 1 mm upstream and downstream positions. Changing the position of this boundary condition does not significantly influence the results unless the gap is set too small. Larger values, such as 100 mm, can cause computational problems because of the need to mesh the fine gap and the entire region outside of the gap. Finite element methods use a computation mesh to help convert the partial differential equations to algebraic equations. Also shown in Figure 3.10 is the typical mesh used in these calculations, which is only visible by looking at an enlargement of the gap region.

A commercial finite element package (COMSOL Multiphysics 4.1) is used to solve the partial differential equations. The geometry is set by specifying the roll diameters at a gap that causes some finite, but small, separation. The region of interest is defined. The circles representing the rolls are subtracted from the region of interest to get Figure 12. The fluid properties can be set to be a Carreau model fluid. The values that fit the two experimental results are given in Table 3.1. These values fit well with the data given in figure 2.2 (see chapter 2 and figure 2.2) for the steady shear viscosities. However, the Carreau model has high and low shear rate viscosities that we need to select, but that the data does not cover. The slow shear rate values do not influence the results because it is the high shear rates at the nip center that are important. The high shear rate viscosity does influence the results. For these suspensions, a value of 1 Pas is selected. However, the high solid suspension may have a higher value here. Significantly different values of this high shear rate viscosity cause it to be impossible to fit the collected data. This issue should be kept in mind when looking at the results of this calculation.

Table 3-1 Carreau model parameters that fit the steady shear data

Solids (%)	$\mu_0$ (Pa-s)	$\mu_\infty$ (Pa-s)	$\lambda$ (s)	N
3.5	3000	1	70	0.15
10.5	45000	1	70	0.09

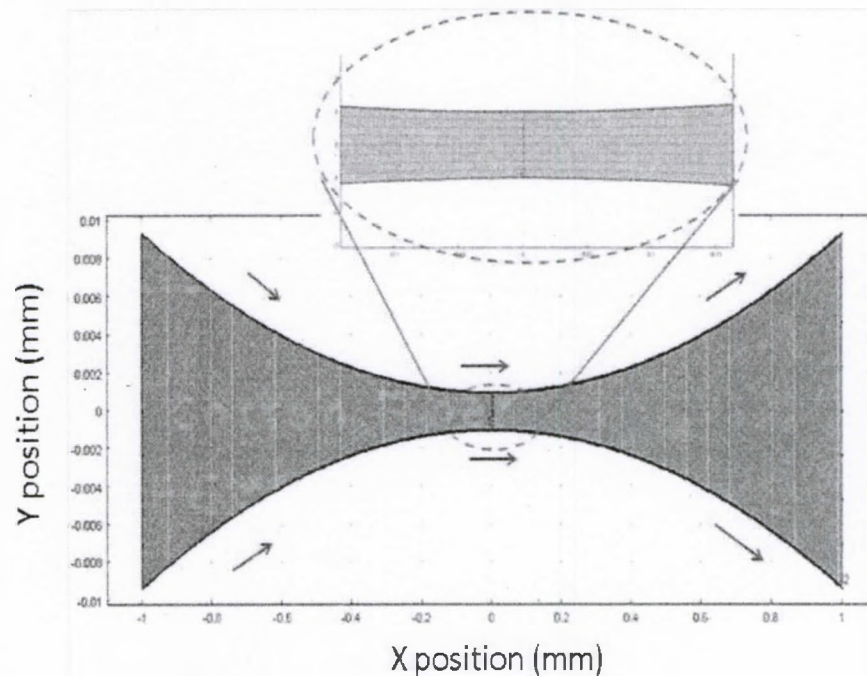


Figure 3-10 Schematic of the forward rolling nip geometry

To obtain a relationship between coat weight and nip loading, the software gives the solution for the pressure and velocity field in the nip region for a specific gap. The flow rate through that gap was obtained by line integration of velocity at any location. The load was obtained by integrating the pressure field from the inlet region to the nip center. The predicted pressure pulse was symmetric. Therefore, if this pressure field was integrated along the entire length, a zero load is obtained. Figure 3.11 shows the velocity field, shear rate field, and pressure distribution for a typical case. (red = 2 m/s, blue = 0

m/s), b) shear rate distribution and c) pressure field (red is high pressure, blue is low) in the nip region for the flow 1 mm inlet and outlet positions and 2 m/s surface velocity of the rolls

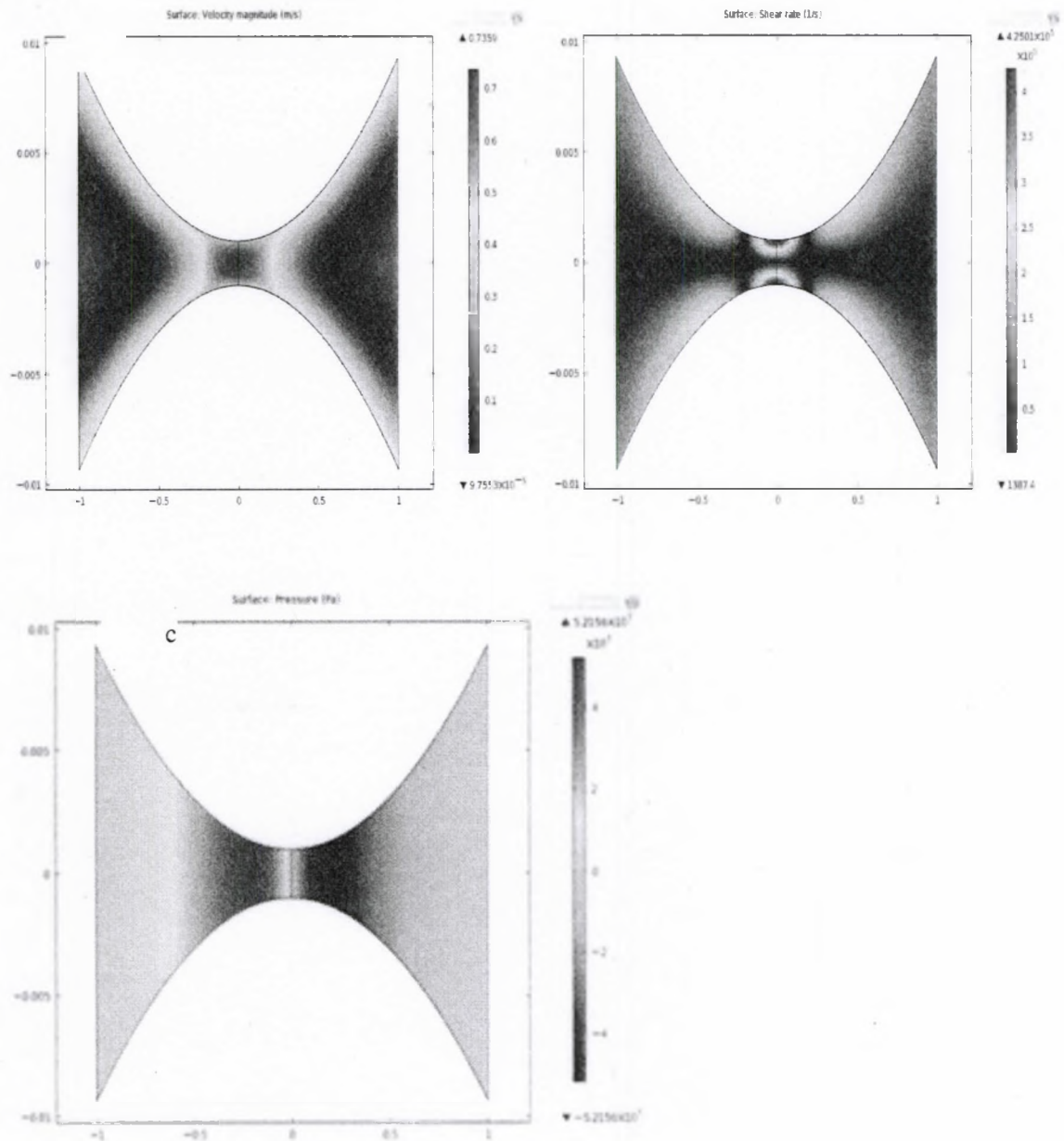


Figure 3-11 An example output of the model for a) velocity magnitude field

Figure 3.12 shows the predicted relationship between the coat weight and the nip loading for a roll surface velocity of 0.5 and 2 m/s. The key difference between the two solids is seen at lower velocities and lower nip loads. The volumetric flow rate through the nip at a given load is influenced by the different viscosities predicted by the Carreau model at moderate shear rates. At high nip velocities and high nip pressure, the CNF suspensions are expected to be shear thinning to similar viscosities at high shear rates. Therefore, the difference in the flow rate through the nip is small. The difference remains regardless how much material, on a dry basis, is deposited on a web. The coat weight values in Fig. 3.12 should be multiplied by a factor of two when compared with the experimental results obtained here because the experiments coat both sides of the web.

Figure 3.11 shows quite a different behavior than seen experimentally in terms of nip pressure. In the experiments, the nip pressure has a minor influence on coat weight, while in the calculations it should be able to reduce coat weight to a low value. What seems to happen is that the capillary and nip pressure drives water from the CNF suspension generating a filter cake on the paper surface. This filter cake results in a higher coat weight than expected from the metering action of the nip. Therefore, the filtration properties of the CNF suspension were determined. The values of coat weight in Figure 3.12 are lower than what is measured by a significant amount.

In addition, as the web speed increases the coat weight is predicted to increase as shown in Figure 3.13, while in the experiments the results do not depict this. Again, the complicating effect of dewatering in the nip can explain these results. A higher speed results in less time for dewatering and with a lower coat weight that contradicts the predictions of this fluid flow model.

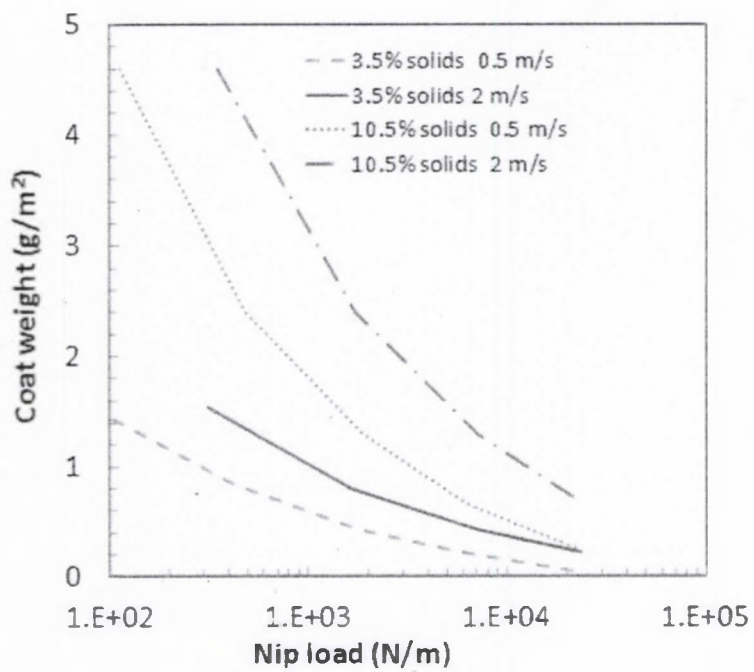


Figure 3-12 Predicted coat weight as a function of nip load for two solid contents and roll surface velocities

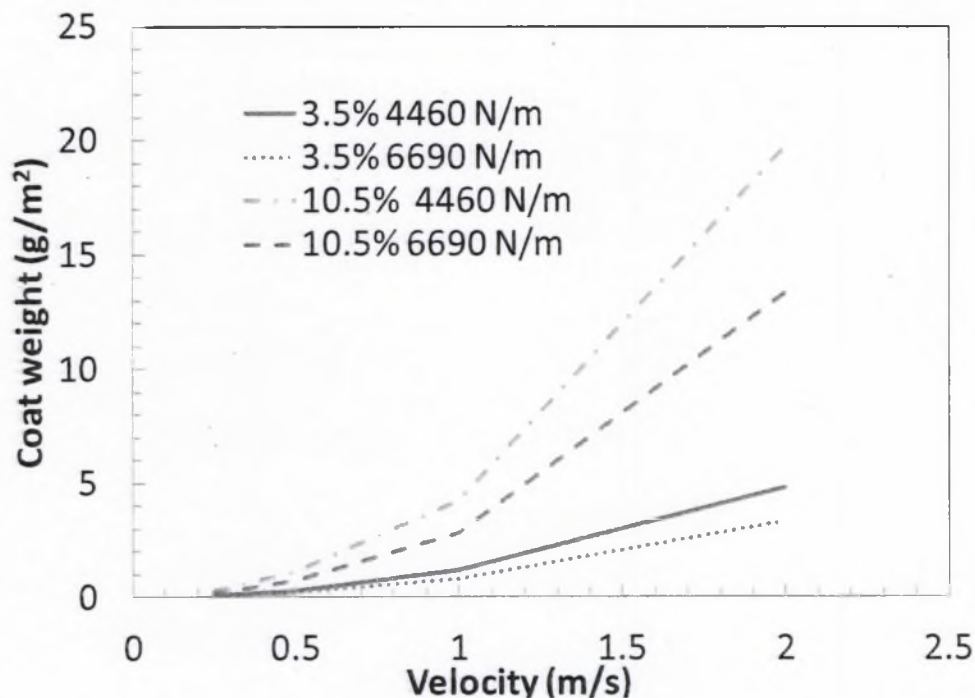


Figure 3-13 Predicted coat weight as a function of roll surface velocity

### 3.6 Filtration Theory

The flow rate of the suspension through a filter medium with resistance  $R_m$  is displayed by the expression below:

$$\frac{1}{A} \frac{dV}{dt} = \frac{\Delta P}{\mu(\alpha C_s V / A + R_m)} \quad (3.2)$$

Where  $V$  is the volume of fluid,  $A$  is the area for filtration,  $\Delta P$  is the pressure driving force,  $\mu$  is the viscosity of the fluid phase,  $\alpha$  is the specific filtercake resistance, and  $C_s$  is the solids of the suspension being filtered. Under the condition that the pressure is constant, Equation. (3.2) can be integrated and arranged as followed:

$$\frac{t}{V} = \frac{K_p V}{2} + B$$

$$K_p = \frac{\mu \alpha C_s}{A^2 \Delta P} \quad (3.3)$$

$$B = \frac{\mu R_m}{A \Delta P}$$

If the data are plotted as  $t/V$  against  $V$ , the slope of the line is related to the specific filtercake resistance  $\alpha$  through the constant  $K_p$  and the intercept is related to the medium resistance through the constant  $B$ . The filtercake resistance is a measure of the resistance to flow through a packed bed or a porous medium. The resistance coefficient does not depend on the concentration of the suspension. The resistance coefficient is related to the Darcy coefficient  $K$  as

$$K = \frac{1}{\alpha \rho (1 - \varepsilon_i)} \quad (3.4)$$

Where  $\rho$  is the particle density and  $\varepsilon_i$  is the void fraction of the porous medium or the ink layer. Therefore, if the specific filtercake resistance is known, and the void fraction can be estimated, using the Darcy coefficient approach.

For the low speed case and the low nip load, the filtration expression provides good results. Higher nip loads experimentally result in an increase in the coat weight, as shown in Figure 3.14. Predicted coat weight compared to the experimental coat weight for all of the flooded nip results for two solids, two nip pressures, and four speeds. At higher velocities, the filtration equations under predict coat weight; there is apparently not enough time in the nip to undergo much dewatering and filter cake growth.

By a simple addition the coat weight predictions due to the fluid flow with that obtained from filtration, a reasonable result is obtained. For example, at 2 m/s and a high nip load, the fluid flow equations predict about 3 g/m<sup>2</sup> and the filtration expression gives 0.8 g/m<sup>2</sup>. The measured amount is 4.8 g/m<sup>2</sup>. Figure 3.14 summarizes the model predictions compared to the measured values. Most of the model predictions are below the 45° line. This could be due to some issues with the fluid flow model or a number of other factors in both the model and the experiments. For example, there is insufficient time for capillary absorption of water while the paper is in contact with the steel roll. If there was enough time, the coat weight could increase on the side of the steel roll. This issue is not taken into account in the model. This issue would lead to a higher measured coat weight compared to the predicted value. Another issue may be due to the viscoelastic nature of the CNF suspension; if normal forces are generated in the nip, the gap would open and allow more suspension through than predicted with this model. In addition, as can be seen in the experimental results, there is much scatter in the values. The filtration calculations and fluid flow calculations could have given results that are much different than what is found here. Therefore, at least to the first order of magnitude, the model seems to be capturing the correct physics.

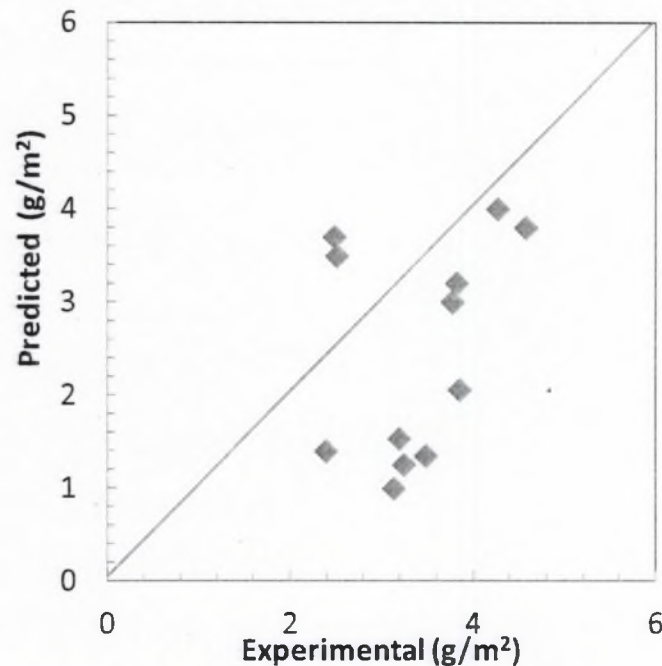


Figure 3-14 Predicted coat weight compared to the experimental coat weight

The interaction of the fluid dynamics and the dewaterings give a reasonable explanation of the experiments. The lack of the dependence of coat weight on velocity comes from two competing effects where the dewatering mechanism decreases due to less time in the nip while the hydrodynamics forces increase dragging more fluid through the nip. The lack of a strong dependence on solids comes from an increase in coat weight due to flow but that is controlled by a decrease in dewatering due to the higher solids and increase in filtercake formation. Increase in the nip load increases the dewatering but decreases the fluid carried through the nip due to the hydrodynamic forces.

The net result, as can be seen in figure. 3.14, is a limited coat weight range that can be obtained for CNF suspensions with this laboratory equipment. High solids and low speeds give high coat weights, but that is limited by a good distribution of the suspension. Flooded size presses would also have this issue with regard to the obtainable coat weight range possible with CNF suspensions. Metered size presses may not have these

limitations but high solids may cause other issues with regard to circulation of the suspensions through the systems and the metering action of the rods.

### **3.7 Conclusion**

CNF suspensions do not produce a 50/50 film split in the laboratory device with steel and rubber rolls. More material moves with the steel roll. This behavior is not seen with a Newtonian fluid such as glycerin. This behavior may be related to the geometry in the film split region and the non-Newtonian nature of the CNF suspension.

The coat weight with the laboratory scale size press device using the flooded and metered size press increases with solids and decreases with speed. The increase in solids is less than expected, but can be explained by considering a dewatering process in the nip. By accounting for the fluid flow through the nip and for the filtration of suspension caused by the nip pressure, a reasonable prediction can be made for coat weight. The coat weight range that could be obtained with the laboratory device is narrow due to the interactions of the dewatering and fluid dynamics.

## CHAPTER 4

### PROPERTIES OF COATED PAPERS COATED WITH CELLULOSE NANOFIBERS (CNF)

#### 4.1 Abstract

The surface properties of papers are important to papermakers because these properties affect the usage such as printing and glueing properties. During the formation of paper, fines are often lost from the sheet during formation and the paper surface becomes depleted of fines. A possible solution is to coat cellulose nanofibers (CNF) on the paper to improve the properties of the paper.

Papers were coated with CNF suspensions with three different methods, a laboratory size press, a rod draw down coater, and a high speed blade coater. Samples were dried and tested for brightness, surface roughness, air permeability, absorbency, stiffness and the pick velocity. CNF coatings cause the paper surface to be less porous and less absorbent, while CNF layers had little effect on other properties.

#### 4.2 Introduction

The interest on cellulosic nanomaterial has been increased rapidly in last decade and especially the material made from wood and other biomass materials. Cellulose can be described as a long and flexible cellulosic nanomaterial and is obtained from cellulose fiber by mechanical disintegration. In the paper coated process, the water base cellulose nanofibers were applied on base papers to analyze the optical behavior of this material on coating paper. The properties of coated paper are mainly controlled by the characteristic

of the base sheet and the materials in function. The behaviors of the base sheet paper get magnified after coated.

There are many mechanisms proposed to explain the influence of base paper on coated paper properties. Bousfield and Wing showed that mixture of CNF and AKD can improve properties of the base sheet of uncoated wood free paper and that play an essential role in determining the coating structure and the printing properties of the final product. The physical properties of cellulose nanofibers coated on papers were performed on different sheets of papers. Some of property results demonstrated the cellulose nanofibers have little influence of coated paper (Hamada et al., 2010; Luu et al., 2011; Richmond et al., 2012).

Two types of papers were evaluated with different thickness to coat MFC with idea to obtain good parking barrier material. MFC may be a good promising barrier material, but there is a need for further study to understand the fundamental behavior of those properties of MFC films and the coating such as the air permeability, moisture-sensitivity and the mechanical properties (Nathalie et al., 2012; Eva-Lena et al., 2010).

The coatings that contained CNF had an increase in brightness, but a decrease in gloss, especially for the rod coated samples. Stiffness increased about 40% for the blade coated samples. At low levels of CNF addition, pick velocity increased, but at higher levels, this value decreased. This result seems to be caused by the coating layers becoming more brittle with CNF addition.

### 4.3 Experimental Methods

The CNF used in this experiment was produced by the University of Maine Process Development Center. The sample was prepared mechanically by using a pilot scale refiner to break down the wood fibers. The wood fibers were a bleached softwood Kraft pulp. The suspensions were obtained at around 3.5% solid. The solid was increased up to 10.5% by using the filtration process. The filtration was done with the standard laboratory equipment using a vacuum and the standard filter paper. The CNF suspension was also diluted to be able to coat on the cylindrical laboratory rod coater (CLC).

The water retention of CNF was measured with the standard device (AA-GWR, Kaltech). The amount of water that passes through a membrane from the CNF suspension was determined at 45, 90 and 180 second at 1 bar pressure. The standard membrane was used (5 micron pore size). The amount of fluid that passed through the membrane was determined by weighing the blotter paper before and after the test. The purpose of this test is to understand the potential release of water from the CNF suspension to paper upon application.

The cylindrical laboratory coater (CLC) was used also to coat CNF. The speed was changed but the blade setting was held constant. This gave a range of coat weights.

All samples including the coated and uncoated papers were calendared with a center rolling temperature of 80° and a roll loading pressure of 150 psi with a high speed calendar (BELOIT WHEELER, MODEL 753) prior to the measurement of properties.

The gloss meter measurement shows the resultant values of the average of three set measurements using a standard device (Micro-tri-gloss, BYK-Gardner, USA). Four different measurements were taken for 85°, and the average mean value for each sample

was determine and recorded. The resultant value of the gloss measurement was recorded in percentage where 100% is the highest value of the gloss and 0% which mean there is no reflectance.

The surface roughness of the coated paper was measured by using an air leak test method (Parker-print-surface, H.E. MESSMER LTD UK.). The flow rate of air that leaks between a rim and the sample is used. This technique was used to measure how much air flow that leaks out between the coated sample and the measurement area which is converted into the average surface roughness  $\mu\text{m}$ .

The air permeability is determined with Tappi standard (T460) where the amount of time that for  $100\text{ cm}^3$  and the atmospheric pressure of air to flow through a single sheet of paper is recorded. This measurement is done with a common device (L&W, Densometer, and Lorenizen & Wettre Sweden).

The brightness of a piece of paper is typically on a scale of 1 to 100, with 100 being the brightest. By using the brightness tester in our lab (Technidyne Corporation USA) the brightness values were obtained.

A sample with a defined dimension is clamped and bent through a specified angle using the stiffness tester (model 150-E, Taber V-5). These measurements followed TAPPI standard method (T489).

The contact angle of water was determined through image analysis of a drop of water on the sample. The contact angle can be defined as the angle formed by the intersection of liquid-solid and liquid vapor interfaces.

The Bristow wheel was used to measure absorption rate. A 25.4 mm wide paper strip is mounted on a rotating wheel. The wheel speed and trough open width determines

the liquid absorption time. By varying the wheel speed and measuring the liquid trace area on the substrate, the total liquid volume (TLV) and absorption time relationship can be measured. This method gives the average permeability rather than the local permeability of the sample.

#### **4.4 Results and Discussion**

The results of the water retention test are shown in Figure 4.1. The y axis is the amount of water that comes through the membrane: more water indicates a more open filtercake that is formed on the membrane by the CNF suspension. One result that was not expected is clear: as the solid of CNF increases, the amount of water that is lost from the sample increases a small amount instead of decreasing. If the solids increase from 1 to 3%, the thickness of the filtercake to remove the same amount of water should triple: this increase should decrease the rate of water transfer by 1/3. However, this trend is not seen. Normal coating formulations would have the opposite result in that less water is removed as the solids increase. Even for starch containing coatings, as the starch content increases, the water release decreases due to the increase of viscosity of the liquid phase. The results here indicate that when the solids of CNF increases, the filtercake formed is more open than at low solids.. Pajari et al., 2012 report that the immobilization solids of a coating formulation that contains pigments decreases with CNF addition: This result indicates that CNF is poorer in packing of pigment.

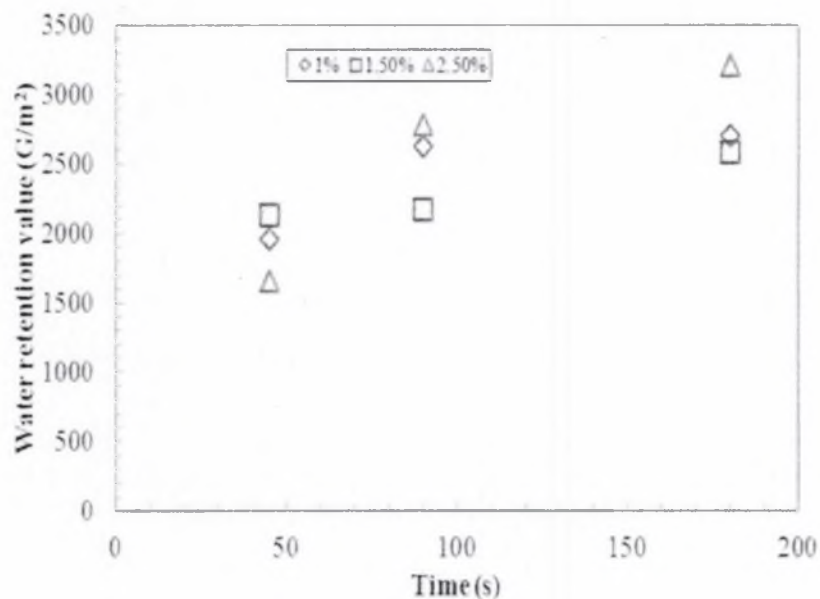


Figure 4-1 Water retention value of CNF as a function of time for different solid contents

The gloss results of the CLC coated samples are shown in Figure 4.2 below. All solids show a decrease in gloss when CNF added. Each point is an average of three repeats. The standard deviations average 10%. Low levels of CNF seem to decrease gloss and this trend seems like to be similar to what (Pajari *et al.*, 2012; Nygårds *et al.*, 2011) report, but both of these had to decrease solids to apply the coating, resulting in more water being in contact with the paper. This increase in water increases the potential of fiber swelling that can decrease gloss even after calendaring.

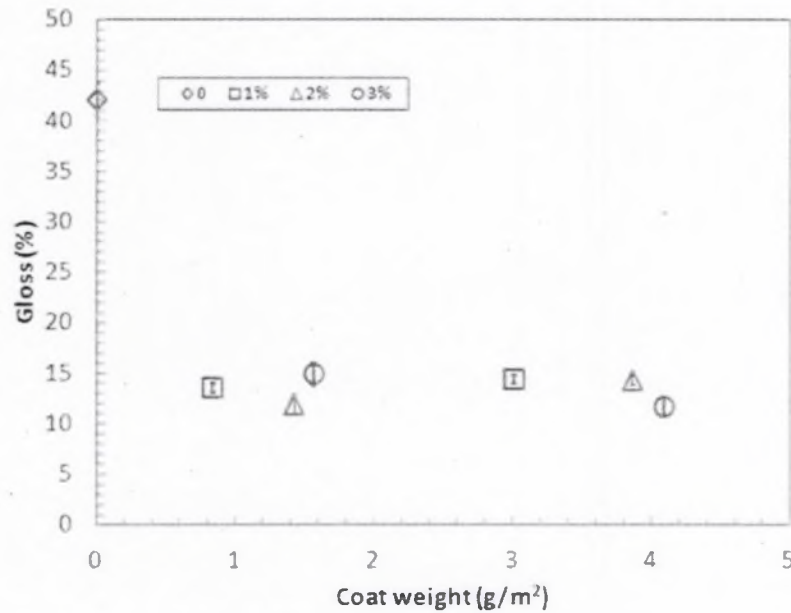


Figure 4-2 Gloss as a function of coat weight for CNF

Figure 4.3 summarizes the brightness results obtained as the function of coat weight for CNF coated on paper with CLC coater. Brightness decreases to some extent as CNF is added. This agrees with work of Pajari *et al.*, 2012. When CNF itself is dried, it gives a brownish color. Therefore, there was a concern with CNF to decrease brightness. However, CNF is used in such small amounts that it does not seem to influence the brightness, but shows a decrease in brightness.

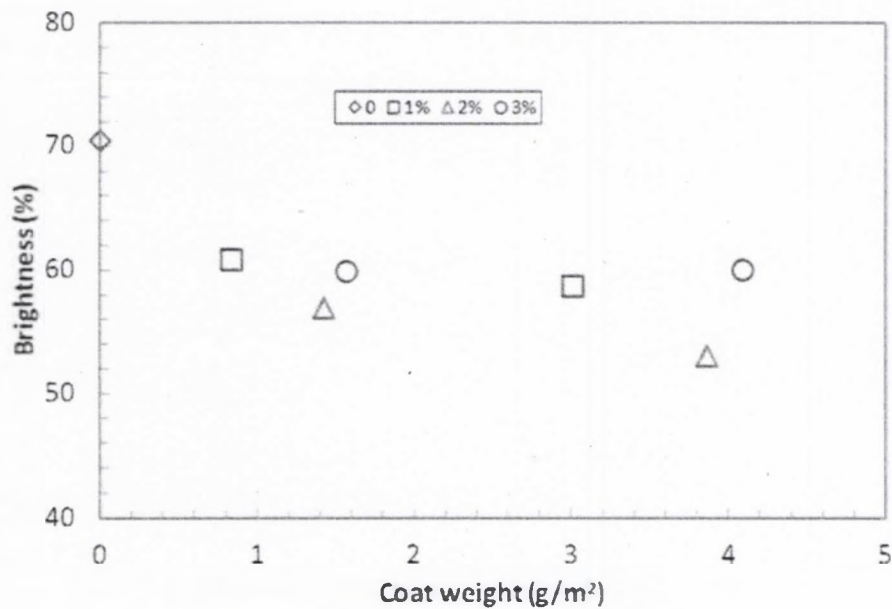


Figure 4-3 Brightness as a function of coat weight for CNF

Figures 4.4 and 4.5 indicate the resultant values for roughness as function of coat weight for different solids of CNF. Each point is an average of three repeats. As the solid of CNF increases the surface roughness increases a small amount. This result is similar to the previous studies, due to the fact they observed an increase in base sheet roughness (Pajari *et al.*, 2012; Nygård *et al.*, 2011). In Fig. 4.5, which the result of the wood free paper coated with laboratory size press device with different solids. As the solid of CNF increases the surface roughness increases a small amount.

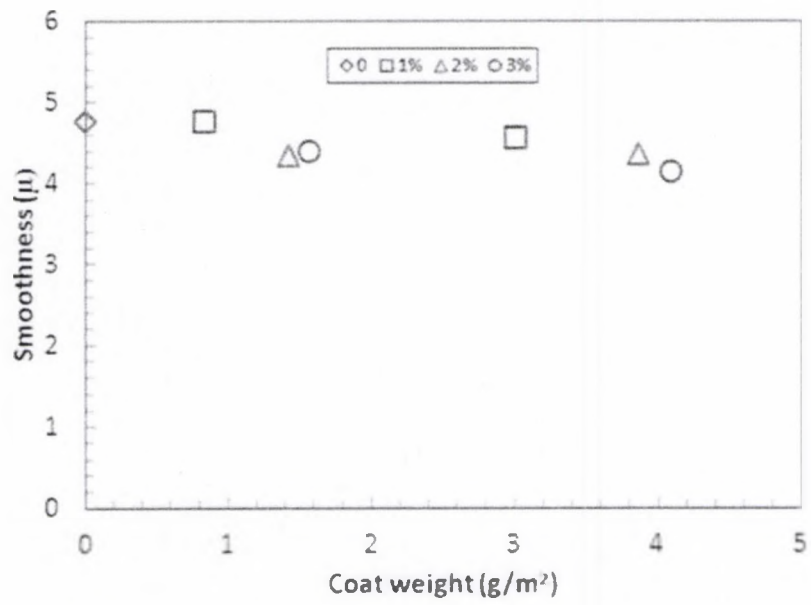


Figure 4-4 Roughness as a function of coat weight for CNF coated with the CLC coater

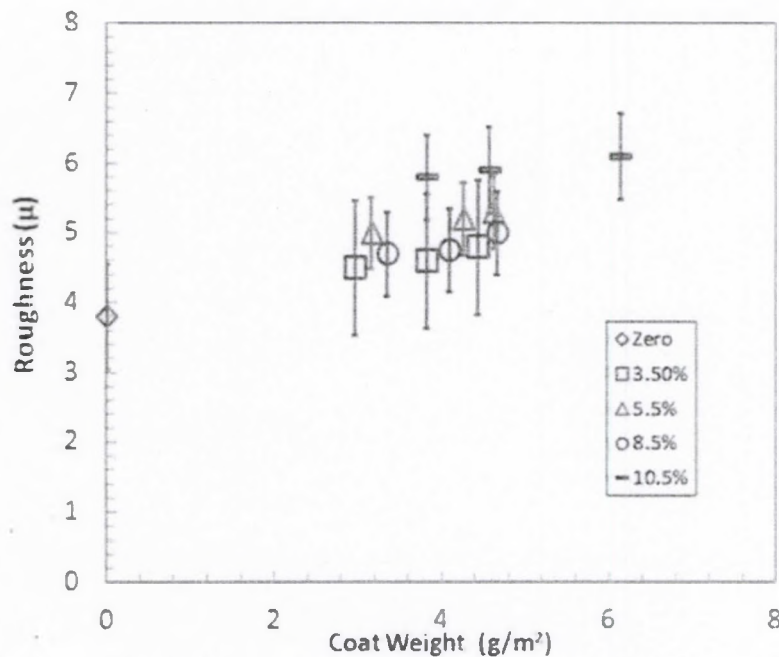


Figure 4-5 Roughness as a function of coat weight coated with a rod draw down coater

Figure 4.6 shows the stiffness for CNF coated on paper as a function of coat weight. The results indicate that the stiffness may increase in a small amount. Each point is an average of three repeats. The standard deviations average 10%. These results agree with Ridgeway et al., 2011 who discussed the “I-beam” effect, even through these samples were coated only on one side. Pure films of CNF are quite stiff: if this high modulus material is captured at the surface of the paper, one would expect an increase in stiffness. The reason that the stiffness increase is not much larger is not clear.

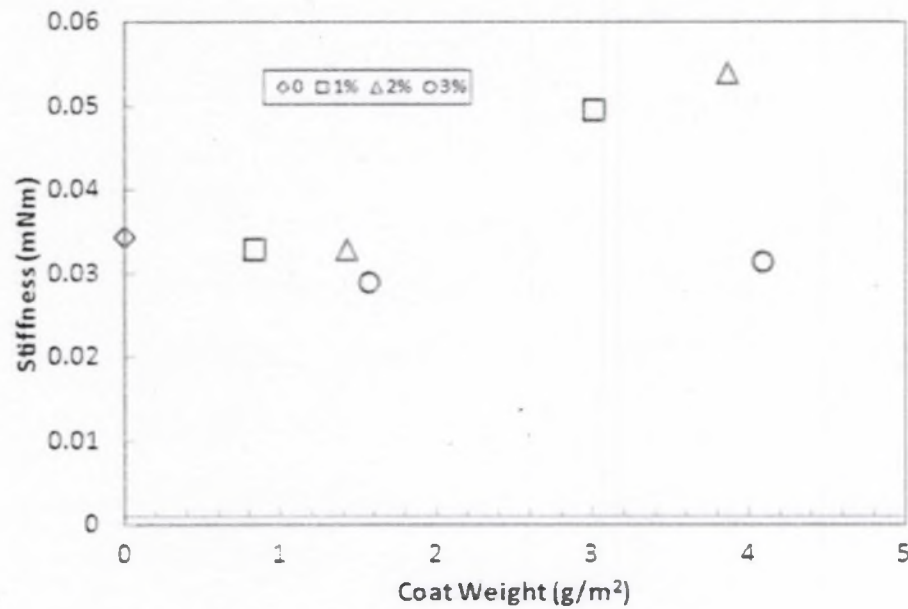


Figure 4-6 Stiffness as a function of coat weight for CNF

As CNF coat weight increases, the amount of air through the sample shows a small increase shown in Figure 4.7. Each point is an average of three repeats. This increase in permeability is not expected because it was thought that CNF would fill in the pore space, decreasing air permeability. As with the GWR water retention tests in Fig. 4.1, this again show that the pore structure generated with CNF is a bit more open than without CNF. The mechanism for this structure change is not clear at present. Pajari *et al.*, 2012 also show an increase in air permeability as CNF content increases for board coatings.

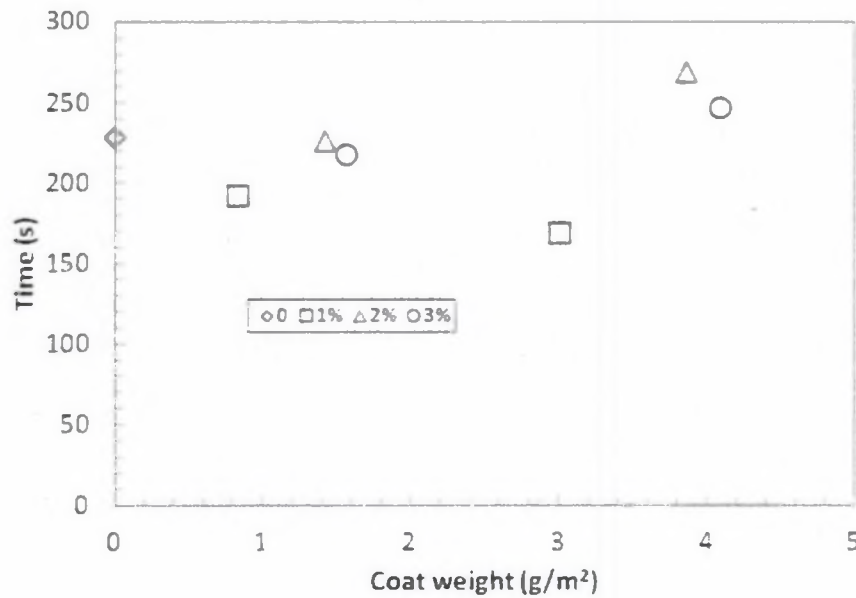


Figure 4-7 Air permeability as a function of coat weight for CNF for CLC coated samples

The permeability is the measure of the amount of fluid that passed through a single sheet of paper. The theory of flow through a single sheet of paper is based on empirical formula known as Darcy's Law. Darcy's Law states that the velocity of a fluid flowing through a porous column is directly proportional to the pressure and inversely proportional to the length of the column. A well known expression that describes the flow through the air is given by Darcy's Law equation.

$$Q = \frac{K\Delta P}{\eta L} A \quad (4.1)$$

Where  $Q$  is the flow rate ( $\text{m}^3/\text{s}$ ),  $\Delta P$  is the pressure drop (Pa),  $\eta$  is the viscosity of the fluid (Pas);  $L$  is the distance that acts in the pressure of the flow direction (m);  $A$  is the cross-section area of the flow; and  $K$  is Darcy's permeability coefficient. Figure 4.8

illustrates the results of Darcy's permeability as function of coat weight for different solids of CNF coated of paper. Each point is an average of three repeats. The result for coated and uncoated paper show to be the same except at higher solid there observed a drop of permeability. A significant amount of CNF seems to be needed to fill the pores and holes of the paper surface. At low coat weights, as in Fig. 4.7, the CNF must be simply going into the paper pores.

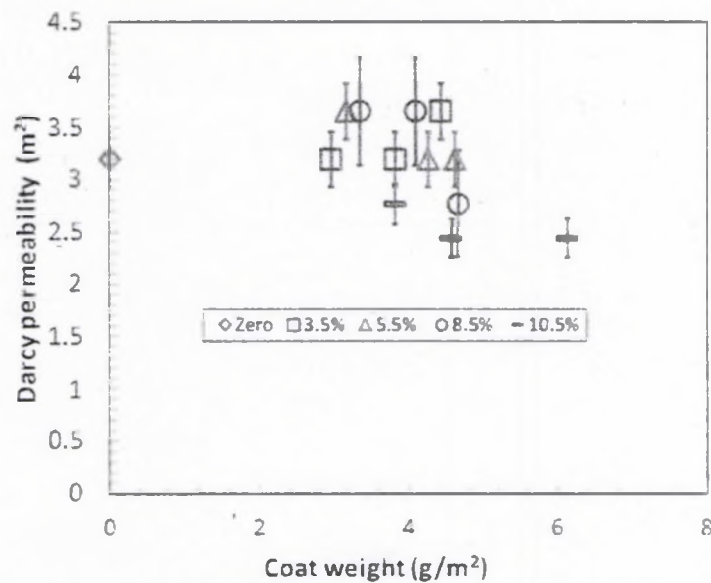


Figure 4-8 Darcy permeability as a function of coat weight for CNF coated with rod draw down coated.

Figure 4.9 displays the contact angle as a function coat weight for uncoated and coated wood free paper (Hansol 80). Each point is an average of three repeats. Results for the coated and uncoated show a small contact angle is observed while the liquid spreads on the surface and indicate that the wetting of the surface is favorable. The contact angle

for uncoated and coated paper seems to have a similar behavior and show a decrease for solids at high coat weight.

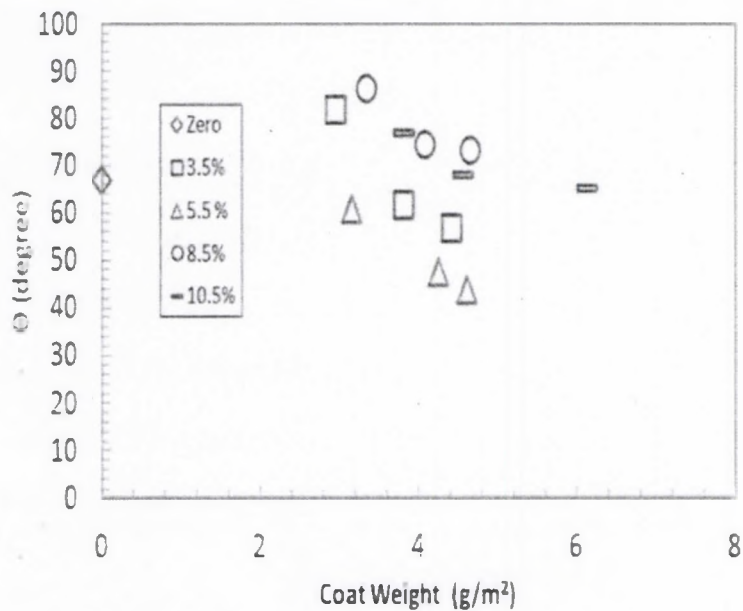


Figure 4-9 Contact angle as a function of coat weight for CNF

Figure below displayed the Bristow wheel of CNF coated on paper as a function of times for different solids of CNF for CNF. Each data set point is an average value from three tests and plotted with error bars which are standard deviation. The result seems to be repeatable, error bars are in the small size. The result shows the decrease in the Bristow wheel as the solids increase. The base sheet has the higher Bristow wheel.

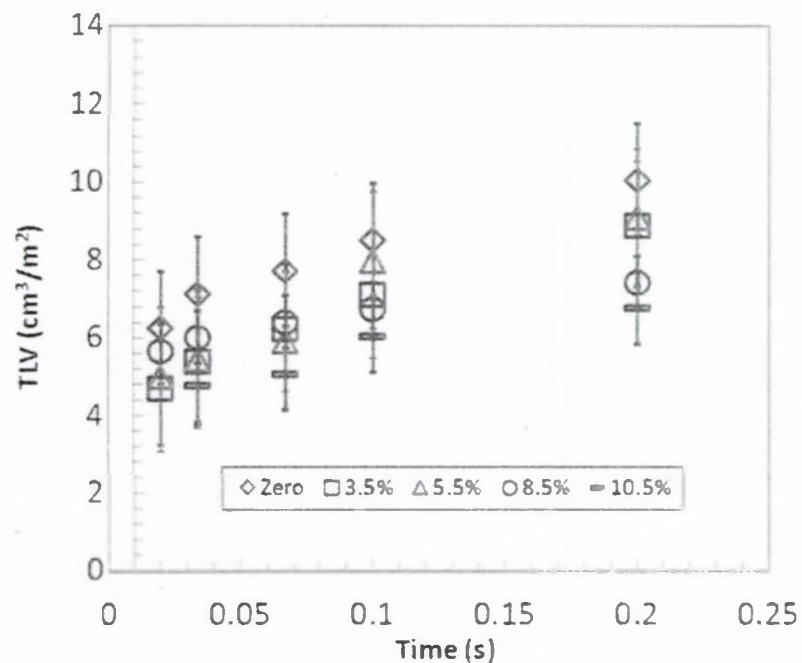


Figure 4-10 Bristow wheel as a function of coat weight for CNF

Figure 4.11 displays the porosity of CNF as a function of coat weight for uncoated and coated wood free paper. The porosity does decrease as CNF must filling up the pore space. The results indicate that CNF does not sit all at the surface of the paper, but sinks into the paper decreasing the void volume.

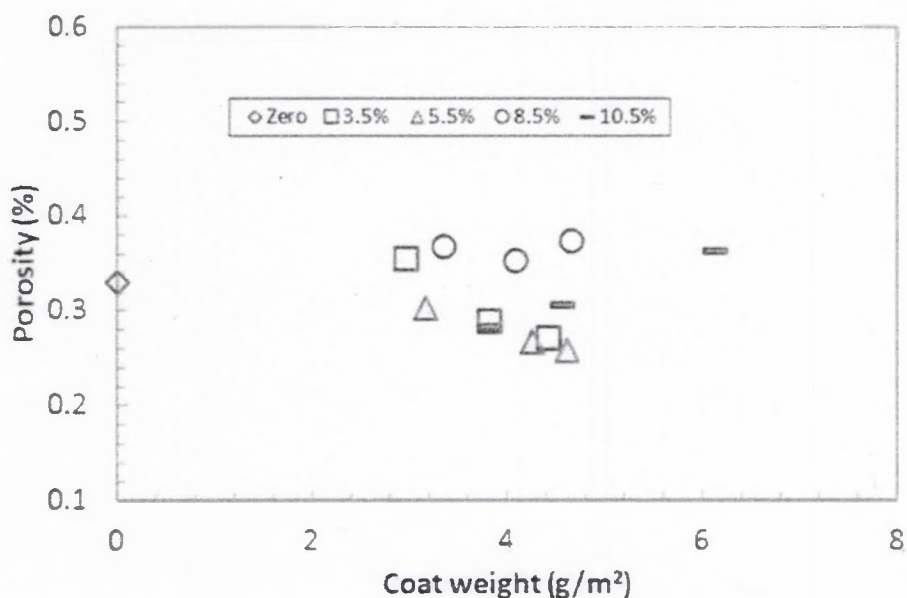


Figure 4-11 Porosity of rod coated samples at various solids and coat weights

Figure 4.12 displays the volume fraction as a function particle size distribution for different solids of CNF. The results described that CNF cannot be seen at low particle size distribution  $<1\mu\text{m}$  which means an electron microscope is needed to measure the size and between 1 to 10 micron the particle size still very small microscope laser diffraction is needed to measure the size of this material. However, most particle sizes are seen between 10 to 50 microns and the overall results showed that the particle sizes are no bigger than 300 micron and afterward the particle size cannot be seen. As expected the particle size results do not change with solids and the different solids of CNF gave the similar particle size distribution.

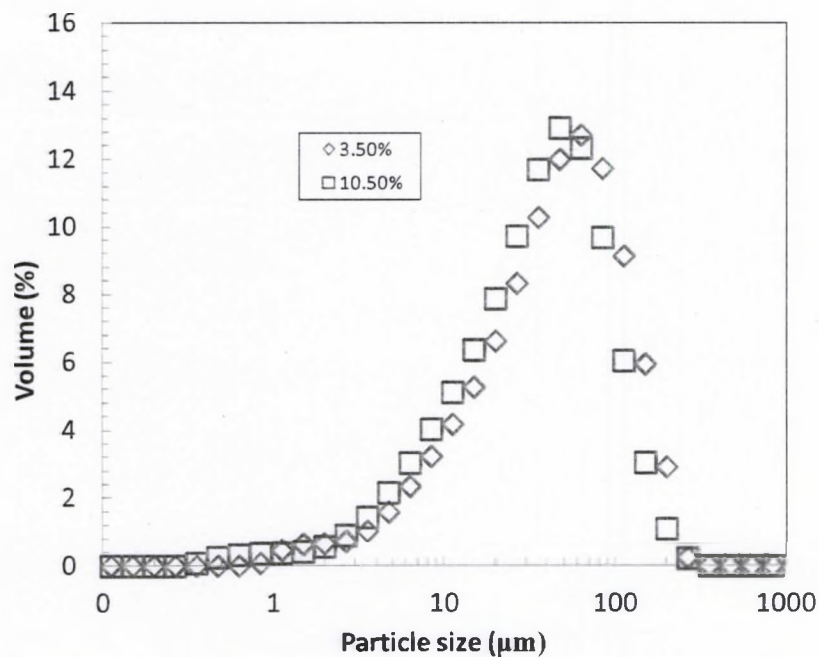


Figure 4-12 Volume as a function particle size for different solids of CNF

#### 4.5 Conclusion

The properties of paper coated with CNF suspensions were characterized. CNF tends to decrease gloss and brightness, likely because of the water exposure of the paper to water and the brown color of CNF. The stiffness of the paper shows little increase even though films of CNF are quite stiff. This lack of stiffness increase, the modest decrease in permeability, and the decrease in porosity all indicate that CNF penetrates into the paper to a significant degree and does not stay at the surface as a coating.

## CHAPTER 5

### THE RHEOLOGY OF COATING FORMULATION THAT COATAIN CELLULOSE NANOFIBERS

#### 5.1 Abstract

Cellulose Nanofibers (CNF) has the potential to be produced at low cost on site of a paper company. A natural use of CNF would be as a component of a paper coating formulation, either as a thickener or as a co-binder. Some preliminary results demonstrate some potential strength improvements of these coatings, but an in-depth study is needed to overcome some of the rheological challenges of using CNF and understanding its ability to be used in a coating layer Pajari *et al.*, 2012. In this chapter, the rheology of coatings that contain CNF are reported and compared to coatings that contain starch. The change in behavior is quite different between CNF and starch: starch acts to modify the viscosity of the liquid phase while CNF seems to influence the overall structure or network strength of the coating.

#### 5.2 Introduction

Many are interested in products made from renewable resources with low environmental impact and minimal safety risks. Cellulose nanofibers (CNF) are biodegradable, natural, and renewable resources made from wood fibers. The CNF suspension can also be extracted from other biomass (Bhat *et al.*, 2003; Klemm *et al.*, 2006). It is expected that this material can be produced at low costs in paper mills Spence *et al.*, 2011. In the paper industry, nano-scale cellulose fibers have gained attention due to

a number of potential applications. Recent journal review articles describe various aspects of the production and use of these materials, and much attention is paid to using this material in plastic composites and other applications (Moon et al., 2011; Eriksen et al. 2011; Klemm et al., 2006; Hubbe et al., 2008; Saito et al., 2010).

Some of the most promising uses for these fibers are in the production of paper and packaging materials. Recent work has shown that CNF coated on paper can increase the capture of ink pigments at the top surface which leads to an increase in print density for ink jet and flexographic printing (Hamada et al., 2010; Luu et al., 2011; Richmond et al., 2012). The use of CNF in the wet end has also been reported (Torvinen et al., 2011; Morseburg et al., 2009) resulting in strength benefits. CNF coated on a paper surface with a pigment pre-coat has also been shown to increase the stiffness of the sheet Ridgeway et al., 2011.

CNF use in paper coatings has been studied by two groups out of Finland (Nygårds et al., 2011; Richmond et al., 2014) used ground calcium carbonate (GCC), binders, and additives to form coating layers. A laboratory rod coater applied the material onto papers. Several physical properties of the coatings were analyzed such as gloss, surface roughness, air permeance, pick strength, surface energy, and ink setting. They were faced with some issues in which at high concentration of CNF, the viscosity of the suspension was too high, and the coating did not spread out to cover the paper uniformly. Their results report coating layers that had a decrease in gloss, and air permeability. However, there was an increase in pick strength as the CNF concentrations increased.

Pajari *et al.*, 2012 reported the use of CNF as a replacement for synthetic latex binders in paper coatings. In their experiment, many trials were considered with different

pigments and latex binders, and different methods of coating were adopted. They found that the partial replacement of latex with CNF increased the viscosity of the coating at low shear rate. Coatings that contain CNF had decreased in gloss and air permeance, but some other properties, like pick strength, were not affected Pajari *et al.*, 2012.

While these two reports show some promise, the difficulties of using CNF becomes clear: addition of CNF into coatings increase viscosities. This increase leads to a challenge with coating using standard equipment at high speeds. More work is needed to understand the rheology of these coatings, the methods that can be used to apply them to paper, and the properties of the coating paper.

In this study, CNF that is produced with a refiner is added to a simple coating formulation. The levels of CNF addition are compared to the behavior with starch. The rheology of these suspensions is characterized.

### **5.3 Experimental Methods**

A simple coating formulation is used to bring out the differences between CNF and starch addition to a coating. A standard kaolin pigment (Capim DG, IMERYYS) is mixed with a styrene butadiene latex (Genflo 557, OMNOVA). The pigment is used in slurry form and is provided at 70 wt% solids. The pigment has an ISO Brightness of 89 with 92 % of particles are < 2  $\mu\text{m}$ . The latex is supplied at 50% solids. An ethylated starch (Ethylex 2025 Tate & Lyle, USA) was used in the coating formulation. The starch was cooked by using the standard of the starch cooker for 60 minutes at 295°F (146°C) at 30% solids before it mixed into the coatings.

The CNF used in this experiment was produced by the University of Maine Process Development Center. The sample was prepared mechanically by using a pilot scale

refiner to break down the wood fibers. The wood fibers were a bleached softwood Kraft pulp. The suspensions were obtained at around 3.5% solid. The solid was increased up to 15% by using a filtration process.

In this work, CNF that is produced with a refiner is added to a simple coating formulation. The levels of addition are compared to the behavior with starch. The rheologies of these suspensions are characterized. Concentrations of latex, starch and CNF are all based on the pigment weight. For example, 10 pph latex means that 10 grams of latex are present for every 100 grams of pigment in the final dried coating.

The coating formulations are displayed in Tables 5.1 and 5.2. All coatings were mixed to the same solids level ( $60\% \pm 1\%$ ). Two series of coatings formulations were tested: 1) CNF and starch were varied from (1-10) pph, with the latex content held constant at 10 pph and 2) CNF and starch were added with reduction of latex on an equal weight basis. After the preparation of each sample, a high speed rotor stator mixer (Kady Mill) was used to mix before the testing for rheology or coating.

Table 5-1. Coating formulations for constant latex amount

	Coating with CNF	Coating with starch
Pigment (Capim DG IMERYYS)	100	100
Latex (GenFlo 557, OMNOVA) (pph)	10	10
CNF (pph), UMaine	1-10	-
Starch (Ethylex 2025), (pph)	-	1-10

Table 5.2. Coating formulations that reduce latex and increase CNF and starch.

Sample No.	0	2-8 (CNF-L)	5-5 (CNF-L)	2-8 (S-L)	5-5 (S-L)
Pigment (Capim DG)	100	100	100	100	100
CNF (pph)	0	2	5	0	0
Starch (pph)	0	0	0	2	5
Latex GenFlo 557 (pph)	10	8	5	8	5

The rheology of the coatings was measured by using a controlled stress rheometer (Bohlin CVO). The parallel disk geometry was used based on past experience with CNF. The fluid was placed between two parallel disks of radius 40 mm separated by a gap of 1 mm. Steady shear viscosity and oscillatory shear tests were used. Enough materials were added to the bottom plate and the excess material was trimmed away after the gap was set. The shear rate was measured using a 10 second delay time with a 10 second integration time. For the oscillatory tests, a shear stress ramp was performed to find the linear viscoelastic region that was less than 0.1 strain. For the frequency sweep test, a range of 0.01 to 30 Hz was used. A power law according to Oswald de Waele empirical model was fitted to the experimental data for the steady shear viscosity after the correction of the data Byron et al., 1987. All data sets reported are the average of triplicate runs where a fresh sample is placed in the rheometer for every run.

## 5.4 Theory

The rheology of a suspension has been the subject of many studies because of the common need to predict the viscosity as a function of concentration of particles in the design and operation of equipment. For a coating, the prediction is difficult because of the colloidal interactions between the pigments and the latex as well as the other additives.

The increase in viscosity of a suspension of spherical particles, at low solids, follows Einstein's equation

$$\eta_r = 1 + 2.5\phi \quad (5.1)$$

Where  $\eta_r$  is the relative viscosity defined as the viscosity of the suspension divided by the viscosity of the fluid phase and  $\phi$  the volume fraction of the spheres. (Barnes et al., 1989).

Bachelor had expanded the Einstein equation by adding a third term which is the square of the second term.

At higher concentration, the empirical data for relative viscosity appear to follow more of an exponential function of concentration. One common expression that seems to give good results (Barnes et al., 1989).

$$\eta_r = \left(1 - \frac{\phi}{\phi_m}\right)^{-2.5} \quad (5.2)$$

Where  $\phi_m$  is the maximum packing volume fraction of the solid phase. As the volume fraction of solids reaches this maximum packing, the viscosity goes to infinity.

There are several factors that can influence the rheology of any suspension, and those factors can be included particle size, particle size distribution, and the volume fraction of solid contents of the substance. It is important to examine the relationship between rheology and particle size parameters. The Krieger Dougherty equation is considered to make the analysis of CNF and starch into the coating formulations. The significance of the relationship is the viscosity which is this concept that describes resistance to flow. High viscosity liquids are relatively immobile when subjected to shear, whereas low viscosity fluids flow relatively easily. Measurement of viscosity, and other rheological properties, can be made using either capillary or rotational rheometers, the choice of system depending on the properties of the material being tested.

'Shear rate' defines the speed with which a material is deformed. In some processes, materials are subjected to high shear rates ( $>10^5 \text{ s}^{-1}$ ); in others, the associated shear rate is low ( $10^{-1} - 10^1 \text{ s}^{-1}$ ). High shear rates tend to occur when a material is being forced rapidly through a narrow gap.

If viscosity remains the same as shear rate increases, a fluid is described as being Newtonian. Non-Newtonian fluids, which fail to exhibit this behavior, fall into one of two categories – shear thinning or shear thickening. With shear thinning materials viscosity decreases as shear rate increases: application of shear leads to a breakdown of the material's structure so that it flows more readily. Most fluids and semi-solids fall into this group. Conversely, the viscosity of shear thickening materials increases at rising shear rates.

Krieger-Dougherty equation stated that the factor 2.5 can be replaced by the intrinsic viscosity  $[\eta]$  times the maximum solids fraction. The intrinsic viscosity for the dilute suspension of particles is related to the initial rate of viscosity increase. This expression allows particles of any shape to be accounted for.

$$\eta_r = \left(1 - \frac{\phi}{\phi_m}\right)^{-[\eta]\phi_m} \quad (5.3)$$

This equation has found great success in predicting the viscosity of a suspension at higher solids. The maximum packing fraction is in theory, a quantity that can be measured directly or estimated from particle packing simulations. This would be the concentration where all the particles are in contact and cannot move relative to each other.

When starch is present in a coating, the starch molecule is dissolved in the liquid phase. If starch is not influencing the colloidal nature of the system, then the suspension viscosity should be possible to predict from the viscosity of the water-starch viscosity with a simple scaling as in the Krieger-Dougherty equation. If the solids concentration is constant, the viscosity of the suspension should increase the same proportion as the starch-water system.

When CNF are in the suspension, it is not clear how to describe the system. If CNF is treated as a dissolved polymer, then the viscosity of the suspension should be increased to the same proportion as the viscosity increase of water when CNF is present. If CNF should be treated as a particle, then the volume fraction of particles should increase as CNF is added.

The above equations are focused on predicting the increase of a Newtonian fluid, but most suspensions are shear thinning. The increase in viscosity with solids should hold to be the same at every shear rate. A shear thinning fluid is often described by the power-law model given as

$$\eta = m\dot{\gamma}^{n-1} \quad (8)$$

Where  $m$  is called the consistency index and  $n$  the power law index. When  $n=1$ , the fluid is Newtonian. When  $n<1$ , the fluid is shear thinning. The change of  $n$  and  $m$  as a function of solids is not clear in the literature even though this has been characterized by a large number of research groups.

## 5.5 Results and Discussion

Figures 5.1-5.2 show the results obtained from the steady shear viscosities for coatings that contain CNF and starch, where the latex content is constant at 10 pph and different concentrations of CNF and starch are added to the mixture. Each set is an average of three runs in the parallel disk geometry with 1 mm gap. Figure 5.3 compares starch and CNF containing coatings where the latex content is replaced by either component. CNF, starch and latex as in Table 5.2. 2-8 (S-L) stands for 2pph starch and 8pph latex. One clear result is that the coatings that contain CNF are a much higher viscosity than coatings that contain the same content of starch; at 5 pph, the viscosity of the CNF is over ten times larger than the starch formulation. The slope of the viscosity-shear rate results increase with CNF concentration showing an increase in the shear thinning nature. In Fig 5.2 with the starch case shows that the thinning behavior does not increase to a large extent with concentration.

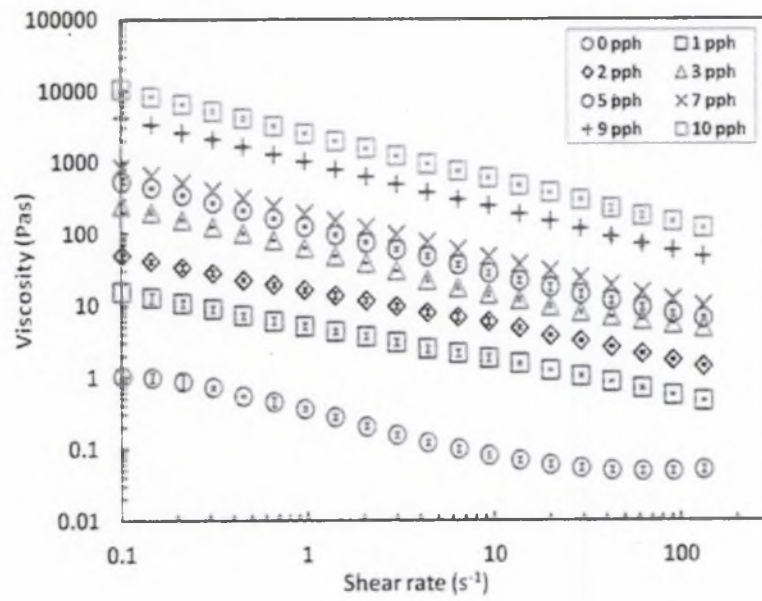


Figure 5-1 Steady shear viscosity as a function of shear rate for different concentrations of CNF holding the latex content constant at 10 pph

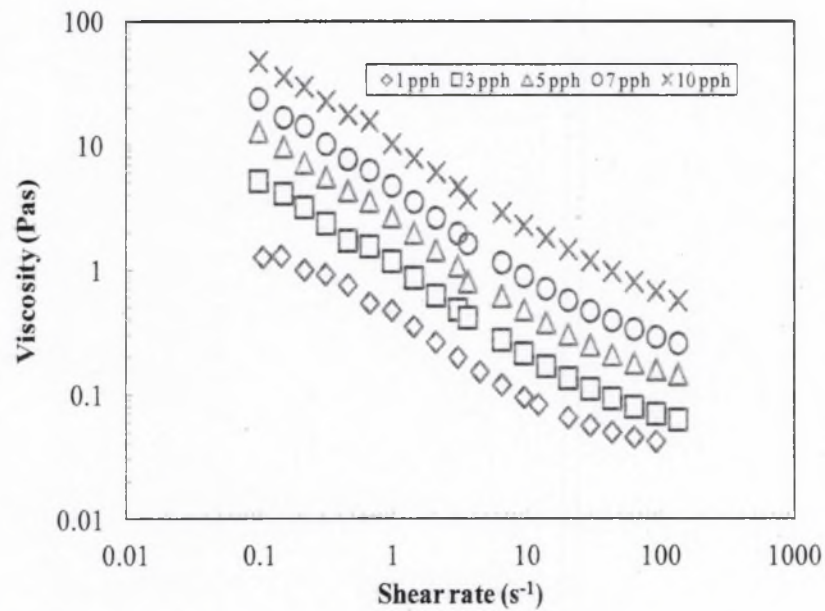


Figure 5-2 Steady shear viscosity as a function of shear rate for different concentration of starch with constant 10 pph of latex

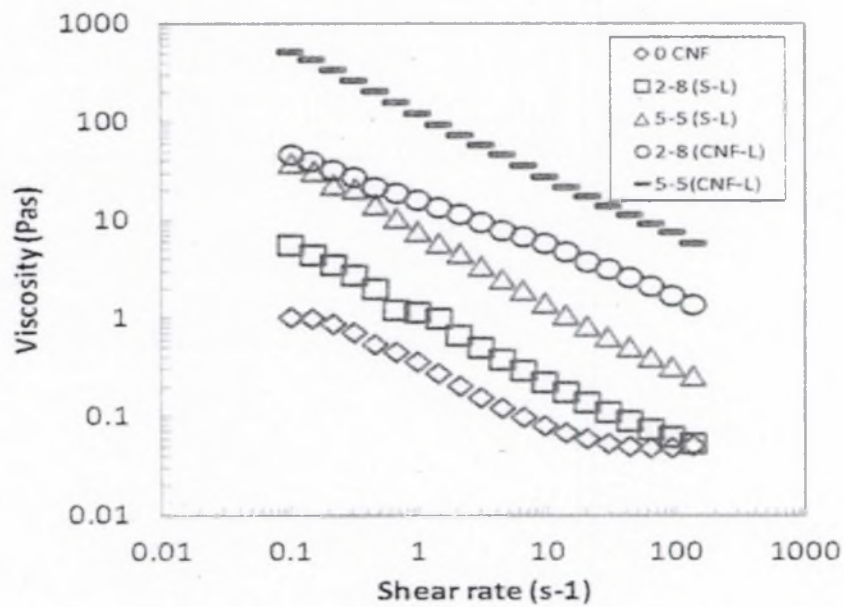


Figure 5-3 Steady shear viscosity as a function of shear rate for different concentrations of CNF, starch

The power law index and consistency index are shown in Figures 5.4 and 5.5. The power law index for coatings that contain CNF or starch is much larger than CNF in water reported in Chapter 2. This indicates that CNF in water can generate some type of structure that does not exist when CNF is mixed with pigments and latex. When latex and pigments are present, it seems like this structure is not as strong and the shear thinning is determined by the pigment-latex interactions. We also observe that the parameters ( $m$ ) for the CNF in water and coatings with CNF look to be the same, but are higher in magnitude than coatings with starch.

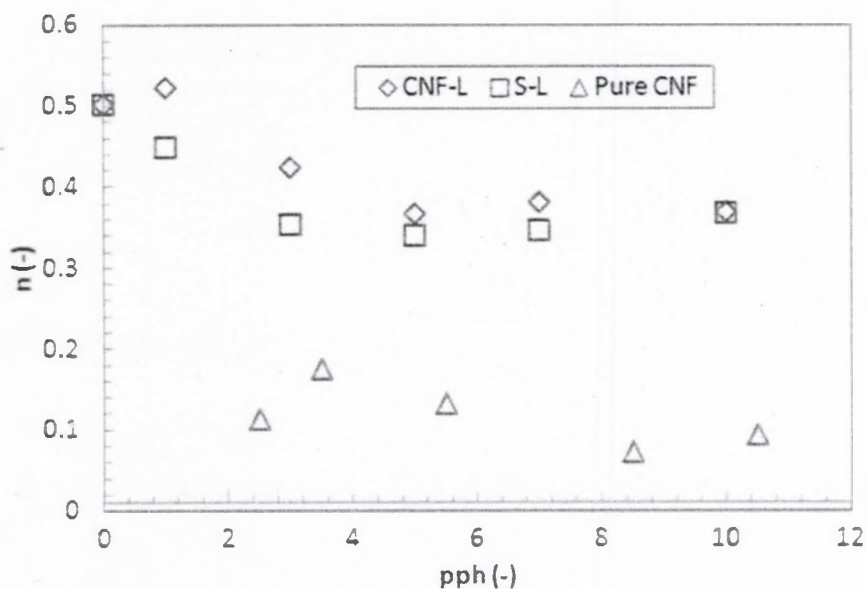


Figure 5-4 Power law index  $n$  as a function of  $pph$  for coatings with CNF, starch and as a function of weight percent in CNF-water system (pure CNF)

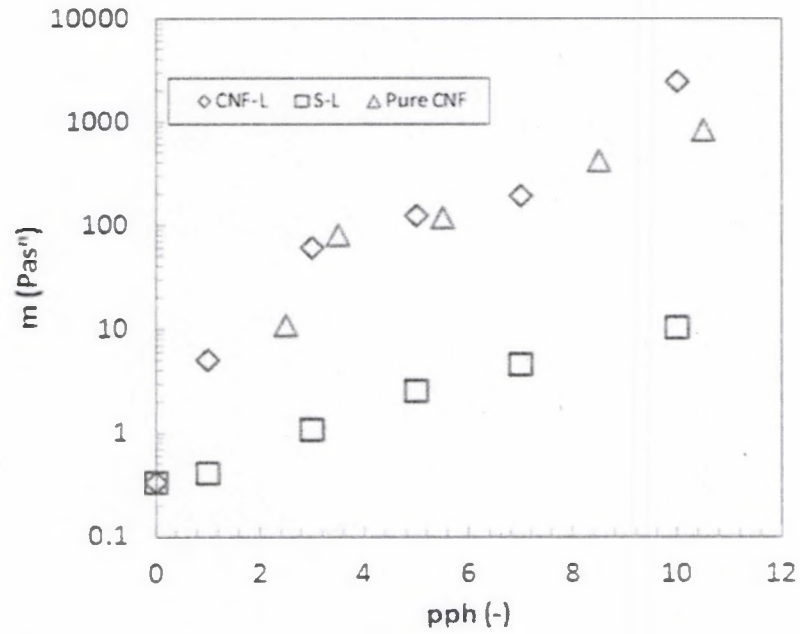


Figure 5-5 Power law parameter  $m$  as a function of  $n$  for coatings with CNF, starch and pure CNF

The figure below displayed the dependence result viscosities of the ethylated starch as a function of solids. The viscosities increase along with the solid contents and showed to be Newtonian in some region.

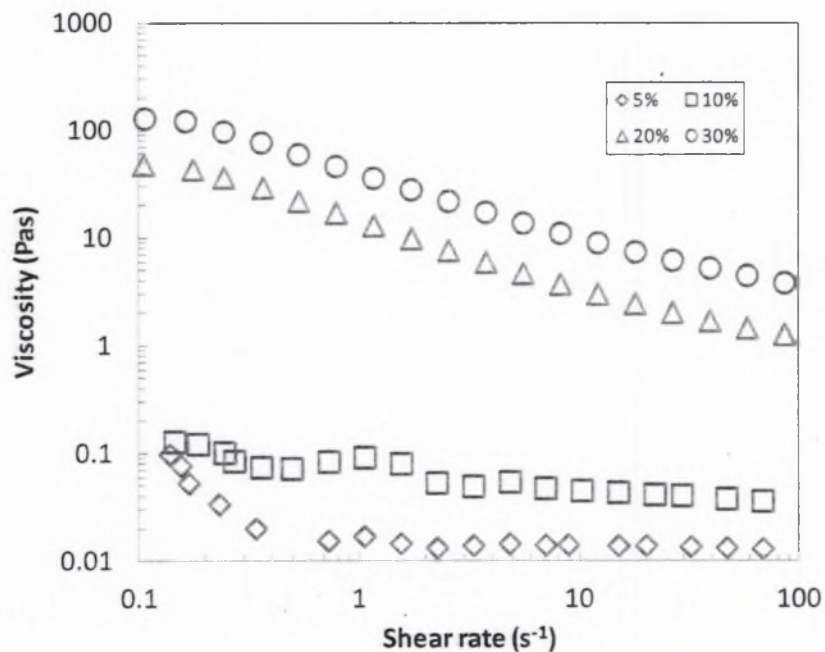


Figure 5-6 Viscosity of starch as a function of shear rate for different solids for ethylated starch Ethylex 2025

Figure 5.7 shows the scaling for coatings with starch for the actual experimental measurement and the predicting result for 5 and 10 pph starch: Predictions are a ratio of water-starch viscosities to the pure water viscosity multiplied by the 0 pph viscosity the predictions are obtained by taking the ratio of the viscosity of starch-water solutions to that of pure water, and multiplying the no starch coating results by this ratio. The results for this scaling works well with some over prediction of the viscosities.

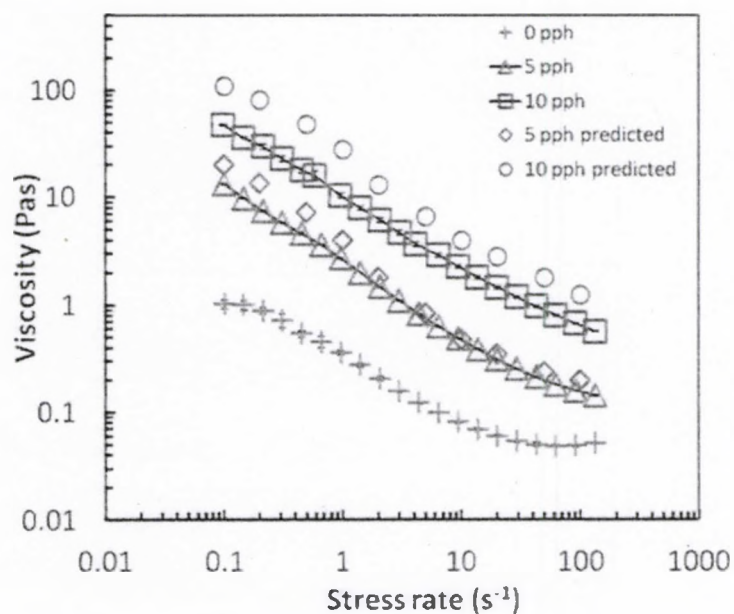


Figure 5-7 Viscosities of coatings that contain starch as a function of shear rate for different 5 and 10pph

Figure 5.8 below is the same scaling as in Fig. 5.6 for coatings that contain CNF for the actual experimental measurement and the predicting result for 5 and 10 pph with constant latex. The viscosity for the CNF-water only systems in Chapter 2 at 1 1/s shear rate are used to predict the behavior. The results show that CNF behaves quite different than starch in terms of the rheology increase with addition. The predicted results are much more shear thinning than the measured values. The magnitude of the increase at moderate shear rates is less than the measured values.

One issue may be that the CNF-water system is quite shear thinning. Therefore, the shear rate of the fluid between pigment particles in a shear field would be much higher than the imposed shear rate. Therefore, the viscosity that should be used to scale the results should be some high shear rate viscosity of the CNF-water system.

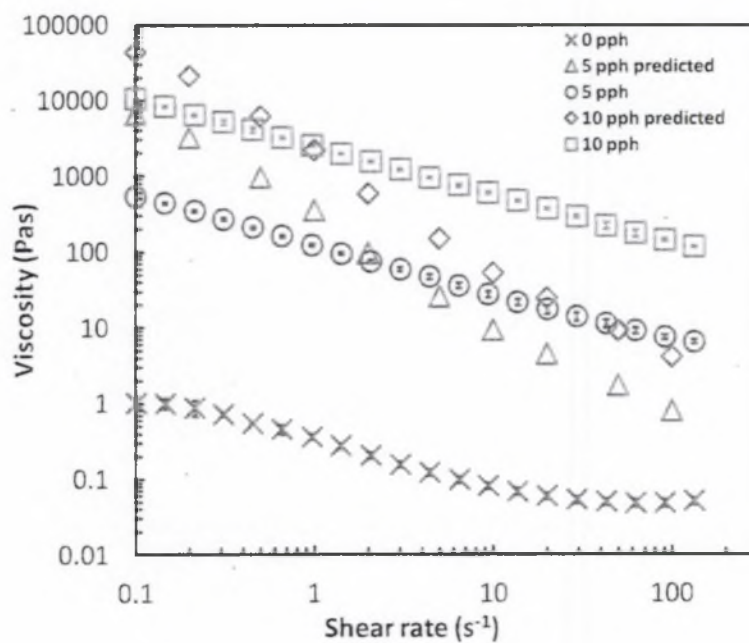


Figure 5-8 Viscosities of proposed scaling for coatings that contain CNF as a function of shear rate for different pph

As the proposed scaling for coatings with CNF results in too much shear thinning, another method to predict the viscosity increase is needed. A simple scale factor may be related to the viscosities at high shear rates. For the 5 and 10 pph CNF cases the constant factor of 450 and 850 respectively, give good results. Figure 5.6 shows the results. These factors may be related to the viscosity of the CNF-water systems at high shear rates, but these shear rates were not possible to obtain in Chapter 2.

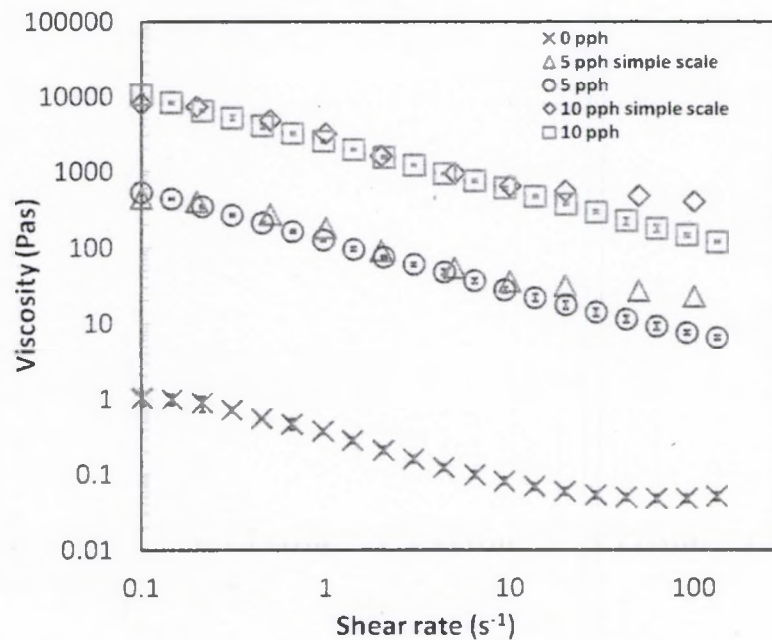


Figure 5-9 Viscosities of proposed scaling for coatings that contain CNF as a function of shear rate for different pph of a constant factor

The effect of shear rate on the variation of complex viscosity was evaluated by measuring complex viscosity response as a function of increasing oscillation frequency (angular frequency  $\omega = 0.628 - 188.50$  rad/s). The complex viscosities for the coatings with CNF and starch are displayed in the figures below. Those are the results that were obtained from the frequency sweep tests and showed to be shear thinning response that help to characterize the rheological properties of the mixtures. As expected, the complex viscosity for the coatings increase with the amount added. The complex viscosities for coatings with CNF are much larger in magnitude than the complex viscosities of starch under the same condition.

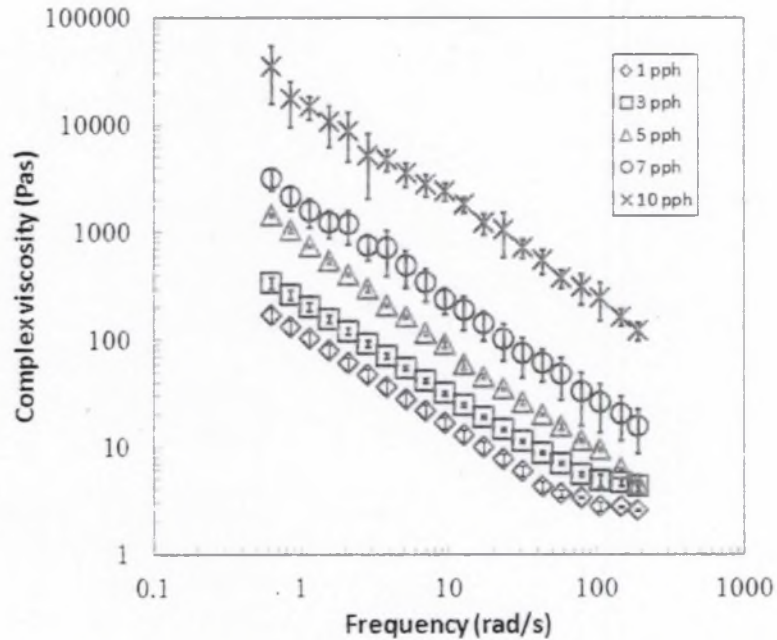


Figure 5-10 Complex viscosity and steady shear viscosity as a function of shear rate-frequency for different concentrations of CNF into a coating

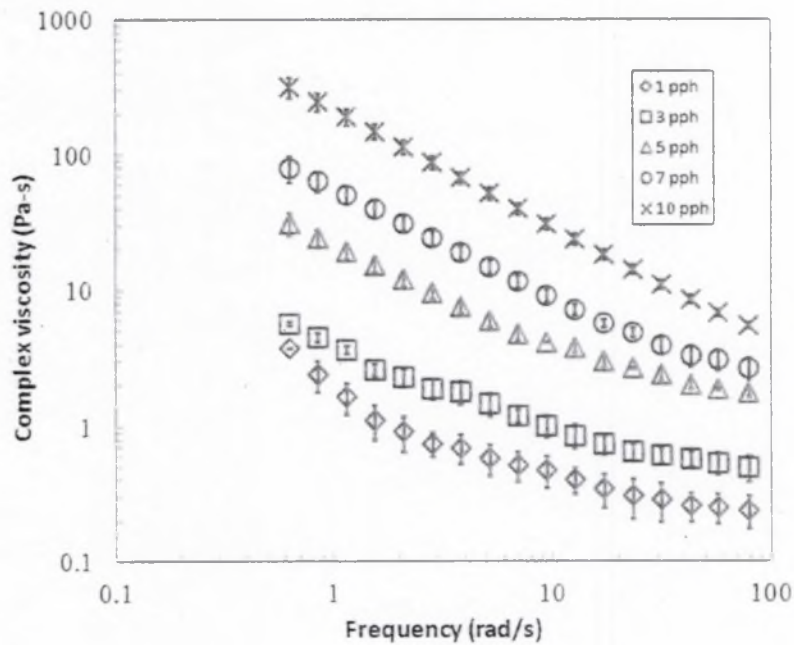


Figure 5-11 Complex viscosity and steady shear viscosity as a function of shear rate-frequency for different concentration of starch in a coating

Figures 5.12 and 5.13 show the results obtained for the storage modulus ( $G'$ ) and the loss modulus ( $G''$ ) against the frequency for different concentrations of CNF and starch. For both cases, a consistent pattern in proportion with the increase of the amount of CNF and starch is observed. The storage modulus ( $G'$ ) is around five times greater in magnitude than the loss modulus ( $G''$ ) for both CNF and starch containing coatings; this results indicates a solid-like behavior of the coatings suspension Katarina et al; 2013 The CNF containing coatings have larger moduli than the starch by more than a factor of ten. The moduli for 10 pph CNF containing coatings are quite high compared to normal paper coating formulations.

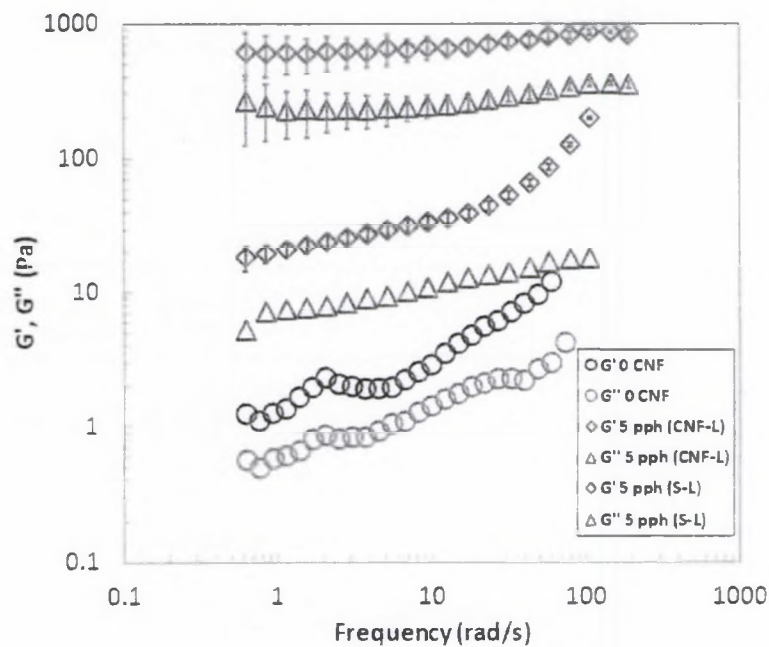


Figure 5-12 Storage and loss moduli as a function of frequency for coatings that contain 5 pph starch or CNF and 10 pph latex

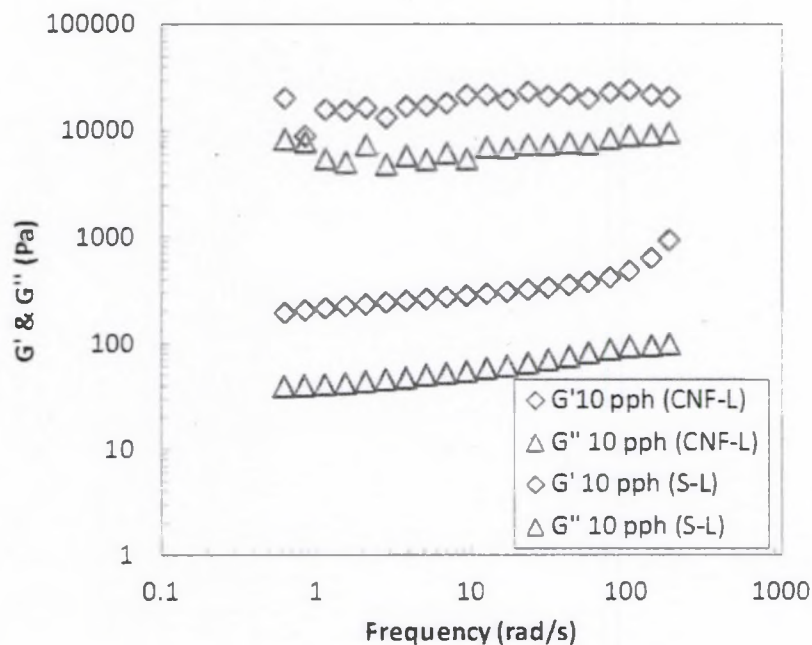


Figure 5-13 Storage and loss moduli as a function of frequency for coatings that contain 10 pph starch or CNF and 10 pph latex

The Cox-Merz rule states that complex viscosity versus the angular frequency obtained from small-amplitude oscillatory shear flow should be similar to the steady shear viscosity against the shear rate (Gleissle et al., 2003). Although there is no fundamental explanation for such a relationship, it is widely accepted and used for isotropic polymeric solutions and polymer melts. Figures 5.14 and 5.15 indicate that the Cox-Merz rule does not follow for the coatings with CNF and starch. The complex viscosity is larger in magnitude than the steady shear viscosity data for both cases. The slopes of the lines are similar for the different solid levels. Other investigations (Doraiswamy et al., 1991) have shown that the complex viscosity is two orders of magnitude larger than the steady shear viscosity for a colloidal suspension. Several other groups reported that Cox-Merz rules relationship do not follow this concept such as Bistany and Kokini (1983) and Jeffrey (2009). Here, the complex viscosity at certain

angular frequencies is much larger than the steady shear viscosity at the equivalent shear rate-frequency.

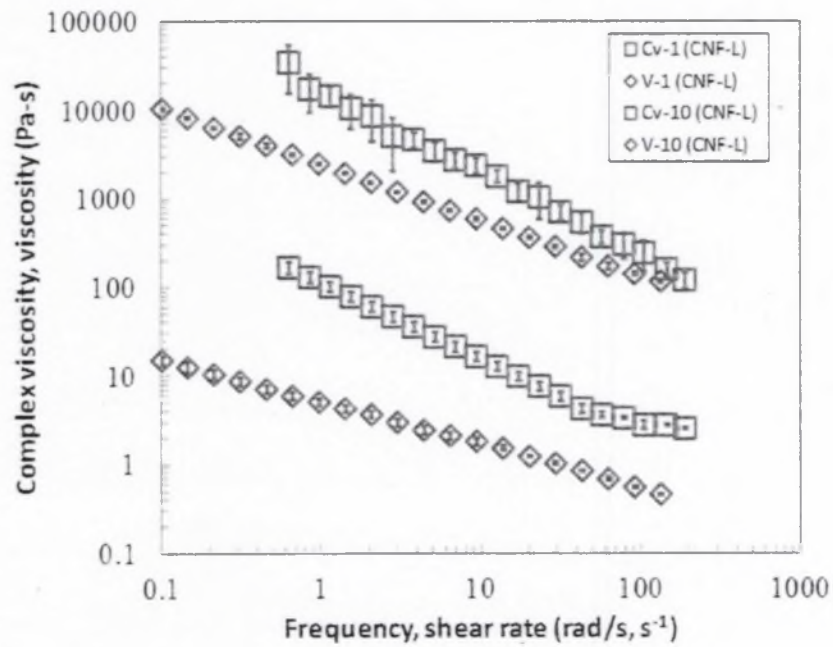


Figure 5-14 Complex viscosity (Cv) and steady shear viscosity (v) as a function of shear rate-frequency for different concentrations of CNF into a coating

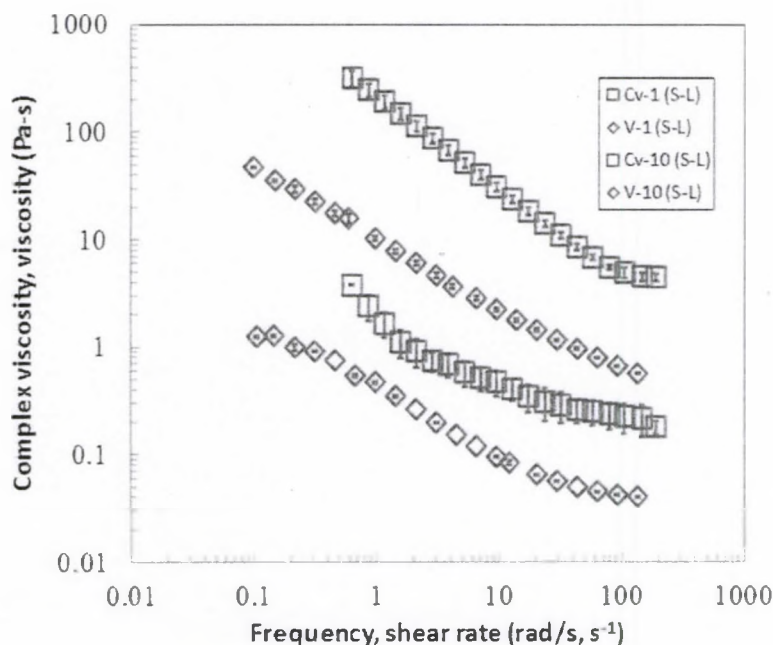


Figure 5-15 Complex viscosity (Cv) and steady shear viscosity ( $v$ ) as a function of shear rate-frequency for different concentration of starch into a coating

Yield stress is the key factor for many processing's pulp fibers suspensions and that can be used in paper industry for the design of process of cellulose nanofibers suspension. Yield stress could be defined as the minimum shear stress that applied initially to a sample to induce flow, and it is considered to be very important entities for the pulp fiber suspension. In literature, there are different methods to measure the yield stress of concentrated suspensions such as: oscillatory techniques, vane tool geometry, concentric cylinder technique, but a lot of those methods are very tedious to perform. However, in this study of cellulose nanofiber suspensions into coatings we will be focused on the vane tool geometry.

Figure 5.15 displays the results that were obtained using the vane geometry for coatings with starch and CNF. 1-9 (CNF-L) means 1 and 9 pph CNF and latex, respectively. As we can see the yield stress for coatings with CNF are much larger in

magnitude than coatings with starch under the same condition. The yield stress increase with increase the amount of CNF and starch (Wikström et al; 1998).

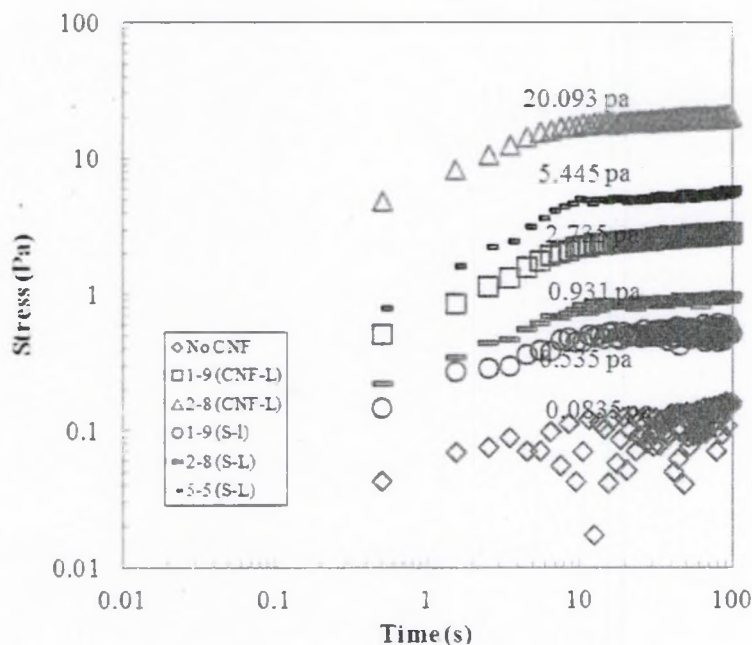


Figure 5-16 Stress as a function of time used to determine the yield stress of CNF-starch into a coating

## 5.6 Conclusion

The addition of CNF increases the viscosity more than the starch at the same addition levels. The structure of CNF must lead to high viscosities, but the power index is determined by the pigment and latex. The simple scaling of viscosities works well for starch but not for CNF. Using an effective shear rate to scale CNF viscosities gives a correct order of magnitude result, but the wrong degree of shear thinning. Both starch and CNF coatings do not follow Cox-Merz rule. The coatings that contained CNF have a larger increase in viscosity, elastic modulus and yield stress compared to coatings that contain starch at the same concentrations.

## CHAPTER 6

### THE USE OF CELLULOSE NANOFIBERS IN PAPER COATING FORMULATION

#### 6.1 Abstract

Cellulose Nanofibers (CNF) have the potential to be produced by mechanical methods at low cost in paper mills. One natural use of CNF would be as a component of a paper coating formulation, either as a thickener or co-binder. Preliminary results demonstrate strength improvements Pajari. 2012, but more work is needed to overcome some of the rheological challenges of using CNF and to document the properties of coating layers than contain CNF.

CNF was produced with a bleached softwood kraft pulp, dispersed with a beater at 3.5% solids and sent to a single disk refiner. The pulp was circulated through the refiner until the fines content was over 90%. The suspension is increased to 15% solids by filtration. In all cases, the total solids of the mixtures remained at 60%. The rheological properties of the coating were characterized with a controlled stress rheometer using parallel plate geometries. The coatings were applied to wood free paper with a laboratory rod coater and a high speed cylindrical laboratory coater (CLC). Samples were calendered and tested for gloss, smoothness, brightness, stiffness, and pick velocity.

Steady shear viscosities increase rapidly with CNF additions compared to starch. The coatings are highly shear thinning and have significant storage and loss moduli. One unexpected finding is that CNF increases the coating formulation viscosity, but it also

increases the dewatering rate. All coatings could be applied with the rod coater, but coatings with 5pph or more of CNF, could not be applied with the CLC coater. This difficulty seems to be a result of the material not flowing to the blade-paper nip when the shutter was opened and not because of some flow problem under the blade itself. Coatings containing CNF had increased in brightness, but decreased in gloss, especially for rod coated samples. Stiffness increased about 40% for blade coated samples. At low levels of CNF, pick velocity increased, but at higher levels, pick velocity decreased. This result seems to be caused by the coating layers becoming brittle with starch and CNF addition.

## **6.2 Introduction**

Many are interested in products made from renewable resources with low environmental impact and minimal safety risks. Cellulose Nanofibers (CNF) are biodegradable, natural, and renewable resources made from wood fibers. The CNF suspension can also be extracted from other biomass (Bhat et al., 2003; Klemm et al., 2006). It is expected that this material can be produced at low costs in paper mills Spence et al.,2011. In the paper industry, nano-scale cellulose fibers have gained attention due to a number of potential applications. Recent journal review articles describe various aspects of the production and use of these materials, and much attention is paid to using this material in plastic composites and other applications (Moon et al., 2011; Eriksen et al. 2011; Klemm et al., 2006; Hubbe et al., 2008; Saito et al., 2010).

However, there may be more natural uses for these fibers in the production of paper and packaging materials. Recent work has shown that CNF coated on paper can increase the capture of ink pigments at the top surface which leads to an increase in print density

for ink jet and flexographic printing (Hamada et al., 2010; Luu et al., 2011; Richmond et al., 2012). The use of CNF in the wet end has also been reported (Torvinen et al., 2011; Morseburg et al., 2009) resulting in strength benefits. CNF coated on a paper surface with a pigment pre-coat has also been shown to increase the stiffness of the sheet Ridgeway et al., 2011.

The first successful production of nanometer scale cellulose was in the 1980's when a wood pulp suspension passed several times through a homogenizer, resulting in a gel-like suspension of highly fibrillated cellulose that was named microfibrillated cellulose (MFC). This process involved forcing the material through a small capillary to break apart fibers. This requires high pressure allowing the wood fibers to break down from a dimension of 30  $\mu\text{m}$  into dimensions of 20-50 nm in diameter. Other mechanical methods have been reported such as microfluidization, micro-grinding, refining, and cryocrushing. Today, the nanoscale material generated through mechanical process is often called microfibrillated cellulose (MFC), nanofibrillated cellulose (NFC) or cellulose nanofibrils (CNF) (Turbak et al., 1983; Henriksson et al., 2007).

Other studies have focused on many aspects of CNF production. For example, chemical pretreatment for reducing energy consumption, such as enzymatic hydrolysis Dufresne et al., 2012, and TEMPO-mediated oxidation Saito et al., 2010 show interesting results. All these studies have focused on the MFC from bleached Kraft pulp wood fiber treatment.

CNF use in pigment coatings has been studied by Linköping University Institute of Technology Nygård et al., 2011. In their work, ground calcium carbonate (GCC), binders, and additives were used to form coating layers. A laboratory rod coater applied

the material onto papers. Several physical properties of the coatings were analyzed such as gloss, surface roughness, air permeance, pick strength, surface energy, and ink setting. They were faced with some issues in which at high concentration of CNF, the viscosity of the suspension was too high, and the coating did not spread out to cover the paper uniformly. Their results report coating layers that had a decrease in gloss, and air permeability. However, there was an increase in pick strength as the CNF concentrations increased.

Pajari *et al.*, 2012 reported the use of CNF as a replacement for synthetic latex binders in paper coatings. In their experiment, many trials were considered with different pigments and latex binders, and different methods of coating were adopted. They found that the partial replacement of latex with CNF increased the viscosity of the coating at low shear rate. Coatings that contain CNF had decreased in gloss and air permeance, but some other properties, like pick strength, were not affected Pajari *et al.*, 2012.

While these two reports show some promise, the difficulties of using CNF becomes clear: addition of CNF into coatings increase viscosities. This increase leads to a challenge with coating using standard equipment at high speeds. More work is needed to understand the rheology of these coatings, the methods that can be used to apply them to paper, and the properties of the coating paper.

In this study, CNF that is produced with a refiner is added to a simple coating formulation. The levels of CNF addition are compared to the behavior with starch. The rheologies of these suspensions are characterized. These coatings are applied to paper with a laboratory rod draw down coater as well as with a high speed coater. Then properties of the coated samples are characterized.

### 6.3 Cellulose Nanofibers as a Coating Additive

A simple coating formulation is used to bring out the differences between CNF and starch into a coating. A standard kaolin pigment (Capim DG, IMERYS) is mixed with styrene butadiene latex (Genflo 557, OMNOVA). This pigment is used in slurry form and is provided at 70 wt% solids. The pigment has an ISO Brightness of 89 with 92 % of particles are  $< 2 \mu\text{m}$ . The latex is supplied at 50% solids. An ethylated starch (Ethylex 2025 Tate & Lyle, USA) was used in the coating formulation. The starch was cooked by using the standard of the starch cooker for 60 minutes at 295°F (146°C) at 30% solids before it mixed into the coatings.

The CNF used in this experiment was produced by the University of Maine Process Development Center. The sample was prepared mechanically by using a pilot scale refiner to break down the wood fibers. The wood fibers were a bleached softwood Kraft pulp. The suspensions were obtained at around 3.5% solid. The solid was increased up to 15% by using a filtration process. Filtration was done with standard laboratory equipment using a vacuum and standard filter paper. Figure 6.1 shows an example of atomic force microscope (AFM) images of the CNF material produced with a refiner. There are a large number of fiber diameters that are under 100 nm, but there are also features that are still 2-3  $\mu\text{m}$  in dimension. It is not clear if these large features are an entanglement of finer fibers, or the fiber wall fractions that have been broken by mechanical action.

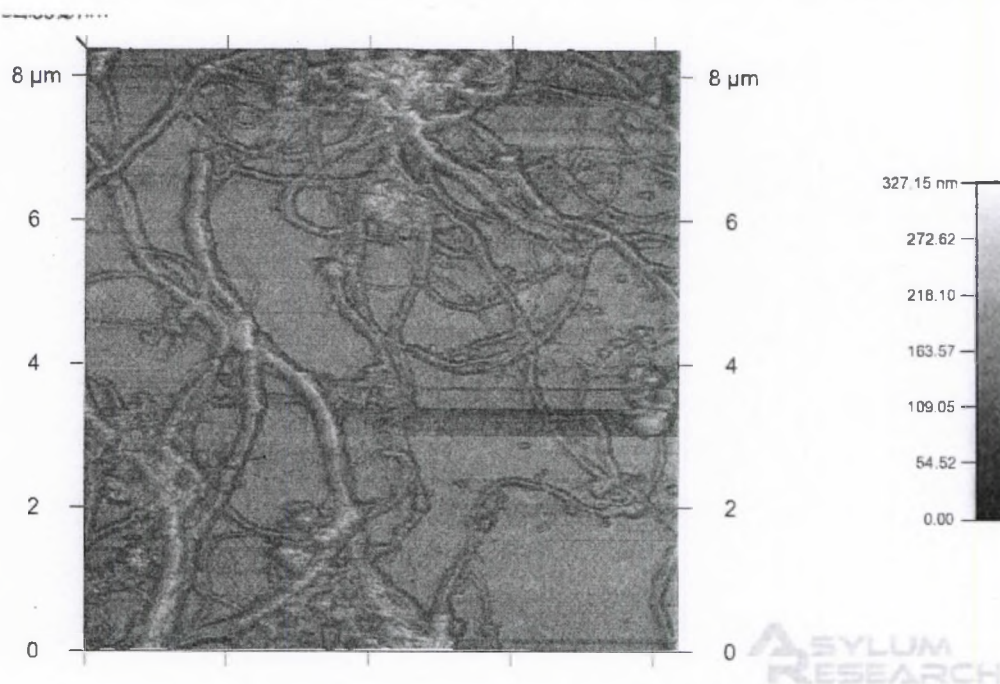


Figure 6-1 An AFM image of the refiner produced CNF

The coating formulations are displayed in tables 6.1 and 6.2. All coatings were mixed to the same solids level ( $60\% \pm 1\%$ ). Two series of coatings formulations were tested: 1) CNF and starch were varied from (1-10) pph, with the latex content held constant at 10 pph and 2) CNF and starch were added with reduction of latex on an equal weight basis. After the preparation of each sample, a high speed rotor stator mixer (Kady Mill) was used to mix before the testing for rheology or coating.

Table 6-1. Coating formulations for constant latex amount

	Coating with CNF	Coating with starch
Pigment (Capim DG IMERYs)	100	100
Latex (GenFlo 557, OMNOVA) (pph)	10	10
CNF (pph), UMaine	1-10	-
Starch (Ethylex 2025), (pph)	-	1-10

Table 6-2. Coating formulations that reduce latex and increase CNF and starch

Sample ID	0	2-8 (CNF-L)	5-5 (CNF-L)	2-8 (S-L)	5-5 (S-L)
Pigment	100	100	100	100	100
CNF (pph)	0	2	5	0	0
Starch (pph)	0	0	0	2	5
Latex (pph)	10	8	5	8	5

The rheology of the coatings was measured by using a controlled stress rheometer (Bohlin CVO). The parallel disk geometry was used based on past experience with CNF. The coating was placed between two parallel disks of radius  $R$  separated by a gap. Steady shear viscosity and oscillatory shear tests were used. Enough materials were added to the

bottom plate and the excess material was trimmed away after the gap was set. The plate had a 40 mm radius and a 1 mm gap was set. The shear rate was measured using a 10 second delay time with a 10 second integration time. For the oscillatory tests, a shear stress ramp was performed to find the linear viscoelastic region that was less than 0.1 strains. For the frequency sweep test, a range of 0.01 to 30 Hz was used. A power law according to Oswald de Waele empirical model was fitted to the experimental data for the steady shear viscosity after the correction of the data Byron et al., 1987.

The water retention of the coatings that contained CNF and starch were measured with the standard device (AA-GWR, Kaltech). The values were determined at 45, 90 and 180 seconds at a pressure of 1 bar. The standard membrane was used (5 micron pore size). The amounts of fluid that passed through the membrane were determined by weighing the blotter paper before and after the test.

A laboratory rod coater was used to apply the coatings. The procedures for this series of coatings are as followed: 1) set up the gap size according to the dimension of the rod, 2) distribute enough material to fill up the gap size, 3) cut the excess material and peel off from the edges of the coated region and 4) calender with a lab scale device. The samples were conditioned and weighed before and after to obtain coat weights.

A cylindrical laboratory coater (CLC) was used also to apply the coatings. The speed was changed and the blade setting was held constant to obtain a range of coat weights.

The gloss measurement was done using a standard device (Micro-tri-gloss, BYK-Gardner, USA). Four different measurements were taken for at 85°, and the average mean value for each sample was determine and recorded. This angle is not the standard angle

for gloss measurements for coated papers, but it gave results more in the middle range of the gloss scale to highlight differences between samples. The resultant value of the gloss measurement was recorded in percentage where 100% shows the highest value of the gloss and 0% shows there is no reflectance.

The surface roughness of the coated paper was measured by using an air leak test method (Parker-print-surface, H.E. MESSMER LTD UK.). The flow rate of air that leaks between a rim and the sample is used. The device converts the air leak rate into a surface roughness  $\mu\text{m}$ .

The air permeability is determined with Tappi standard (T460) where the amount of time for 100  $\text{cm}^3$  of air to flow through a single sheet of paper is recorded. This measurement is done with a common device (L&W, Densometer, Lorenizen & Wettre Sweden).

The brightness of a piece of paper is typically on a scale of 1 to 100, with 100 being the brightest. By using the brightness tester in our lab (Technidyne Corporation USA) the brightness values were obtained.

A sample with a defined dimension is clamped and bent through a specified angle using the stiffness tester (model 150-E, Taber V-5). These measurements followed TAPPI standard method (T489). The pick strength of the samples were characterized with the standard method using the print tester (AIC-5, IGT). The medium tack oil was used. For the samples here, the samples were accelerated to 2 m/s. Visual inspection of the start of picking gives a pick velocity.

## 6.4 Results and Discussion

Figures 6.2 and 6.3 compares the steady shear viscosity results for coatings that contain CNF and starch for the two cases. (CNF-L and S-L). Each set is an average of three runs. The results follow a shear thinning behavior and a consistent pattern. The slopes of the lines also increase with CNF and starch concentration showing an increase in the shear thinning nature. As expected, the viscosities increase as the concentration of CNF and starch increase. The viscosities of coatings with CNF are more than ten times the viscosities of coatings with starch.

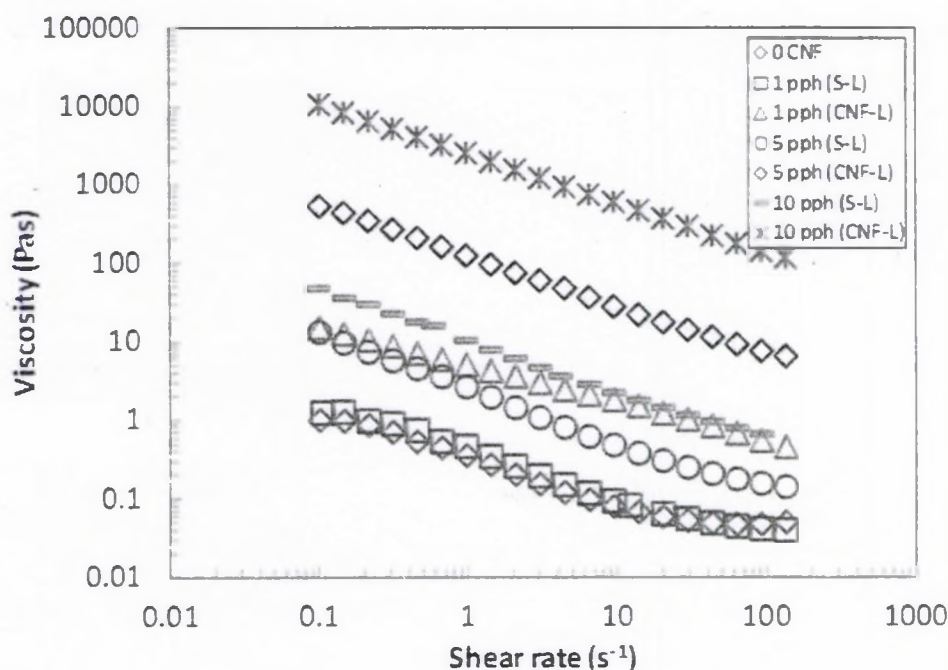


Figure 6-2 Comparison of steady shear viscosity as a function of shear rate for different pph of coatings with CNF and starch

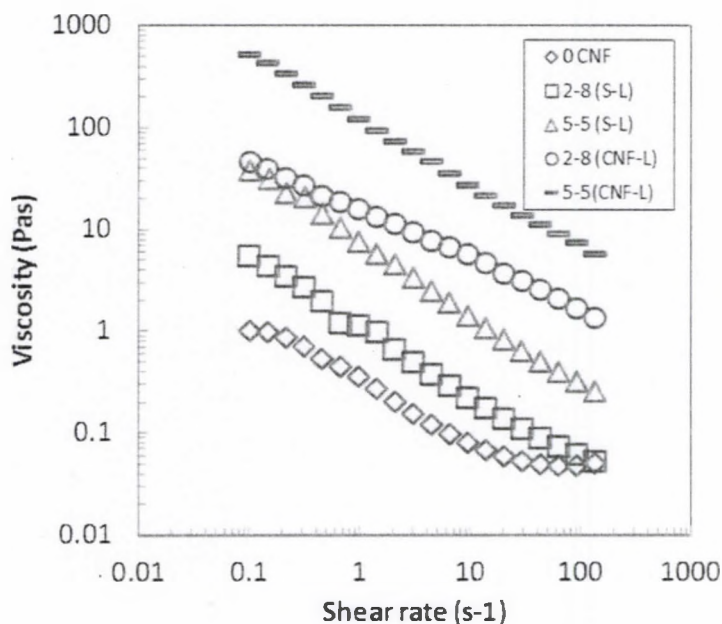


Figure 6-3 Steady shear viscosity as a function of shear rate for different pph of coatings with CNF, starch and latex

Figures 6.4 and 6.5 show the results obtained for the storage modulus ( $G'$ ) and the loss modulus ( $G''$ ) against the frequency for different concentrations of CNF and starch. For both cases, a consistency pattern in proportion with the increase of the amount of CNF and starch is observed. The storage modulus ( $G'$ ) is around five times greater in magnitude than the loss modulus ( $G''$ ) for both CNF and starch containing coatings; this results indicates a solid-like behavior of the coatings suspension Katarina et al; 2013. The CNF containing coatings have larger moduli than the starch by more than a factor of ten. The moduli for 10 pph CNF containing coatings are quite high compared to normal paper coating formulations.

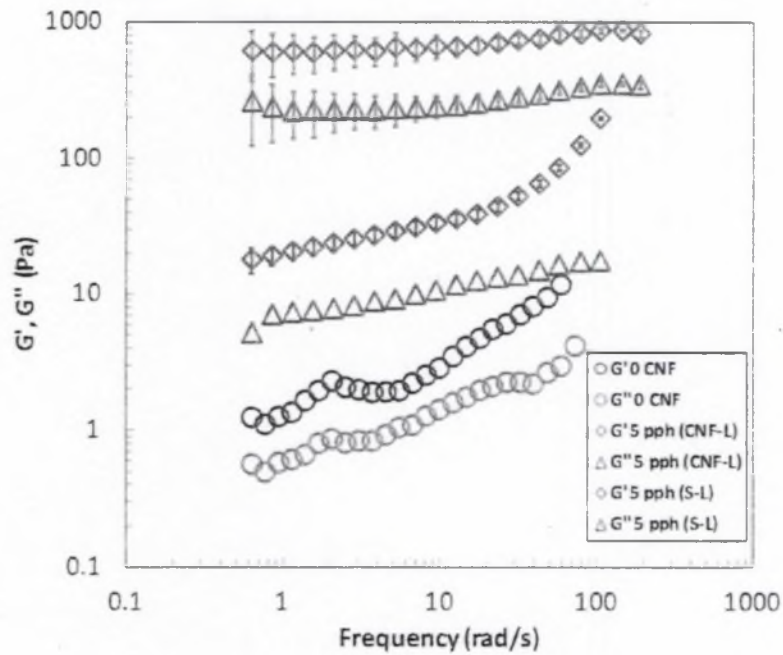


Figure 6-4 Storage and loss moduli as a function of frequency for coatings that contain 0 CNF and 5 pph starch or CNF and 10 pph latex

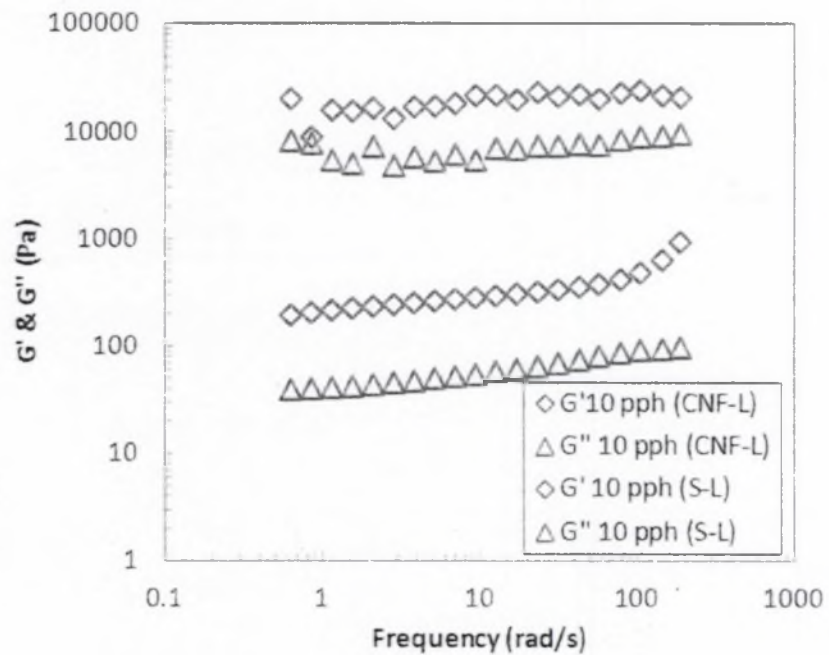


Figure 6-5 Storage and loss moduli as a function of frequency for coatings that contain 10 pph starch or CNF and 10 pph latex

The results of the water retention test are shown in Figure 6.6. Each point is an average of three trials. One result that was not expected is clear: as the content of CNF increases, the amount of water released from the coating formulation increases, even though the viscosity of the coating system increases. The starch containing coatings respond as expected in that an increase in starch content decreases the amount of water that passes through the membrane. This decrease is explained by the increase in the liquid phase viscosity that would result in a decrease in the rate of flow through the porous filtercake of the coating. The results indicate that when CNF is present, the filtercake formed is more open than when CNF is not present and the water can flow through the filtercake (which means as CNF holding more water and being able to release the water during the experiment). These results show a difference between starch and CNF. Starch molecules are truly a water soluble polymer that increase the viscosity of the liquid phase. This increase of viscosity increases the viscosity of the coating and decreases the water released in the GWR test. CNF used here still has micron length scales that act to increase the viscosity, but are also captured in the coating layer during dewatering. This capture must influence the pigment packing and the coating layer structure. Pajari *et al.*, 2012 report that the immobilization solids decrease with CNF addition representing poorer packing. However, they report that the water drainage rates decrease with CNF addition which is opposite of the results in Fig. 5.

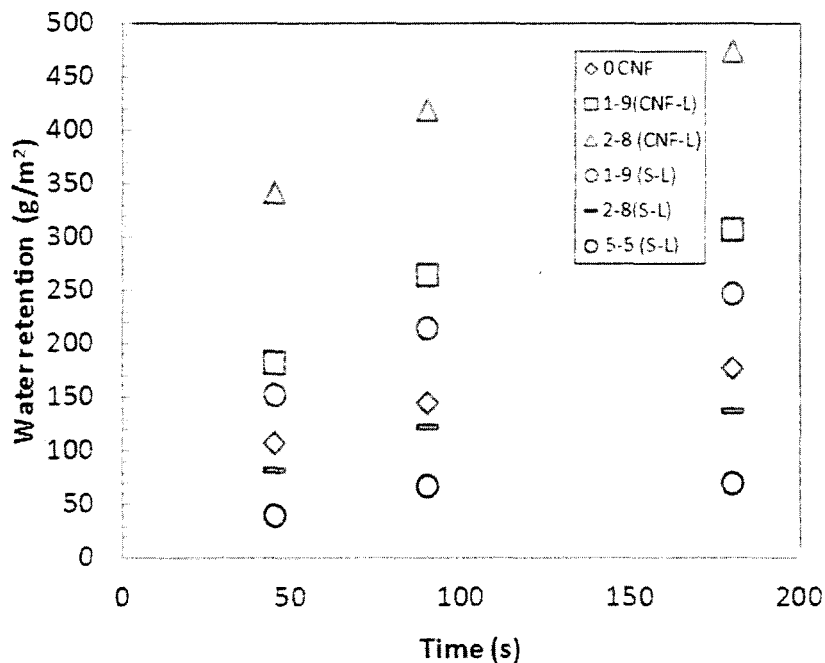


Figure 6-6 Water retention value for coatings with CNF and starch as a function of time for series 2 formulations

Figure 6.7 shows the total coat weight obtained with the cylindrical laboratory coater (CLC). The blade setting was not adjusted but the speed was adjusted from 1500 to 3500 ft/min to change coat weight. The results show that as the concentration of starch or CNF increases, the coat weight also increases. This result is expected in that as the speed or viscosity increases, the blade forces would increase, deforming the blade and allowing more coating to flow under the blade.

The concentration of CNF at 5 pph could not be coated with our CLC. The coating was quite thick and had a yield stress. When the shutter of the pond opens, coating is too thick to flow by gravity to the blade-paper nip. If the pond was pressurized and this flow could be induced; it seems like it would be possible to coat this higher concentration with the blade.

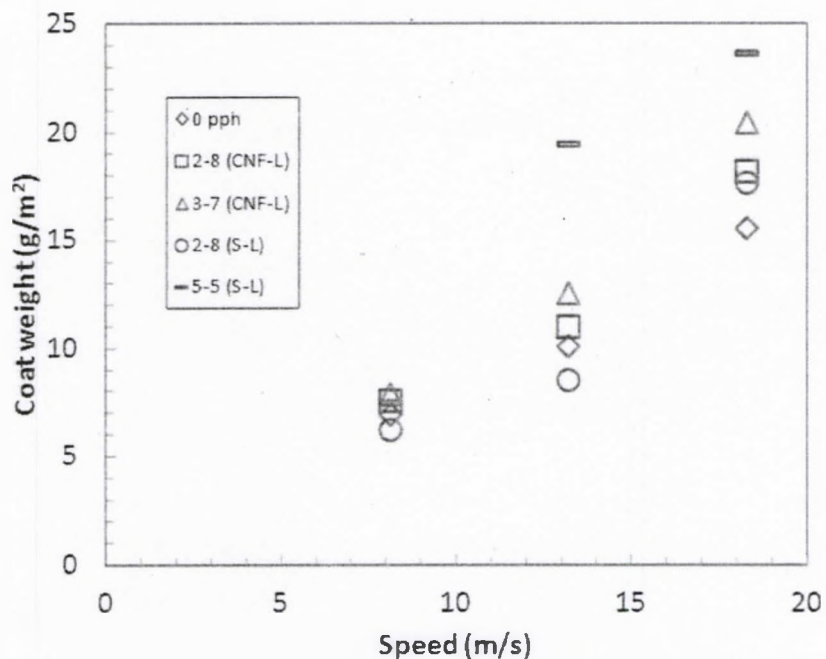


Figure 6-7 Coat weight as a function speed for different coating formulation by using the CLC coater

The gloss results of the rod coated samples all show a decrease as starch or CNF are added. It is clear that the wire marks from the rod are not leveled in the coating layers, resulting in low gloss values. This low gloss is similar to what others have reported (Pajari *et al.*, 2012; Nygård *et al.*, 2012).

The gloss results of the CLC coated samples are shown in Figure 6-8. The amount of CNF or starch seems to not influence gloss within the scatter of the data. Each point is an average of three values. The standard deviation is often around 2 points. The line is the trend for the 0 pph case. Low levels of starch or CNF seem to even increase gloss, but the results are within a narrow range. This trend is different than what (Pajari *et al.*, 2012; Nygård *et al.*, 2012) report, but both of these had to decrease solids to apply the coating,

resulting in more water being in contact with the paper. This increase in water increases the potential of fiber swelling that can decrease gloss even after calendaring.

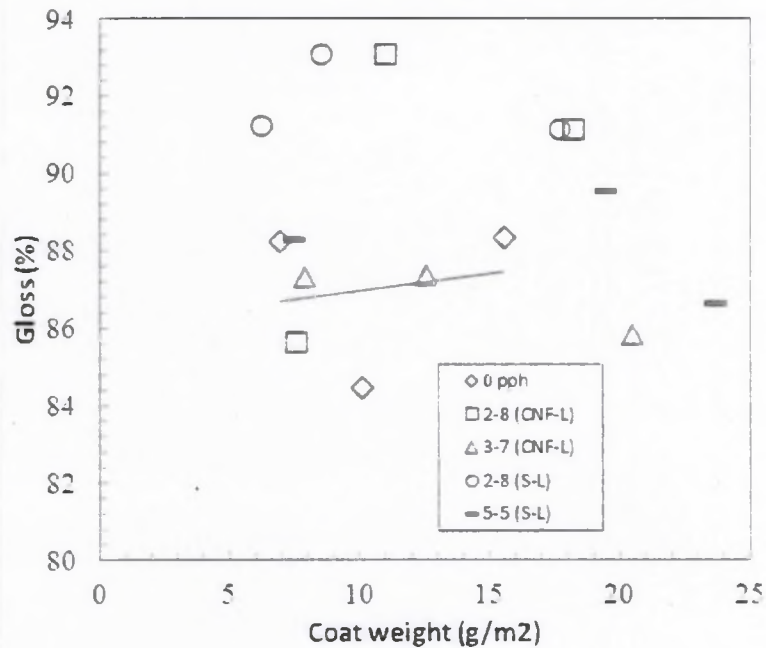


Figure 6-8 Gloss as a function of coat weight for coatings with CNF and starch applied with CLC coater

The roughness as function of coat weight for different concentrations of starch and CNF is shown in Figure 6.9. “c” denotes CLC coated sample and “r” denotes rod coated sample. Each value is an average of three repeats. Lines are trendlines for base sheet with no CNF and starch. As the concentration of CNF increases, the surface roughness increases a small amount. This result is similar to the previous studies, because of the fact they observed an increase in base sheet roughness (Pajari *et al.*, 2012; Nygård *et al.*, 2012). As we can see, the roughness obtained with the laboratory rod coater is less than the CLC.

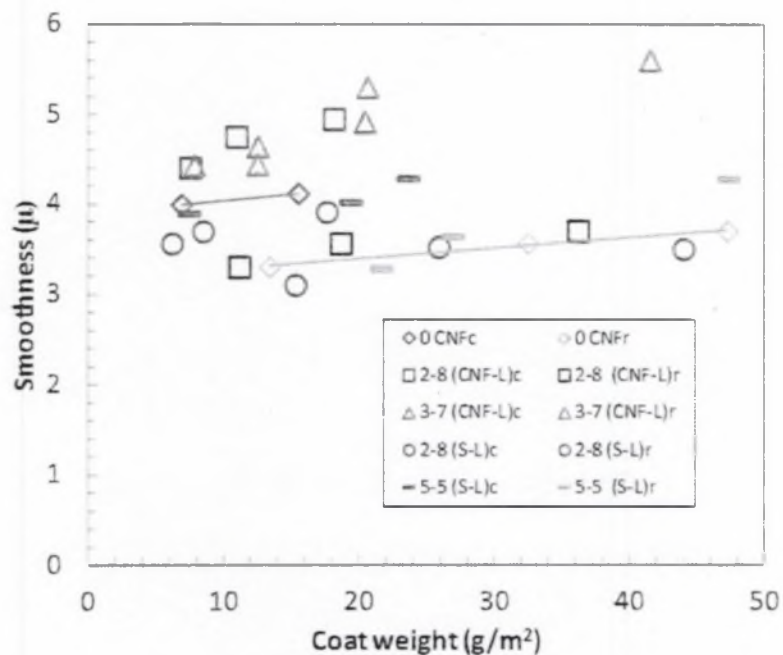


Figure 6-9 Roughness as a function of coat weight for coatings with CNF and starch

Figure 6.10 shows the brightness obtained as the function of coat weight. brightness is not influenced by CNF content. The letter “c” denotes CLC coated sample and “r” denotes rod coated sample. Each value is an average of three repeats. Lines are trendline for the base case with no CNF or starch. This agrees with work of Pajari *et al.* Pajari *et al.*, 2012. When CNF itself is dried, it gives a brownish color. Therefore, there was a concern with CNF to decrease brightness. However, CNF is used in such small amounts that it does not seem to influence the brightness.

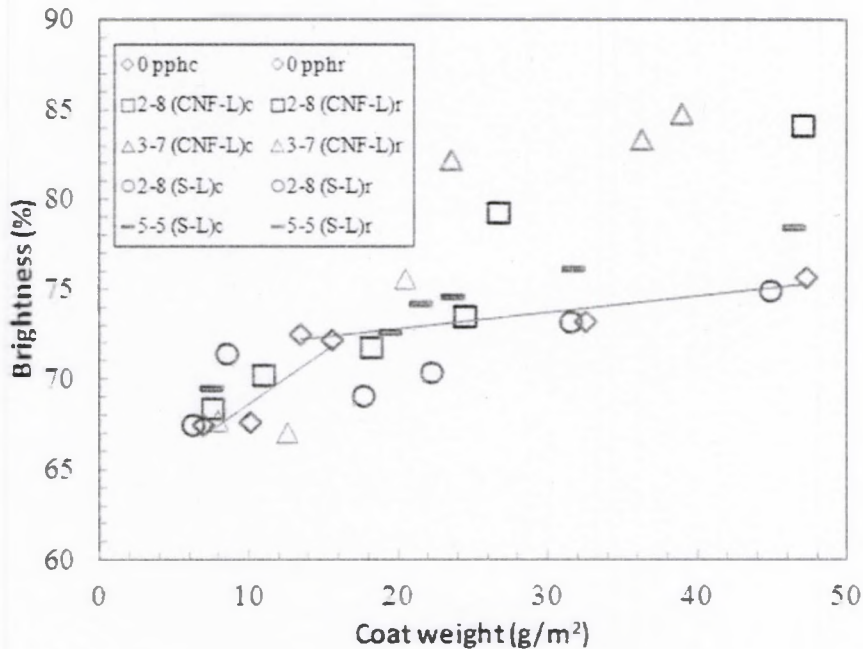


Figure 6-10 Brightness as a function of coat weight for coatings with CNF and starch

As CNF concentration increases, the time to flow a set amount of air through the sample shows a small increase given in Figure 6.11. Lines are trend lines of the base case with no starch or CNF. Higher coat weights were obtained with rod coater and are denoted "r". Each point is an average of three repeats. Standard deviation average 10%. This result is different than the GWR results in Fig. 6.6 that show in the wet state that the pore structure is more open when CNF is present. It seems like during drying, the CNF must be able to collapse into a dense packing closing up the pore space. Pajari *et al.*, 2012 also show an increase in air permeability as CNF content increases for board coatings; this result and the decrease in immobilization solids suggests the CNF can generate a more open coating layer. More work is needed around this topic.

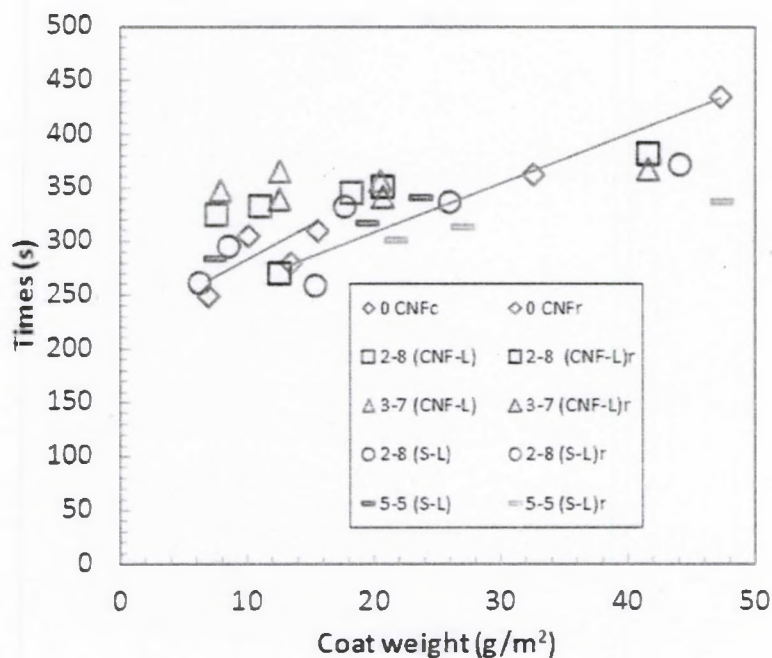


Figure 6-11 Air permeability as a function of coat weight for coatings with CNF and starch

Figure 6.12 shows the stiffness results for coatings with CNF and starch as a function of coat weight. “c” denotes CLC coated sample and “r” denotes rod coated sample. Value is an average of three repeats. Lines are trendlines for the base case with no starch or CNF coatings with CNF have higher stiffness than coatings with starch under the same condition. This increase in stiffness seems to be significant. These results also agree with Ridgeway et al., 2011 who discussed the “I-beam” effect, even though these samples were coated only on one side. Pure films of CNF are quite stiff: if this high modulus material is captured at the surface of the paper, one would expect an increase in stiffness. The stiffness increase for rod coated samples is not significant. The reason for this result is not clear.

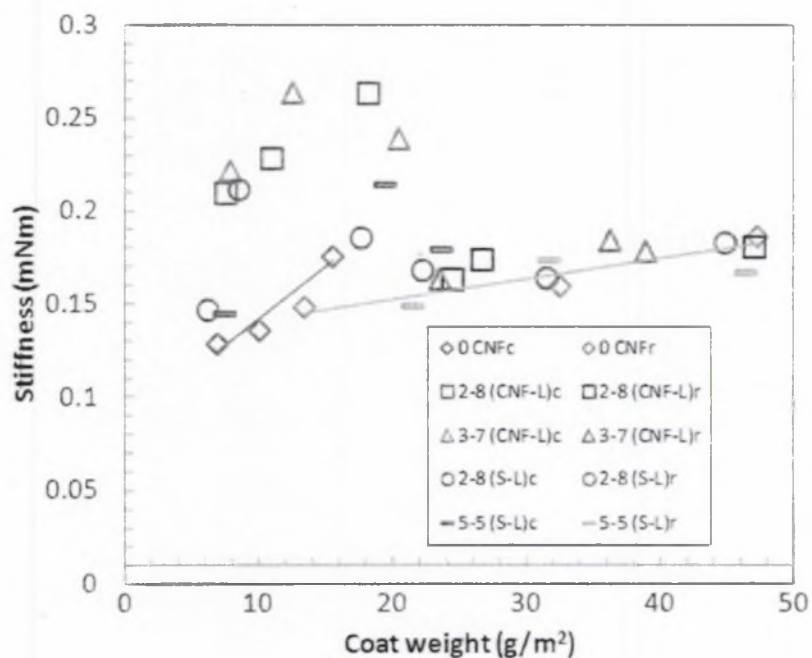


Figure 6-12 Stiffness as a function of coat weight for coatings with CNF and starch

The pick velocity for coating with CNF and starch is shown in figure 6.13. Lines are trend lines of the base sheet case. “c” is for CLC coated samples and “r” is for rod coated samples. Each value is average of three repeats. Standard deviations are around 30%. The pick strength increased for the low concentrations of coatings with CNF and starch, but decreased at higher concentrations. For CNF, 2 pph content of CNF increases the pick velocity by 50%. The results obtained for both cases seem to have the similar behavior and may be due that the coating becoming more brittle at high levels of pph of CNF. Pajari *et al.*, 2012 showed a small decrease in pick velocity as CNF content increased, but the change was not large.

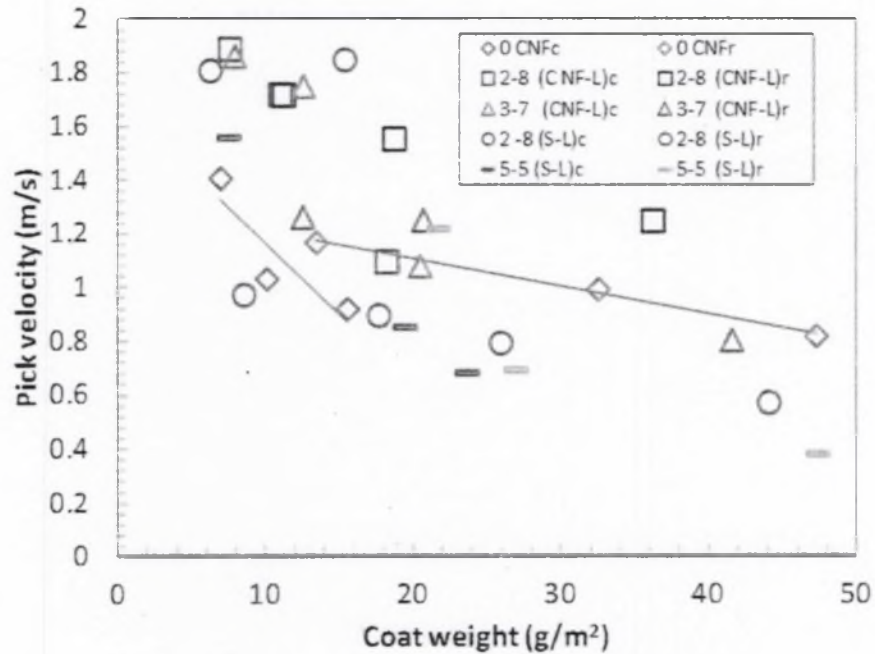


Figure 6-13 Pick velocity as a function of coat weight for coatings with CNF and starch

The biggest challenge on this topic is to understand better the issues related to applying CNF containing coatings at high CNF content. Blade coating of these CNF containing coating may not be viable because of the high viscosities. At present, it is not clear if the lack of ability to coat the 5pph CNF coating with the CLC is due to flow in the pond, or flow uniformity under the blade.

## 6.5 Conclusion

The coatings that contain CNF have a larger increase in viscosity and elastic modulus compared to coatings that contain starch. Coatings with CNF of 5 pph were not able to be applied with CLC coater due to solid like behavior of the coating: the issue seems to be the ability of the coating to flow in the pond by gravity to the blade-paper nip and not the flow in the blade region itself.

The water retention tests and the air permeability tests show a surprising difference between starch and CNF containing coatings: CNF seems to generate a more open pore structure in the wet state while starch does not. In the final dry coating, CNF and starch show a slight decrease in permeability. The CNF used here must have micron scale features that influence the packing of pigments and changes the coating structure.

The coatings with CNF had higher stiffness and coating strength than coatings that contained starch. CNF acts similar to starch in terms of being a co-binder. A decrease in pick resistance is seen at 5 pph CNF or starch content; this decrease likely comes from the coating layer becoming more brittle.

## CHAPTER 7

### RECOMMENDATIONS FOR FUTURE WORK

CNF is an interesting nanomaterial that has great potential in packaging materials, foamed structure, barrier films properties, absorbent materials and CNF synthesis in bioplastics. A number of unexplained results came up during the work.

For both the parallel plate and cone and plate geometries, the sample tends to eject from the sides of the device at moderate shear rates. The mechanism for this discharge is not clear and should be further investigated because this behavior may influence some processes such as coating. This ejection may be related to the generation of flocs in the material during shear.

Cellulose nanofibers show some potential improving coatings and reducing the use of latex binder. It would be useful to have a systematic study by applying the material into coating formulations for different type of papers, and compare the results.

Some preliminary results show that CNF generates a normal force during shear. In future work, the normal forces of CNF water base and the CNF coating formulations should be characterized. This would be important to understand blade loading during the blade coating process.

The laboratory size scale press device experiments should be repeated with the new update device for flooded and the metered size press methods with different speeds and nip pressures. A good place to start should be the same speeds and nip load pressures used in Chapter 3. Coating formulations could also be studied as well with this device and the influence of CNF into starch suspensions to size paper. Develop a predicted

method with the significance that can explain the main issues face during the experimental

## REFERENCES

- Agoda-Tandjawa., Durand S., Berot S., Blassel C., Gaillard C., Garnie C., and Doublier J. L. "Rheological characterization of microfibrillated cellulose suspensions after freezing". *Cabohydrate Polymers* 205: 677-686, 2010.
- Bhat G, Lee Y, "Recent advancements in Electrospun nanofibers." Proceedings of the twelfth international symposium of Processing and Fabrication of Advanced materials, Ed TS Srivatsan & RA Vain, TMS 1-10, 2003.
- Barnes, H. A., Hutton, J. F., Walters, K." *An Introduction to Rheology*", Elsevier, Amsterdam, 1989.
- Barud H. S., Ribeiro C. A., Crespi M. S. et al., "Thermal characterization of bacterial cellulose-phosphate composite membranes," *Journal of Thermal Analysis and Calorimetry*, 87(3): 815–818, 2007.
- Battista, O. A., Microcrystal Polymer Science. McGraw Hill Book Company: New York, 208, 1975.
- Benjamin D., T.J. Anderson, and L.E. Scriven, "Multiple roll systems, steady state analysis", *AIChE J.* 41(5): 1045-1060, 1995.
- Bennigton, C.P.J., Kerekes, R.J., and Grace, J.R.,"The yield stress of Fibers Suspensions." *The Canadian Journal of Chemical Engineering* 68: 748-57,1990.
- Bird R. Byron; Robert C. Armstrong; Ole Hassager "Dynamics of Polymerics of Liquids" volume 1, *Fluid Mechanic*, second edition, 1987.
- Bristow, J. A., *Liquid Absorption into Paper During Short Time Intervals. Svensk Papperstidning-Nordisk Cellulosa* 1967, 70, (19), 623-629.

Caner E; Farnood R., and Yan N “Effect of the coating formulation on the gloss properties of coated papers” *Tappi J.* 1-14, 2010.

Chakraborty A., Sain M., Kortschot M., *Holzforschung* “A comparative study of energy consumption and physical properties of microfibrillated cellulose produced by different processing methods 59(1), 102, 2005.

Cohen E. and E. Guttoff, Modern Coating and Drying Technology, VCH Publishing, New York, 1992.

Devisetti S.K. and Bousfield D.W., Fluid absorption during forward roll coating of porous webs, *Chem. Eng. Sci.*, 65: 3528-3537, 2010.

Doraiswamy D., Mujumdar A.N., Tsao I., Beris A.N., Danforth S.C., and Metzner A.B., “The Cox-Merz rule extended” A rheological model for concentrated suspensions and other materials with a yield stress, *J. Rheol.*, 35(4): 647-685, 1991.

Dufresne A. *Nanocellulose: From nature to high performance tailored materials*. Chapter 6, rheological behavior of nanocellulose suspensions and self-assembly, 2012.

Eva-Lena Hult, Marco Lotti, Marianne Lenes “Efficient approach to high barrier packaging using microfibrillar cellulose and shellac”.575-586, 2010.

Eichorn, S.J., A. Dufresne, M. Aranguren, N.E. Marcovich, J.R. Capadona, S.J. Rowan, C. Weder, W. Thielmans, M. Roman, S. Renneckar, W. Gindl, S. Veigel, J. Keckes, H. Yano, K. Abe, M. Nogi, A. N. Nakagaito, A. Mangalam, J. Simonsen, A.S. Benight, A. Bismarck, L.A. Berglund, T. Peijs: “Review: current international research into cellulose nanofibres and nanocomposites”, *J. Mater. Sci* 45:1-33, 2010.

Eklund R. W., LeBlanc H.A and Halley, D. G. “CLC- A New High Speed Blade Coater for the Laboratory,” *Tappi J.* 71(12), 55, 1988.

Eriksen et al. "Strength and barriers of cellulose nanofibers for utilization of packaging materials" Springer, 2008.

Eichorn, S.J., A. Dufresne, M. Aranguren, N.E. Marcovich, J.R. Capadona, S.J. Rowan, C. Weder, W. Thielmans, M. Roman, S. Renneckar, W. Gindl, S. Veigel, J. Keckes, H. Yano, K. Abe, M. Nogi, A. N. Nakagaito, A. Mangalam, J. Simonsen, A.S. Benight, A. Bismarck, L.A. Berglund, T. Peijs: "Review: current international research into cellulose nanofibres and nanocomposites", *J. Mater. Sci* 45:1-33, 2010.

Eriksen et al. "Strength and barriers of cellulose nanobers for utilization of packaging materials" Springer, 2008.

Eyholzer C., N. Bordeanu, F. Lopez-Suevos, D. Rentsch, T. Zimmermann, and K. Oksman, "Preparation and characterization of water redispersable nano fibrillated cellulose in powder form", *Cellulose* 17:19-30, 2010.

Gardner D.J, G.S. Oporto, R. Mills, and M.A.S.A. Samir. "Adhesion and surface issues in cellulose and nanocellulose," *Journal of Adhesion Science and Technology*, 22, 545-567, 2008.

Gardner, K.; Blackwell, J. "Structure of native cellulose". *Biopolymers* 13: 1975-2001, 1974.

Geankoplis C. Transport Processes and Separation Process Principles, Prentice Hall, 2003.

Gleissle W. and Hochstein B. "Validity of the Cox Merz -rule for concentrated suspensions" *Journal of Rheology* 47, 897, 2003.

Gonzales et al. "Cellulose Nanofibers as paper additive". *Bioresources* 7(4), 5163-5180, 2008.

Haavisto S., Liukkonen J., Jasberg A., Koponen A., Lille M. and Salmela J., "Laboratory-Scale Pipe Rheometry: A study of a microfibrillated cellulose suspension" Proc. Tappi PAPERCON, 2011.

H.A. Barnes, J.F. Hutton, K. Walters "An introduction to rheology". Chapter 3, 46-49 second edition 1989.

Hatzikiriakos S., Hamad W, and Safiei-Sabet S. "Rheology of nanocrystalline cellulose aqueous suspension". Langmuir, 28(49), 17124-33, 2012.

Hamada H., and Bousfield D.W., Nano-fibrillated cellulose as a coating agent to improve print quality of synthetic fiber sheets, Proc. Technical Association of Pulp and Paper Advanced Coating Fundamentals Symposium, 2010.

Hamada H., J. Beckvermit, and Bousfield D. W., Nanofibrillated cellulose with fine clay as a coating agent to improve print quality, Technical Association of Pulp and Paper PAPERCON conference, 2010.

Herrick, F. W., Casebier, R. L, Hamilton, J. K, Sandberg K. R. "Microfibrillated Cellulose: Morphology and Accessibility". 37, 815, 1983.

Henriksson et al. "An environmentally friendly method for enzyme-assisted preparation of microfibrillated cellulose (MFC) Nanofibers", European Polymer Journal 43(8), 3434-3441, 2007.

Higuchi, T. *Lignin Biochemistry. Biosynthesis and Biodegradation*. Wood Sci. Technol. 24: 23-63, 1990.

Hentze H., "From nanocellulose science towards applications" VTT Technical Research Centre of Finland. Pulpaper, 2010.

Hessler N., Klemm D., "Control of structure and shape of bacterial synthesized nanocellulose". 235<sup>th</sup> ACS National Meeting, New Orleans, LA, United States 2008.

Hon, D.N.S.; Shiraishi, N. *Wood and Cellulosic Chemistry*. Ed. 2, 1-108, 2000.

Hubbe M.A., O.J. Rojas, L.A. Lucia, and M. Sain, "Cellulosic nanocomposites: A review", *BioResources* 3(3): 929-980 (2008).

Jan C. Walter, the Coating Processes" Tappi Press Atlanta, GA USA 1993.

Katarina Dimic-Misc, Patrick A.C. Gane, Jouni Paltakari "Micro and nanofibrillated cellulose as rheology modifier additive in CMC-Containing pigment coating formulations. American Chemical Society. October 21,2013.

Karppinen A, Saarinen T, Salma J., Laukkanen A., Nuopponen M, Seppälä J. "Flocculation of microfibrillated cellulose in shear flow", *Springer* 19, 1807-1819, 2012.

Kellog T., Huber J.M. Corp, Clay Division "Coating formulation. The Coating Processes" *Tappi J.* 147-149, 1993.

Klemm, D.; Schumann, D.; Kramer, F.; Hessler, N.; Hornung, M.; Schmauder, H. P.; Marsch, S., Nanocelluloses as innovative polymers in research and application. *Adv Polym Sci*, 205, 49-96, 2006.

Klemm, D.; Schumann, D.; Kramer, F.; Hessler, N.; Koth, D.; Sultanova, B., "Nanocellulose Materials - Different Cellulose, Different Functionality". *Macromol Symp*, 280, 60-71, 2009.

Klemm D., Schumann D., Udhardt U., and Marsch S., "Bacterial synthesized cellulose artificial blood vessels for microsurgery," *Progress in Polymer Science*, 26 (9), 1561–1603, 2001.

Klemm D., Heublein B., Fink H., and Bohn A., "Cellulose: Fascinating Biopolymer and Sustainable Raw Material", *Angew. Chem. Int. Ed.*, 44, 3358-3393, 2005.

Lepoutre, P., and Rigdahl, M., "Analysis of the effect of porosity and pigment shape on the stiffness of coating layers," *Journal of Materials Science*, 24: 2971, 1989.

Liang C., Yan N., Vidal D., Zou X. "Effect of the coating formulation on the gloss Properties of coated papers" *Proc. Technical Association of Pulp and Paper PAPERCON symposium*", 2012.

Luu W., J. Kettle, Bousfield D.W, "Application of Nano-fibrillated cellulose as a paper surface treatment for inkjet printing', *Proc. Technical Association of Pulp and Paper PAPERCON symposium*", 2011.

Marco Lotti, Oyvind Weiby Gregersen, Storker Moe, Marianne Lenes "Rheological studies of microfibrillar cellulose water dispersion" 137-145, 2011.

Missoum, K., Belgacem, N., Krouit, M., Martin, C., Tapin-Lingua, S., & Bras, J. (2010). Influence of fibrillation degree & surface grafting of micro-fibrillated cellulose on their rheological behavior in aqueous suspension. In Presented at the 2010 TAPPI nanotechnology conference for the forest product industry Espoo, Finland.

Missoum, K., Corre L., Dufresne D., Belgacem A., Martin N., and Bras, J. (2010). Rheological behavior of different bio-based nanoparticles suspensions. Rheological behavior of different bio-based nanoparticles suspensions. Presented at the 2010 TAPPI Nanotechnology conference for the forest product industry, Espoo.

Moon, R.J., Martini, A., Nairn, J., Simonsen, J. and Youngblood, J. 2011. Cellulose nanomaterials review: structure, properties and nanocomposites. *Chemical Society Reviews*, 40: 3941-3994, 2011.

- Morseburg K. and Chinga-Carrasco G., Assessing the combined benefits of clay and nanofibrillated cellulose in layered TMP-based sheets, *Cellulose* 16:795-806, 2009.
- Nathalie Lavoine; Isabelle Desloges; Alain Dufresne; Julien Bras “Microfibrillated cellulose-Its barrier properties and applications in cellulosic materials, 735-764, 2012.
- Nygårds S; Aulin C; Ström G; Ederth T” Nanocellulose in pigment coatings- Aspects of barrier properties and printability offset. Linköping University Institute of Technology, 8-28, 2011.
- Ozin, G. A., and Arsenault, A. C. *Nanochemistry: “A Chemical Approach to Nanomaterials”*, The royal society of chemistry, Cambridge, 2005.
- Pääkkö, M., Ankerfors, M., Kosonen, H., Nykanen, A., Ahola, S., Osterberg, M., et al. “Enzymatic hydrolysis combined with mechanical shearing and high-pressure homogenization for nanoscale cellulose fibrils and strong gels”. *Biomacromolecules*, 8(6), 1934–194, 2007.
- Pajari H., Rautkoski H., Moilanen P., replacement of synthetic binders with nanofibrillated cellulose in board coating: pilot scale studies. TAPPI International Conference on Nanotechnology for renewable material. June 5-7, 2012.
- Ranby, B. G., “The Colloidal Properties of Cellulose Micelles”. *Discussions of the Faraday Society*, 11, 158-164, 1951.
- Revol, J. F.; Bradford, H.; Giasson, J.; Marchessault, R. H.; Gray, D. G., Helicoidal self-ordering of cellulose microfibrils in aqueous suspension. *International Journal of Biological Macromolecules* 14 (3):170-172, 1992.

Richmond F., Luu W., Bilodeau M., Bousfield D.W., “Nanofibrillated Cellulose as a surface treatment for inkjet printing.” Proc. Technical Association of Pulp and Paper, Nanotechnology of renewable materials conference. 2011.

Ridgeway, C., Gane P., ‘Constructing NFC –Pigment composite surface treatment for enhanced paper stiffness and surface properties, Proc. Technical Association of Pulp and Paper, Nanotechnology of renewable materials conference. 2011.

R. Byron Bird, Robert C. Armstrong, Ole Hassager “Dynamics of polymeric liquids”. Chapter 10 second edition 1989.

Saarikoki E., Saarinem T., Salma J, Seppälä J., Flocculated flow of microfibrillated cellulose water suspension: an imaging approach for characterization of rheological behavior. Springer, 19, 647-659, 2012.

Saito et al. “TEMPO-oxidized cellulose Nanofibers prepared from chemical wood pulps”. TAPPI International Conference on Nanotechnology for the Forest Product Industry, 2010.

Saito, T., Nishiyama, Y. Putaux, J. L., Vignon, M. and Isogai, A., “Homogeneous suspensions of individualized microfibrils from TEMPO-Catalyzed oxidation of native cellulose”, *Biomacromolecules*, 7: 1687-1691, 2006.

Siqueira, G., Bras, J., & Dufresne, A. Cellulose whiskers versus microfibrils: “Influence of the nature of the nanoparticle and its surface functionalization on the thermal and mechanical properties of nanocomposites”. *Biomacromolecules*, 10(2), 425–432, 2009.

Siro I., and Plackett D., “Microfibrillated cellulose and new nanocomposite material: a review”, *Cellulose*, 10-1007, 2010.

Spence K., Venditti R., Rojas R., Habibi Y., Pawlak J. "A comparative study of energy consumption and physical properties of microfibrillated cellulose produced by different processing methods" 18:1097-1111,2011.

Spence K.L., R.A. Venditti, Y. Habibi, O. J. Rojas, and J. J. Pawlak, "Aspects of Raw Materials and Processing Conditions on the production and Utilization of Microfibrillated Cellulose", Proc. Technical Association of Pulp and Paper, Nanotechnology of renewable materials conference, 2010.

Torvinen K., Helin T, Kiiskinen H, Hellen E, Hohenthal K, and Ketoja J "Nanofibrillated cellulose as a strength additive in filler-rich SC paper", Proc. Technical Association of Pulp and Paper, Nanotechnology of renewable materials conference, 2011.

Turbak A.F, Snyder F.W, and Sandberg K.R... Microfibrillated cellulose, a new cellulose product; properties, uses and commercial potential. J Appl Polym Sci: Appl Polym Symp 37:815-827, 1983.

Walls H.J., Caines S.B., Sanchez A.M., and Khan S.A., "Yield stress and wall slip phenomena in colloidal silica gels". J. Rheol 47(4):847-868, 2003.

Wikström T., Rasmuson A. Yield stress of pulp suspension: The influence of fibre properties and processing conditions. Nordic pulp and paper research Journal, 13(3), 243-250, 1998.

Whitesides, G. M. (2005). "Nanoscience, nanotechnology, and chemistry." Small,1(2), 172-179.

Wielen V., Lorraine. "The Structure and Physical Properties of Pulpwood Fibers". Georgia Tech: 2004.

Yano H., Y Okahista, K. Abe, M. Nogi, A. N. Nakagaito, "Potential of wood-based nanofibers material", Proceeding of TAPPI International of Conference on Nanotechnology, 2010.

Zimmermann T, Bordeanu Nicolae, Strub E. "properties of cellulose from different raw material and its reinforcement potential" Carbohydrate polymers, 79 1086-1093, 2010

## **BIOGRAPHY OF THE AUTHOR**

Finley Richmond was born in Gros-Morne, Haiti on February 13, 1972. He was raised in Gros-Morne, Haiti and graduated from the local High School in 1989. He received the certificate in accounting from The Centre profession of Chris-Roi, Haiti and entered the Mechanical Engineering program in 1991. He left Haiti in 1999 and started the school from Montgomery County Community College and graduated from MC3 Pennsylvania in May 2004 with two associate degrees in general science and mathematics. He entered Widener University of Chester, PA in September 2004 with a Associate degree in Chemical Engineering, and entered the Master of Science program in the summer of 2006. His research topic was the biodiesel production from waste cooking oils. Finley earned the Master of Science degree in Chemical Engineering from The Widener University of Chester, PA in 2008. After graduation, he worked as a Research Engineer for some local companies doing contract Jobs. In 2010, he left PA, and attended full-time studies in the Ph.D. program at University of Maine. Finley contributed papers to TAPPI PaperCon 2011 and 2014 was awarded "Best student paper presented at PaperCon 2014", as well as the Advanced Coating Fundamentals Symposium 2014, International Coating Science and Technology Symposium, The Rheology Conferences and the Nanotechnology for Renewable Materials conferences, etc. Finley Richmond is a candidate for the Doctor of Philosophy degree in Chemical Engineering from The University of Maine in December 2014.